

5-2009

Biology-Inspired Adaptive and Nonlinear Robust Control of BAUV Using Pectoral-Like Fins

Subramanian Ramasamy
University of Nevada, Las Vegas

Follow this and additional works at: <https://digitalscholarship.unlv.edu/thesesdissertations>



Part of the [Electrical and Computer Engineering Commons](#), and the [Ocean Engineering Commons](#)

Repository Citation

Ramasamy, Subramanian, "Biology-Inspired Adaptive and Nonlinear Robust Control of BAUV Using Pectoral-Like Fins" (2009). *UNLV Theses, Dissertations, Professional Papers, and Capstones*. 1197.
<http://dx.doi.org/10.34917/2753738>

This Thesis is protected by copyright and/or related rights. It has been brought to you by Digital Scholarship@UNLV with permission from the rights-holder(s). You are free to use this Thesis in any way that is permitted by the copyright and related rights legislation that applies to your use. For other uses you need to obtain permission from the rights-holder(s) directly, unless additional rights are indicated by a Creative Commons license in the record and/or on the work itself.

This Thesis has been accepted for inclusion in UNLV Theses, Dissertations, Professional Papers, and Capstones by an authorized administrator of Digital Scholarship@UNLV. For more information, please contact digitalscholarship@unlv.edu.

BIOLOGY-INSPIRED ADAPTIVE AND NONLINEAR ROBUST CONTROL OF BAUV
USING PECTORAL-LIKE FINS

by

Subramanian Ramasamy

Bachelor of Engineering
Anna University, Tamil Nadu, India
2006

A thesis submitted in partial fulfillment
of the requirements for the

**Master of Science Degree in Electrical Engineering
Department of Electrical and Computer Engineering
Howard R. Hughes College of Engineering**

**Graduate College
University of Nevada, Las Vegas
May 2009**

UMI Number: 1472435

INFORMATION TO USERS

The quality of this reproduction is dependent upon the quality of the copy submitted. Broken or indistinct print, colored or poor quality illustrations and photographs, print bleed-through, substandard margins, and improper alignment can adversely affect reproduction.

In the unlikely event that the author did not send a complete manuscript and there are missing pages, these will be noted. Also, if unauthorized copyright material had to be removed, a note will indicate the deletion.

UMI[®]

UMI Microform 1472435
Copyright 2009 by ProQuest LLC
All rights reserved. This microform edition is protected against
unauthorized copying under Title 17, United States Code.

ProQuest LLC
789 East Eisenhower Parkway
P.O. Box 1346
Ann Arbor, MI 48106-1346



Thesis Approval
The Graduate College
University of Nevada, Las Vegas

_____ April 24 _____, 20.09

The Thesis prepared by

_____ Subramanian Ramasamy _____

Entitled

_____ Biology-inspired Adaptive And Nonlinear _____

_____ Robust Control of Bauv Using Pectoral-like Fins _____

is approved in partial fulfillment of the requirements for the degree of

_____ Master of Science in Electrical Engineering _____

[Redacted Signature]

Examination Committee Chair

[Redacted Signature]

Dean of the Graduate College

[Redacted Signature]

Examination Committee Member

[Redacted Signature]

Examination Committee Member

[Redacted Signature]

Graduate College Faculty Representative

ABSTRACT

Biology-Inspired Adaptive and Nonlinear Robust Control of BAUV Using Pectoral-Like Fins

by

Subramanian Ramasamy

Dr. Sahjendra N. Singh, Examination Committee Chair
Professor of Electrical and Computer Engineering Department
University of Nevada, Las Vegas

Aquatic animals have splendid ability to move smoothly through water using variety of oscillating fins. Presently researchers are involved in developing biorobotic autonomous underwater vehicles (BAUVs) which have the ability to swim like marine animals. Multiple oscillating fins (dorsal, caudal, pectoral, pelvic, etc.) can be mounted on BAUVs to generate control forces for propulsion and maneuvering. In this research work, control of the BAUVs using pectoral fins alone is considered. The oscillating pectoral fins produce unsteady periodic forces. The control of motion of an BAUV in yaw and dive planes are considered.

We first design an adaptive controller for controlling the heading angle of an BAUV in the yaw plane. The fins are assumed to be oscillating with a combined sway and yaw motion. The bias angle of the angular motion of the fin is used as the control input. The yaw angle is considered as the output variable. The adaptive controller requires the tuning of a single gain and uses only the yaw angle and its derivative for feedback.

Then, a robust servoregulator for the control of BAUVs based on the nonlinear internal model principle is designed. This design methodology is applied to control of BAUV both in the dive plane and yaw plane. In the dive plane, the fins attached to the vehicle have oscillatory pitching and heaving motion. The pitch bias angle of the fin is taken as the control input. The depth is taken as the output variable. In the yaw plane, the yaw angle command tracking of the BAUV is desired. In both the cases, the same design strategy is adopted. For the control law derivation, an exosystem of third-order is introduced, and the nonlinear time-varying BAUV model, including the fin forces, is represented as a nonlinear autonomous system in an extended state space. Based on this representation, a nonlinear robust regulator for the set point control of the depth is derived. The control system includes the internal model of a k -fold exosystem, where k is a positive integer chosen by the designer. It is shown that the control system suppresses all the harmonic components of order up to k of the tracking error.

Finally, the servoregulation of BAUVs in the dive plane using indirect adaptive output feedback control is considered. It is assumed that the physical vehicle parameters, hydrodynamic coefficients, fin forces and fin moments are unknown. This entails the design of a parameter identifier to estimate the nonlinear BAUV system parameters. A sampled-data control system is designed for the reference trajectory tracking using output feedback. The design of a stabilizing control law requires an internal model of the exosignals. The constant reference signal and also the constant disturbance input together are taken as the exosignals. The closed-loop indirect adaptive feedback control law derived is applicable to both minimum phase and non-minimum phase BAUV systems.

Simulation results show that in spite of uncertainties in the system parameters, precise tracking of the BAUV is achieved for the various control design methods indicated.

TABLE OF CONTENTS

ABSTRACT	iii
LIST OF FIGURES	vii
ACKNOWLEDGMENTS	ix
CHAPTER 1 INTRODUCTION	1
Biological Inspiration	1
Literature Review	1
Scope of Thesis	3
CHAPTER 2 BAUV DYNAMICS	8
Mathematical Model of BAUV In Dive Plane	8
Fin Force And Moment In Dive Plane	10
Mathematical Model of BAUV In Yaw Plane	11
Fin Force And Moment In Yaw Plane	13
CHAPTER 3 ADAPTIVE YAW PLANE CONTROL OF BAUV USING PECTORAL- LIKE FINS	16
Problem Definition	16
Adaptive Control Law	17
Simulation Results	22
CHAPTER 4 NONLINEAR ROBUST DIVE PLANE CONTROL OF BAUV USING INTERNAL MODEL PRINCIPLE	29
Problem Definition	30
Third-Order Exosystem	31
Control Law	34
Internal Model	35
Stabilizer Design	37
Simulation Results	39
CHAPTER 5 NONLINEAR ROBUST YAW PLANE CONTROL OF BAUV USING INTERNAL MODEL PRINCIPLE	54
Problem Formulation	55
Exosystem and Control Law Design	56
Simulation Results	58
CHAPTER 6 MODULAR DIVE PLANE ADAPTIVE CONTROL OF BAUV USING MECHANICAL PECTORAL FINS	71
Problem Statement	72

Estimation of BAUV System Parameters	73
Adaptive Output Feedback Control Law	78
Simulation Results For Depth Trajectory Tracking	82
CHAPTER 7 CONCLUSION	90
APPENDIX I SYSTEM PARAMETERS	93
APPENDIX II MATHEMATICAL CALCULATIONS	95
REFERENCES	98
VITA	104

LIST OF FIGURES

1.1	Fin patterns in a fish	7
2.1	Model of BAUV in dive plane	14
2.2	Model of BAUV in yaw plane	15
3.1	Closed-loop system	25
3.2	Adaptive yaw plane BAUV control: Constant reference trajectory $\psi^* = 25$ deg, $\omega_f = 8$ Hz, nominal parameters	26
3.3	Adaptive yaw plane BAUV control: Constant reference trajectory $\psi^* = 25$ deg, $\omega_f = 8$ Hz, -25 % uncertainty	27
3.4	Adaptive yaw plane BAUV control: Constant reference trajectory $\psi^* = 25$ deg, $\omega_f = 8$ Hz, +25 % uncertainty	28
4.1	BAUV control using first-order servocompensator: $\omega_f = 6$ Hz, nominal param- eters	46
4.2	BAUV control using first-order servocompensator: $\omega_f = 6$ Hz, -25% uncertainty	47
4.3	BAUV control using internal model of 2-fold exosystem: $\omega_f = 6$ Hz, nominal parameters	48
4.4	BAUV control using internal model of 2-fold exosystem: $\omega_f = 6$ Hz, +25% uncertainty	49
4.5	BAUV control using first-order servocompensator: $\omega_f = 8$ Hz, nominal param- eters	50
4.6	BAUV control using first-order servocompensator: $\omega_f = 8$ Hz, +25% uncertainty	51
4.7	BAUV control using internal model of 2-fold exosystem: $\omega_f = 8$ Hz, nominal parameters	52
4.8	BAUV control using internal model of 2-fold exosystem: $\omega_f = 8$ Hz, -25% uncertainty	53
5.1	BAUV control using first-order servocompensator: $\omega_f = 6$ Hz, nominal param- eters	63
5.2	BAUV control using first-order servocompensator: $\omega_f = 6$ Hz, -25% uncertainty	64
5.3	BAUV control using internal model of 2-fold exosystem: $\omega_f = 6$ Hz, nominal parameters	65
5.4	BAUV control using internal model of 2-fold exosystem: $\omega_f = 6$ Hz, +25% uncertainty	66
5.5	BAUV control using first-order servocompensator: $\omega_f = 8$ Hz, nominal param- eters	67
5.6	BAUV control using first-order servocompensator: $\omega_f = 8$ Hz, +25% uncertainty	68
5.7	BAUV control using internal model of 2-fold exosystem: $\omega_f = 8$ Hz, nominal parameters	69

5.8	BAUV control using internal model of 2-fold exosystem: $\omega_f = 8$ Hz, -25% uncertainty	70
6.1	Closed-loop BAUV system	87
6.2	BAUV depth control for constant reference command, frequency of fin oscillation $\omega_f = 8$ Hz, parameter uncertainty: + 20 %	88
6.3	BAUV depth control for sinusoidal reference command, frequency of fin oscillation $\omega_f = 8$ Hz, parameter uncertainty: + 20 %	89

ACKNOWLEDGMENTS

I joined the Electrical and Computer Engineering department at UNLV in Fall 2007, since then I have been closely working with Dr. Sahjendra Singh in the field of Control Systems. He has been a constant source of motivation and guidance throughout my research work. I express my sincere gratitude to Dr. Singh, for sharing his knowledge and experience with me and for mentoring me throughout my Masters research.

I express my sincere thanks to Dr. Keum W. Lee for his guidance, support and interest in my research work.

I am thankful to Dr. Woosoon Yim, Dr. Pushkin Kachroo and Dr. Venkatesan Muthukumar for their valuable suggestions, which helped me present my thesis in a good standard.

I would like to thank Dr. Henry Selvaraj for providing me with a Teaching Assistantship, which helped me gain academic knowledge outside my curriculum and directly helped in my research work. I would also thank the administrative staff in the Electrical and Computer Engineering Department for their support.

I am grateful to my mom, dad, brother, Dr. Robert Abella and my friends Karthik, Arjun, Priyank for believing in me and encouraging me all through.

CHAPTER 1

INTRODUCTION

1.1 Biological Inspiration

The marine animals have remarkable navigational and maneuvering capabilities due to their various fin structures. Extensive research is going on to understand and mimic the swimming mechanism of these aquatic animals. The fishes have extensive control over fin conformation. A fish with its fin structures is shown in Figure 1.1. The fin structures in fishes can be broadly categorized into; paired fins and median fins. Most of the known fishes have a total of at least seven individual fins. There are four paired fins; pectoral and pelvic of two each. Dorsal, caudal and anal fins are the median fins. In this research work, the control of autonomous underwater vehicles has been considered by using pectoral fins. The pectoral fins contribute to low speed maneuvering. A steady rectilinear motion of an BAUV can be achieved by using the pectoral fins. A nonlinear model of a BAUV is considered to be attached with two pectoral fins symmetrically placed on either sides of the vehicle and various control design methods have been studied for the smooth maneuvering of an BAUV.

1.2 Literature Review

Aquatic animals are excellent swimmers and possess a natural ability to navigate smoothly through water bodies using their various fin patterns [1, 12, 5, 16]. Presently, lot of research is being conducted in the field of biologically inspired underwater vehicle control [2]. The fish

motion mechanism can be adapted in the control of BAUVs. In literature, multiple oscillating fins mounted on AUVs have been proposed to generate control forces for propulsion and maneuvering [10, 11, 4, 20, 18]. Laboratory experiments have been performed to obtain fin forces of oscillating fins [20, 18, 19, 3]. Computational fluid dynamics methods have been also used to derive the fin forces [17, 15]. The unsteady forces are complex periodic functions of the oscillation parameters (bias angle, amplitude, frequency of oscillation, relative phase angle, etc.). The mathematical models of BAUVs including the fin forces are nonlinear and time-varying.

Many fishes use oscillating pectoral fins for their smooth maneuvers [44]. The lead-lag motion, feathering motion, flapping motion and spanning motion patterns can be observed in the pectoral fin motion and these aide their smooth navigation through the water body [1]. The adaptive closed-loop feedback control is used when the system parameters are unknown or partially known. Since, in the case of the nonlinear BAUVs the hydrodynamic coefficients are poorly known, the identification schemes can be used to determine the system parameters. Flapping foils have been designed for propulsion and smoother maneuverability of BAUVs. The control forces and moments generated by the flapping foils have been measured using various computational methods [24, 30, 37]. A lot of research has been done to design control systems using traditional methods, whereas the area of pectoral fin control is still relatively new field of study. Speed, performance and maneuverability are the striking features of pectoral fin control that make it a perfect fit for the control of BAUVs. The design of a smart fin has been considered [50]. Inverse feedback linearization technique has been used for the design of an adaptive controller [15]. In recent papers [15, 45], the control of BAUV's in the dive and yaw planes was considered using pectoral fins, but the system parameters have been assumed to be known. The assumption of precise knowledge of system parameters is very restrictive.

Furthermore in these papers, it is assumed that state variables are available for feedback. In recent papers adaptive control laws have been designed for the trajectory control of the yaw angle [13, 14]. However, from the literature it appears that an in depth study into use of pectoral fins for control of BAUVs in the dive plane in the presence of parametric uncertainties has not been done yet.

In literature, methods of averaging and discretization of time-periodic systems have been proposed for the control of BAUVs. By averaging method, one obtains an approximate average time-invariant representation of the BAUV model for simplicity in control law design [39]. But the control system designed based on the time-invariant average model ignores the effect of time-varying fin forces on the vehicle motion. As such in the closed-loop system, the tracking error responses exhibit fluctuations caused by the harmonic components of the fin forces in the steady-state. Based on exact discrete-time models of BAUVs [17, 15] sampled-data control systems have been developed. For BAUV models with parametric uncertainties, discrete-time adaptive laws have been also designed [13, 14]. Of course, exact discretization is not possible for nonlinear models of BAUVs. Moreover, discrete-time controllers can give zero tracking error only at the sampling instants; and in the closed-loop system, large intersample excursions may exist. Besides these approaches, fuzzy and neural control of BAUVs have been considered [10, 11, 21]. Open-loop control of a BAUV equipped with six oscillating fins using a cluster of inferior olive neurons has been also attempted [4].

1.3 Scope of Thesis

This thesis considers the control of BAUVs using various closed-loop control design methods, being motivated by the natural ability of the aquatic animals to smoothly navigate through water bodies. The adaption of this fish motion mechanism for the control of BAUVs

in yaw and dive planes is considered. Though, the marine animals are characterized by a variety of their fin patterns, only the contribution of the pectoral fins to their smooth maneuvering is studied. The scope of this research work covers the design of an yaw plane adaptive controller for a continuous time-varying system by the method of averaging, design of dive and yaw plane robust nonlinear controller for a continuous system using internal model principle and modular dive plane sampled-data indirect adaptive control law design for the set point control of depth.

The mathematical model for the motion of an BAUV in the dive plane and yaw plane is given in chapter 2. Similar to the pectoral fin flapping mechanism found in the fishes, the BAUV is designed with a pair of pectoral attached symmetrically to either sides of the vehicle. The fins produce a combined heaving and pitching motion in the dive plane. In the yaw plane, the fins are assumed to oscillate with a sway and yaw motion. The control forces and moments produced by the fins in both dive and yaw planes are nonlinear functions of the bias angle, which is taken as the control input. Also, the expression and formulation of the net fin forces and moments are shown in chapter 2.

In chapter 3, an adaptive controller is designed for the control of an BAUV in the yaw plane. The fins attached to the vehicle have an oscillatory swaying and yawing motion. The bias angle of the fin is taken as the control input. The oscillatory motion of the fins produce periodic forces. The method of averaging is used for designing the control law. Even though the derivation of the control law is performed for an averaged system, simulations are performed on the complete system with time-varying force and moment components included. The closed-loop responses show that precise set point control for the yaw angle can be achieved in spite of the approximations assumed in the control law derivation.

In chapter 4, a new approach for the control of nonlinear BAUVs equipped with oscil-

lating fins is presented. The method is based on the nonlinear servoregulation theory [7, 8]. Although, this design approach is applicable to multi-input nonlinear BAUV models, here for simplicity, control of a BAUV in the dive plane using a pair of mechanical pectoral fins is considered. The fins are assumed to oscillate harmonically, and have a combined pitch and heave motion. The pitch bias angle of the fin is treated as a control input. Oscillating fins produce time-periodic forces. An exosystem of third-order is introduced to model the periodic forces, and the time-varying nonlinear model of the BAUV is represented as an autonomous nonlinear system in an extended state space. For the depth control, based on the nonlinear servoregulation theory, an internal model of k -fold exosystem driven by the tracking error is constructed, where k is a positive integer chosen to give desirable tracking accuracy. The k -fold exosystem has ability to produce monomials of degree up to k of the state variables of the exosystem. Then the composite system including the linearized model of the BAUV and the internal model of the k -fold exosystem is stabilized to obtain a robust state feedback control law for the depth control. It is shown that the controller, including the internal model in the loop, suppresses harmonic fluctuations of degree up to k in the tracking error responses. This desirable closed-loop property is not possible using the method of averaging [39] or discretization [17, 15, 13]. Simulation results are presented which show that the servoregulator accomplishes set point control of the depth precisely in spite of large parameter uncertainties in fin forces. Chapter 5 considers the control of a BAUV in the yaw plane using a control design that is similar to the one used in chapter 4. The fins are assumed to be oscillating with a combined sway and yaw motion and produce unsteady periodic forces. The bias angle of the angular motion of the fin is treated as the control input and only the yaw angle is measured for output feedback. The problem of servoregulation is addressed with the design of an internal model of the k -fold exosystem. It is desired to accurately achieve the set point

control of the yaw angle. Simulation results presented show that in spite of the parametric uncertainties precise yaw angle trajectory control is accomplished with all other parameters bounded.

Finally, the design of an indirect adaptive closed-loop servoregulator for the dive plane control of a nonlinear BAUV using mechanical pectoral-like fins is considered in chapter 6. The pectoral fins oscillate with a pitch and heave motion. The pitch bias angle of the oscillating fins is taken as the control input. Accurate depth trajectory tracking is desired in the dive plane and also constant disturbance rejection is to be taken care off. Since the nonlinear BAUV hydrodynamic coefficients and fin forces are poorly known, an adaptive control technique is used for control system design. The modular control system consists of an identifier and a stabilizer. The parameter identifier is designed which estimates the unknown system parameters. For the convenient design of stabilizer a sampled-data control system is used. The depth is taken as the output variable and only output feedback is employed for the synthesis of the control design. The stabilizer is designed using the pole placement technique. The advantage of designing an indirect control law lies in its application to both minimum phase and non-minimum phase systems. This control method is very significant, as the system is found to be non-minimum phase for all choices of the pectoral fin location. It is shown that in spite of the uncertainties in the system parameters accurate depth control is achieved in the dive plane and also the remaining state variables remain bounded when the tracking error converges to zero.

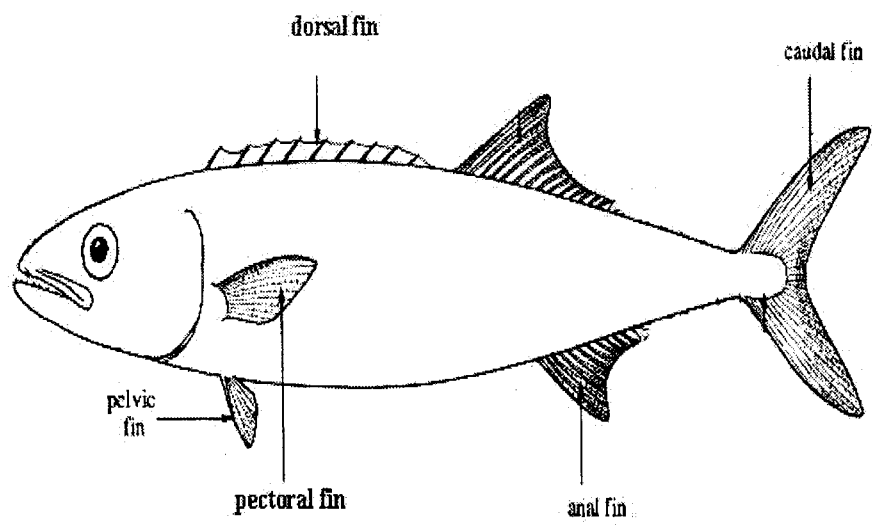


Figure 1.1: Fin patterns in a fish

CHAPTER 2

BAUV DYNAMICS

2.1 Mathematical Model of BAUV In Dive Plane

The model of a BAUV in dive plane is given in Figure. 2.1. On either sides of the vehicle two fins similar to the pectoral fins are attached. The vehicle moves in the dive plane ($X_I - Z_I$ plane), where $O_I X_I Z_I$ is an inertial coordinate system. $O_B X_B Z_B$ is body-fixed coordinate system with its origin at the center of buoyancy. X_B is in the forward direction, and Z_B points down. Each of the pectoral fins oscillates with with a combined heave and pitch motion. The motion of the fin is described by

$$h(t) = h_m \sin(\omega_f t) \quad (2.1)$$

$$\theta_d(t) = \beta + \theta_{dm} \sin(\omega_f t + \nu_1) \quad (2.2)$$

where h and θ are the heave and pitch angles of the fin, h_m and θ_m are the amplitudes of linear and angular oscillations, β is the pitch bias angle, ω_f (rad/sec) is the frequency of oscillations of fins, and ν_1 is the phase difference between the pitching and heaving motion.

We assume that vehicle's forward speed $u = U$ is held constant by some control mechanism.

The equations of motion of a neutrally buoyant vehicle are described by [6]

$$m(\dot{w}_d - uq - z_G \dot{q}^2 - x_G \dot{q}) = 0.5\rho l^4 z'_q \dot{q} + 0.5\rho l^3 (z'_w \dot{w} + z'_q qu) + 0.5\rho l^2 z'_w w_d u + f_{pd}$$

$$I_y \dot{q} + m z_G (\dot{u} + w_d q) - m x_G (\dot{w}_d - uq) = 0.5\rho l^5 M'_q \dot{q} + 0.5\rho l^4 (M'_w +$$

$$M'_q qu) + 0.5\rho l^3 M'_w w_d u - x_{GB} W \cos\theta - z_{GB} W \sin\theta + m_{pd}$$

$$\dot{z}_d = -u\sin(\theta) + w\cos(\theta) \quad (2.3)$$

where θ is the pitch angle; $q = \dot{\theta}$, $x_{GB} = x_G - x_B$, m is the mass of the vehicle, $z_{GB} = z_G - z_B$, $l =$ body length. $\rho =$ density; and z_d is the depth. f_{pd} and m_{pd} are the net force and moment acting on the vehicle due to the pectoral fins. The primed variables are the nondimensionalized hydrodynamic coefficients. Here $((x_B, z_B) = 0)$ and (x_G, z_G) denote the coordinates of the center of buoyancy and center of gravity (cg), respectively. For control law design, a linearized BAUV system is used. But, for simulation purposes the nonlinear BAUV model is considered. Linearizing the equations of motion (Eqn 2.3) about $w_d = 0$, $q = 0$, $z_d = 0$, and $\theta = 0$, we obtain

$$\begin{bmatrix} m - z_{\dot{w}} & -mx_G - z_{\dot{q}} & 0 \\ -mx_G - M_{\dot{w}} & I_y - M_{\dot{q}} & 0 \\ 0 & 0 & 1 \end{bmatrix} \begin{bmatrix} \dot{w}_d \\ \dot{q} \\ \dot{z}_d \end{bmatrix} = \begin{bmatrix} z_w U & z_q + mU & 0 \\ M_w U & M_q - mx_G U & 0 \\ 1 & 0 & 0 \end{bmatrix} \begin{bmatrix} w_d \\ q \\ z_d \end{bmatrix} + \begin{bmatrix} 0 \\ -z_{GB} W \\ -U \end{bmatrix} \theta + \begin{bmatrix} f_{pd} \\ m_{pd} \\ 0 \end{bmatrix}$$

where, $(x_{GB} = 0)$, $(z_{\dot{w}}, M_{\dot{q}}$, etc.) are obtained from the hydrodynamic coefficients.

Simplying the above linearized equations, we can the express the BAUV system model in a state-space representation by

$$\dot{x}_d = A_d x_d + B_d \begin{bmatrix} f_{pd} \\ m_{pd} \end{bmatrix}$$

$$y_d = \begin{bmatrix} 0 & 0 & 1 & 0 \end{bmatrix} x_d$$

where, the state vector x_d is defined as $x_d = (w_d, q, z_d, \theta)^T \in R^4$. The constant matrices, $A_d \in R^{4 \times 4}$ and $B_d \in R^{4 \times 2}$. The output variable is given as y_d (depth).

2.2 Fin Force And Moment In Dive Plane

The computation of periodic force and moment coefficients are based on the CFD analysis. The control force and moment for a single pectoral fin in the dive plane is given by f_d and m_d . The control force and moment coefficients generated by the oscillating fin in the dive plane can be described by the Fourier series given by [15]

$$\begin{aligned} f_d(t) &= \sum_{n=0}^M [f_n^s(\beta) \sin(n\omega_f t) + f_n^c(\beta) \cos(n\omega_f t)] \\ m_d(t) &= \sum_{n=0}^M [m_n^s(\beta) \sin(n\omega_f t) + f_n^c(\beta) \cos(n\omega_f t)] \end{aligned} \quad (2.4)$$

where $f_n^a(\beta)$ and $m_n^a(\beta)$, $a \in \{s, c\}$ are the Fourier coefficients, and M is an integer. The control design does not depend on the value of M . The Fourier coefficients are nonlinear functions of the pitch bias angle. The control force and moment for a single pectoral fin is given by f_d and m_d . For smaller bias angles, f_d and m_d can be approximated as

$$\begin{aligned} f_n^a(\beta) &= f_n^a(0) + \left(\frac{\partial f_n^a(0)}{\partial \beta} \right) \beta \\ m_n^a(\beta) &= m_n^a(0) + \left(\frac{\partial m_n^a(0)}{\partial \beta} \right) \beta \end{aligned} \quad (2.5)$$

Here a time-varying vector $\phi(t)$ is defined. It is comprised of sinusoidal functions

$$\begin{aligned} \phi(t) &= [1, \sin(\omega_0 t), \cos(\omega_0 t), \dots, \sin(M\omega_0 t), \\ &\quad \cos(M\omega_0 t)]^T \in R^{2M+1} \end{aligned} \quad (2.6)$$

The control force and moment produced by each fin can be written by using Eqns 2.4 - 2.6 as

$$f_d(t) = \phi^T (f_a + \beta f_b)$$

$$m_d(t) = \phi^T(m_a + \beta m_b) \quad (2.7)$$

where $f_a, f_b, m_a, m_b \in R^{2M+1}$. For our control design we have used $M=4$. The superscript T denotes the matrix transposition. The net normal force due to both the fins is given by $f_{pd} = -2f_d$ and $m_{pd} = 2(d_{cgd} \cdot f_d + m_d)$, respectively, where d_{cgd} is the distance of the fin from the nose of the vehicle.

2.3 Mathematical Model of BAUV In Yaw Plane

Figure. 2.2 shows the schematic of a typical BAUV in yaw plane. Two fins resembling the pectoral fins of fish are symmetrically attached to the vehicle. The vehicle moves in the yaw plane ($X_I - Y_I$ plane), where $O_I X_I Y_I$ is an inertial coordinate system. $O_B X_B Y_B$ is body-fixed coordinate system with its origin at the center of buoyancy. X_B is in the forward direction. Each fin has two degrees of freedom (sway and yaw) and oscillates harmonically. We assume that the combined sway-yaw motion of the fin is described as follows:

$$\delta(t) = \delta_m \sin(2\pi ft)$$

$$\theta_y(t) = \beta + \theta_{ym} \sin(2\pi ft + \nu) \quad (2.8)$$

where δ and θ_y correspond to sway and yaw angle of the fin, δ_m and θ_{ym} are the amplitudes of linear and angular oscillations, β is the bias angle, f (Hz) is the frequency of oscillations, and ν is the phase difference between the sway and yaw motion.

We assume that vehicle's forward speed $u = U$ is held constant by some control mechanism. The equations of motion of a neutrally buoyant vehicle is described by [35]

$$\begin{aligned} m(\dot{v} + Ur + X_G \dot{r} - Y_G r^2) &= Y_r \dot{r} + (Y_v \dot{v} + Y_r Ur) + Y_v Uv + f_{py} \\ I_z \dot{r} + m(X_G \dot{v} + X_G Ur + Y_G vr) &= N_r \dot{r} + (N_v \dot{v} + N_r Ur) + N_v Uv + m_{py} \\ \dot{\psi} &= r \end{aligned} \quad (2.9)$$

where ψ is the heading angle, $r = \dot{\psi}$ is the yaw rate, v is the lateral velocity along the Y_B -axis, $(X_G, Y_G) = (X_G, 0)$ is the coordinate of the center of gravity with respect to O_B , m is the mass, and I_z is the moment of inertia of the vehicle. $Y_{\dot{v}}, N_{\dot{r}}, Y_{\dot{\psi}}$, etc are the hydrodynamic coefficients, and f_{py} and m_{py} are the net fin force and moment. The global position coordinates X and Y of the vehicle are described by the kinematic equations

$$\begin{aligned}\dot{X} &= U\cos(\psi) - v\sin(\psi) \\ \dot{Y} &= U\sin(\psi) + v\cos(\psi)\end{aligned}\tag{2.10}$$

As in section 2.1, we linearize the equations of motion (Eqn 2.9) of the BAUV in yaw plane to get

$$\begin{aligned}\begin{bmatrix} m - Y_{\dot{v}} & mX_G - Y_{\dot{r}} & 0 \\ mX_G - N_{\dot{v}} & I_z - N_{\dot{r}} & 0 \\ 0 & 0 & 1 \end{bmatrix} \begin{bmatrix} \dot{v} \\ \dot{r} \\ \dot{\psi} \end{bmatrix} &= \\ \begin{bmatrix} Y_v U & Y_r U - mU & 0 \\ N_v U & N_r U - mX_G U & 0 \\ 0 & 1 & 0 \end{bmatrix} \begin{bmatrix} v \\ r \\ \psi \end{bmatrix} &+ \\ &+ \begin{bmatrix} f_{py} \\ m_{py} \\ 0 \end{bmatrix}\end{aligned}$$

where, the state vector $x_y = (v, r, \psi)^T \in R^3$. From the above linearized equations of motion, the state variable form can be expressed as

$$\begin{aligned}\dot{x}_y &= A_y x_y + B_y \begin{bmatrix} f_{py} \\ m_{py} \end{bmatrix} \\ y_v &= \begin{bmatrix} 0 & 0 & 1 \end{bmatrix} x_y\end{aligned}$$

where $A_y \in R^{3 \times 3}$ and $B_y \in R^{3 \times 2}$ are constant matrices. The output variable is y_v (yaw angle).

2.4 Fin Force And Moment In Yaw Plane

The periodic force and moment calculation are similar to section 2.2. The lateral force is shown by f_p and yawing moment is shown by m_p . The control force and moment coefficients generated by the oscillating fins in yaw plane is computed using Eqns. 2.4-2.7.

$$f_p(t) = \phi^T(f_a + \beta f_b)$$

$$m_p(t) = \phi^T(m_a + \beta m_b) \quad (2.11)$$

where f_a , f_b , m_a , m_b , ϕ , β are defined in section 2.2. The net lateral force due to two fins is given by $f_{py} = -2f_p$ and $m_{py} = 2(d_{cgy} \cdot f_p + m_p)$, respectively, where d_{cgy} is the moment arm due to fin location.

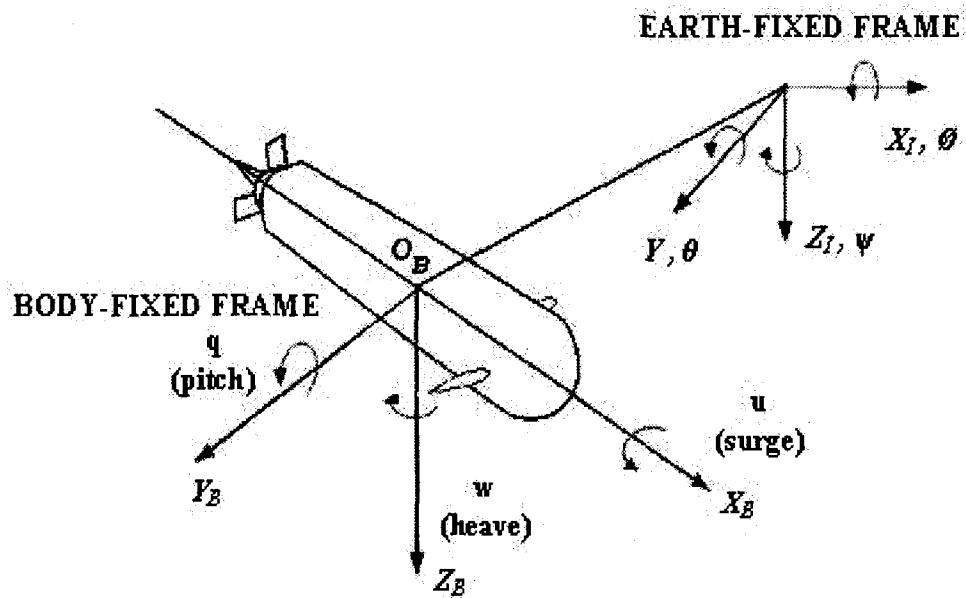


Figure 2.1: Model of BAUV in dive plane

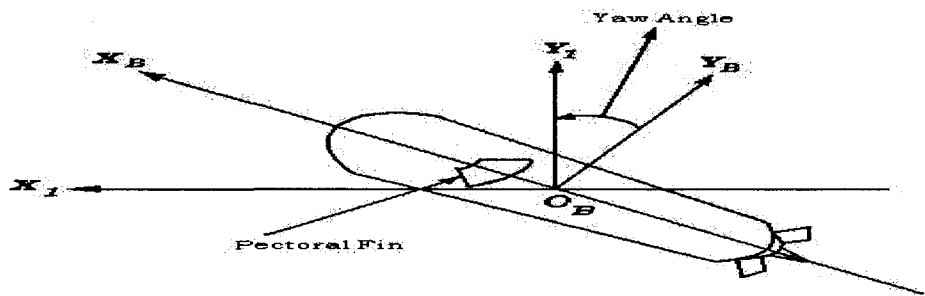


Figure 2.2: Model of BAUV in yaw plane

CHAPTER 3

ADAPTIVE YAW PLANE CONTROL OF BAUV USING PECTORAL-LIKE FINS

In this chapter, an adaptive servoregulator is designed for the yaw plane control of an BAUV using pectoral-like fins. This controller design can be applied to the control of BAUVs both in yaw plane and dive plane. The yaw plane control is considered here. A pair of pectoral fins is attached symmetrically to either sides of the BAUV and are assumed to be oscillating with swaying and yawing motion. The motion of the fins generate unsteady periodic forces. The bias angle of the angular motion of the fin is taken as the only control input. The yaw angle is the controlled output variable. The force and moment coefficients of the fin are computed by Fourier decomposition methods. For the heading angle control of the BAUV, an adaptive servoregulator is designed. The yaw angle and its derivative are used for feedback. The physical parameters of the system and also the hydrodynamic coefficients are not known. This adaptive design control law design does not require the full knowledge of the system parameters. In steady-state, the set point control of the yaw angle is precisely achieved. Simulation results show that the other simulation parameters also show bounded oscillations.

3.1 Problem Definition

The yaw plane control of an BAUV could be achieved by various methods. In this case, the design of an adaptive controller is considered for the BAUV control in the yaw plane. The physical model of an BAUV in the yaw plane is given in Figure. 2.2. The equations of

motion of the BAUV have been given in section 2.3. For the convenience of the readers they are described again [35].

$$\begin{aligned}
m(\dot{v} + Ur + X_G\dot{r} - Y_G r^2) &= Y_r\dot{r} + (Y_v\dot{v} + Y_rUr) + Y_vUv + f_{py} \\
I_z\dot{r} + m(X_G\dot{v} + X_GUr + Y_Gvr) &= N_r\dot{r} + (N_v\dot{v} + N_rUr) + N_vUv + m_{py} \\
\dot{\psi} &= r
\end{aligned} \tag{3.1}$$

where ψ is the yaw angle, $r = \dot{\psi}$ is the yaw rate, v is the lateral velocity along the Y_B -axis, $(X_G, Y_G) = (X_G, 0)$ is the coordinate of the center of gravity with respect to O_B , m is the mass, and I_z is the moment of inertia of the vehicle. The forward velocity $u = U$ is held constant by some control mechanism. Y_v, N_r, Y_v , etc are the hydrodynamic coefficients, and f_{py} and m_{py} are the net fin force and moment. The global position coordinates X and Y of the vehicle are described by the kinematic equations

$$\begin{aligned}
\dot{X} &= U\cos(\psi) - v\sin(\psi) \\
\dot{Y} &= U\sin(\psi) + v\cos(\psi)
\end{aligned} \tag{3.2}$$

The fin force and control moment calculations are shown in detail in section 2.4. In the next section, the adaptive control law is designed.

3.2 Adaptive Control Law

In this section, the design of an adaptive controller is considered. This thesis work focuses on multiple control law design techniques for the control of BAUVs in yaw and dive planes. To analyze the performance of different controllers designed, an uniform reference signal is given throughout. For the yaw plane control, a constant reference signal is given by $\psi_r = \psi^*$ and $e = \psi - \psi_r$ is the tracking error. Defining the state vector $x = (x_1, x_2, x_3)^T = (v, r, \psi)^T \in$

R^3 , solving Eqn 3.1 and substituting f_{py} and m_{py} using Eqn 2.4, gives the state variable representation of the linearized model of the BAUV by

$$\begin{aligned}\dot{x} &= Ax + B \begin{pmatrix} f_{py} \\ m_{py} \end{pmatrix} + D \\ y &= [0, 0, 1]x = Cx \\ e &= x_3 - \psi_r\end{aligned}\tag{3.3}$$

where A, B are constant matrices and D is the nonlinear disturbance matrix.

The output variable is expressed as

$$y = \dot{\psi} + \lambda\psi \triangleq Cx\tag{3.4}$$

where $\lambda > 0$ is a design parameter. Using Eqns 3.3 and 3.4, we can write

$$\hat{y}(s) = C(sI - A)^{-1}B\hat{u}(s) + C(sI - A)^{-1}D\hat{v}(s)\tag{3.5}$$

$$\triangleq \frac{n_c(s)\hat{u}(s) + n_d(s)\hat{v}(s)}{d_c(s)}\tag{3.6}$$

In Laplace form, s is taken as a Laplace variable. Then, $\hat{u}(s)$ is the control input and $\hat{v}(s)$ is the unknown disturbance vector, and

$$n_c(s) = Cadj(sI - A)B$$

$$n_d(s) = Cadj(sI - A)F$$

$$d_c(s) = det(sI - A)$$

where, $n_c(s)$ was computed and found to be a Hurwitz polynomial. Therefore, $n_c(s)/d_c(s)$ is minimum phase.

We consider a reference trajectory $y_m = \lambda\psi^*$ and the tracking error is given by $e_1 = y - y_m$.

From Eqn 3.4 it can be seen that, as e_1 tends to zero ψ converges to ψ^* . The tracking error can be written as

$$e_1 = \frac{n_c(s)}{d_c(s)}\hat{u}(s) + \frac{n_d(s)}{d_c(s)}\hat{v}(s) - \hat{y}_m(s) \quad (3.7)$$

It is our objective to remove the unknown disturbance vector v . For this purpose, we filter both sides of Eqn 3.7 by $(s/s + \mu)$, where μ is the design parameter ($\mu > 0$)[43]. Since y_m is a constant signal, $sy_m = 0$. Therefore, from Eqn 3.7

$$\left(\frac{s}{s + \mu}\right) e_1 = \frac{n_c(s)}{d_c(s)} \left(\frac{s}{s + \mu}\right) \left[\hat{u}(s) + \frac{n_d(s)}{n_c(s)}\hat{v}(s) \right]$$

The exponentially decaying signals in Eqn 3.8 have been neglected.

The modified input and disturbance signals can be written as

$$\begin{aligned} \hat{u}_f(s) &= \left(\frac{s}{s + \mu}\right) \hat{u}(s) \\ \hat{\omega}_f(s) &= \left(\frac{s}{s + \mu}\right) \frac{n_d(s)}{n_c(s)} \hat{v}(s) \end{aligned} \quad (3.8)$$

where $\omega_f(t)$ is a bounded function because $n_c(s)$ is a Hurwitz polynomial. Further, Eqn 3.8 can be rearranged as

$$e_1 = \frac{(s + \mu)n_c(s)}{sd_c(s)} [\hat{u}_f(s) + \hat{\omega}_f(s)] = H(s) [\hat{u}_f(s) + \hat{\omega}_f(s)] \quad (3.9)$$

A control law $u_f(t)$ has to be designed, so that, the tracking error $e_1(t)$ asymptotically tends to zero.

We already saw that $n_c(s)$ is Hurwitz and $\mu > 0$, hence for the given BAUV model $H(s)$ is minimum phase and has relative degree one. From the root-locus technique, we infer that a negative feedback law of the form

$$u_f(t) = -K_e e_1 \quad (3.10)$$

can stabilize the system Eqn 3.9, where $K_e > 0$.

A minimal realization of $H(s)$ is given by

$$\begin{aligned}\dot{x}_a &= A_a x_a + B_a [u_f + \omega_f] \\ e_1 &= C_a x_a\end{aligned}\tag{3.11}$$

where A_a , B_a , and C_a are the constant matrices. Since $H(s)$ is minimum phase with relative degree one, it follows that there exists a unknown gain $K^* > 0$ such that [48, 49]

$$\begin{aligned}P(A - K^* B_a C_a) + (A - K^* B_a C_a)^T P &= -Q < 0 \\ P B_a &= C_a^T\end{aligned}\tag{3.12}$$

where P and Q are positive definite symmetric matrices. Let \hat{K} be an estimate of K^* and consider an output feedback control law

$$u_f = -\hat{K} e_1\tag{3.13}$$

One of the advantages of designing an adaptive controller is that, tuning of a single adaptive gain is sufficient for the stabilizing the closed-loop system. Now, we adaptively tune \hat{K} . Using Eqn 3.13 in Eqn 3.11 gives

$$\dot{x}_a = (A_a - K^* B_a C_a) x_a + (K^* B_a C_a x_a - \hat{K} B_a e_1) + B_a \omega_f\tag{3.14}$$

The parameter error is defined as, $\tilde{K} = K^* - \hat{K}$, Eqn 3.14 gives

$$\dot{x}_a = \bar{A} x_a + \tilde{K} B_a e_1 + B_a \omega_f\tag{3.15}$$

where eigenvalues of $\bar{A} = (A_a - K^* B_a C_a)$ are found to be in the left half of the s plane.

For stability analysis, we consider a positive definite quadratic Lyapunov function

$$W = x_a^T P x_a + \gamma \tilde{K}^2\tag{3.16}$$

where $\gamma > 0$. From Eqn 3.15, the derivative of W is given by

$$\dot{W} = x_a^T(P\bar{A} + \bar{A}^T P)x_a + 2x_a^T P\tilde{K}B_a e_1 + 2\gamma\tilde{K}\dot{\tilde{K}} + 2x_a^T P B_a \omega_f \quad (3.17)$$

Using Eqn 3.12 in Eqn 3.17 and noting that $x_a^T P B_a = x_a^T C_a^T = e_1$ gives

$$\dot{W} = -x_a^T Q x_a + 2\tilde{K}(\gamma\dot{\tilde{K}} + e_1^2) + 2e_1\omega_f \quad (3.18)$$

It is desired to eliminate \tilde{K} from Eqn 3.18, for this purpose the adaptation law is taken as

$$\dot{\tilde{K}} = -\dot{\tilde{K}} = -\gamma^{-1}e_1^2 \quad (3.19)$$

Substituting Eqn 3.19 in Eqn 3.18 and using Young's inequality gives

$$\dot{W} = -x_a^T Q x_a + 2e_1\omega_f = -\lambda_{\min}(Q)\|x_a\|^2 + \epsilon\|x\|^2 + \frac{\|C_a\|^2}{\epsilon}|\omega_f| \leq 0 \quad (3.20)$$

According to Eqn 3.8, $\omega_f(t) \rightarrow 0$, as $t \rightarrow \infty$, because v is a constant signal. Thus asymptotically Eqn 3.2 becomes

$$\dot{W} \leq -[\lambda_{\min}(Q) + \epsilon]\|x_a\|^2 \quad (3.21)$$

For a choice of $\epsilon < \lambda_{\min}(Q)$; from Eqn 3.2, we can see that $W(x_a, \tilde{K})$ is positive definite and $\dot{W} \leq 0$, x_a and \tilde{K} are bounded. We can show that x_a [43] (from Barbalat's lemma) tends to zero, which implies that $e_1 = C_a x_a$ converges to zero and ψ tends to ψ^* .

Using Eqn 3.8, the control input $u(t)$ can be obtained. From Eqn 3.8 we have

$$\hat{u} = \left(\frac{s + \mu}{s} \right) \hat{u}_f \quad (3.22)$$

which yields

$$u(t) = u_f(t) + \mu \int_0^1 u_f(\tau) d\tau \quad (3.23)$$

Using $u_f(t) = -\hat{K}(t)e_1(t)$ in Eqn 3.22 gives

$$u(t) = -\hat{K}(t)e_1(t) - \mu \int_0^1 \hat{K}(\tau)e_1(\tau) d\tau \quad (3.24)$$

3.3 Simulation Results

In this section, simulation results for control of BAUV using an adaptive servoregulator is presented. The parameters of the vehicle are unknown, but the adaptive controller design law does not require the full knowledge of the system. It is desired to achieve set point control of the yaw angle, with the bias angle of the fin as the control input. The parameters of the model are taken from [15]. The vehicle parameters are $l = 1.391$ m, mass=18.826 kg, $I_z = 1.77$ kgm², $X_G = -0.012$, $Y_G = 0$. The hydrodynamic parameters for a forward velocity of 0.7 m/sec are $Y_{\dot{r}} = -0.3781$, $Y_{\dot{v}} = -5.6198$, $Y_r = 1.1694$, $Y_v = -12.0868$, $N_{\dot{r}} = -0.3781$, $N_{\dot{v}} = -0.8967$, $N_r = -1.0186$, and $N_v = -4.9587$. The fins are set with an oscillation frequency of 8 Hz.

The computation of the chord length (c) and surface area of the foil requires the knowledge of the Strouhal number, $S_t = 0.6$, where $S_t = \frac{cf}{U_\infty}$, U_∞ is 0.8 m/sec, f is the frequency of the fin oscillation. The fin force and moment coefficients are calculated for this Strouhal number. The distance of the fin from the center of gravity cg is $d_{cgy} = 0.02$ m. For this choice of d_{cgy} , the BAUV model is found to be minimum phase.

From the CFD analysis, the parameter vectors f_a , f_b , m_a , and m_b used for simulations are

$$\begin{aligned} f_a &= (f_0^c(0), f_1^s(0), f_1^c(0), \dots, f_M^s(0), f_M^c(0))^T \\ f_b &= \left(\frac{\partial f_0^c}{\partial \beta}(0), \frac{\partial f_1^s}{\partial \beta}(0), \frac{\partial f_1^c}{\partial \beta}(0), \dots, \frac{\partial f_s^M}{\partial \beta}(0), \frac{\partial f_c^M}{\partial \beta}(0) \right)^T \\ m_a &= (m_0^c(0), m_1^s(0), m_1^c(0), \dots, m_M^s(0), m_M^c(0))^T \\ m_b &= \left(\frac{\partial m_0^c}{\partial \beta}(0), \frac{\partial m_1^s}{\partial \beta}(0), \frac{\partial m_1^c}{\partial \beta}(0), \dots, \frac{\partial m_s^M}{\partial \beta}(0), \frac{\partial m_c^M}{\partial \beta}(0) \right)^T \end{aligned}$$

where $f_a, f_b, m_a, m_b \in R^{2M+1}$. Only the four significant harmonics are considered ($M = 4$).

Then the values of f_a, f_b, m_a, m_b for $M=4$ are

$$f_a = (0, -40.0893, -43.6632, -0.3885, 0.6215, 6.2154, -10.1777, -0.1554, 0.6992)$$

$$f_b = (68.9975, 0.4451, -16.4704, 64.1009, -19.5864, -0.8903, -2.2257, 2.2257, 4.8966)$$

$$m_a = (0, 0.6037, 0.4895, 0, -0.0054, 0, -0.0925, 0, -0.0054)$$

$$m_b = (-0.4986, -0.3739, -0.0935, -0.2493, 0.1246, 0.0312, -0.0312, 0.0935, 0)$$

(Readers may refer to [15] for the details.) It is pointed out that these parameters are obtained using the Fourier decomposition of the fin force and moment, and are computed by multiplying the Fourier coefficients by $\frac{1}{2}\rho.W_a.U_\infty^2$ and $\frac{1}{2}\rho.W_a.c.U_\infty^2$, respectively, where W_a is the surface area of the foil. For simulation, the initial conditions of the vehicle are assumed to be $x(0) = 0$. The initial value of the gain \hat{K} is taken as 20. The design parameters λ and μ are taken as 0.01 and 40, respectively.

Simulations are carried out for a constant reference trajectory ψ_r converging to $\psi^*=25$ deg. We note that a fourth-order filter is used to generate the constant reference trajectory. A gradually rising exponential command is combined with a third-order filter and is given by

$$G_c(s) = \frac{\lambda_1 \omega_{nc}^2}{(s + \lambda_{c1})(s + \lambda_{c2})(s^2 + 2\zeta_c \omega_{nc} s + \omega_{nc}^2)}$$

is generated, where $\omega_{nc} = 4.95$, $\zeta_c = 0.707$, $\lambda_{c1} = 0.14$ and $\lambda_{c2} = 3.5$ are the real poles. The initial filter conditions are taken as zero.

Case I: Adaptive yaw plane BAUV control: Constant reference trajectory $\psi^* = 25$ deg, $\omega_f = 8$ Hz, nominal parameters

The pectoral fin oscillation frequency is set at 8 Hz. A smooth reference trajectory ψ_r converging to $\psi^* = 25$ deg is generated using a fourth-order filter, as seen above. Simulation results for the nominal values of the fin force and moment coefficients are shown in Figure 3.2. It is seen that the yaw angle converges to the desired values in little over 30 seconds. The control bias input required is around 20 deg. This can be easily provided by the pectoral fins.

The magnitude of the tracking error is 0.01 deg. The tracking error has time-zero bias due to the averaging of the fin force and control moment. The desired yaw angle output is found to oscillate with zero bias around the reference input ψ_r . Hence the tracking error does not converge to zero in steady-state. The control force and moment required are 45 N and around 0.4 Nm, respectively.

Case II: Adaptive yaw plane BAUV control: Constant reference trajectory
 $\psi^* = 25 \text{ deg}, \omega_f = 8 \text{ Hz}, -25 \% \text{ uncertainty}$

A smooth set point control of the yaw angle was achieved for the nominal values of the fin force and moment coefficients. Now the performance of the adaptive controller for perturbed values of the fin force and moment coefficients are examined. The values of f_a , f_b , m_a and m_b are perturbed by a factor of 0.75. The frequency of the fin oscillation is retained at 8 Hz. The simulation results are presented in Figure. 3.3. The performance of the controller in this case is almost similar to Figure. 3.2. The response time taken to achieve the target value is around 30 seconds. The magnitude of the tracking error is slightly lesser when compared to Figure. 3.2. The control input is around 20 deg.

Case III: Adaptive yaw plane BAUV control: Constant reference trajectory
 $\psi^* = 25 \text{ deg}, \omega_f = 8 \text{ Hz}, +25 \% \text{ uncertainty}$

In this case, an uncertainty factor of 1.25 is added to the fin force and moment. The simulation results are shown in Figure. 3.4. The performance of the controller has slightly deteriorated when compared to Figure. 3.2 and Figure. 3.3. Even though the response time taken for the BAUV to reach ψ_r is around 30 seconds, the control bias required is has increased to around 30 deg. It can be intuitively seen that for further perturbations to force coefficients, the control input required would increase.

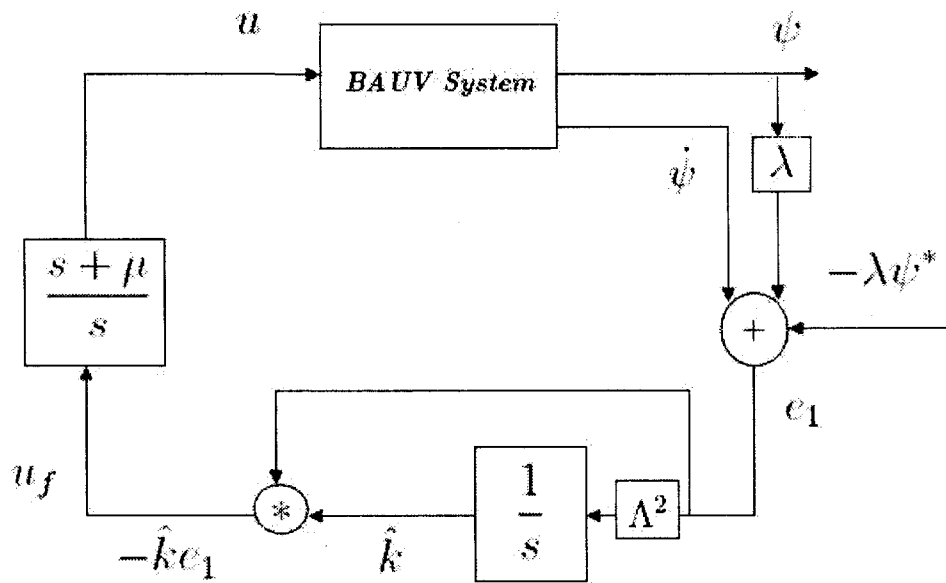


Figure 3.1: Closed-loop system

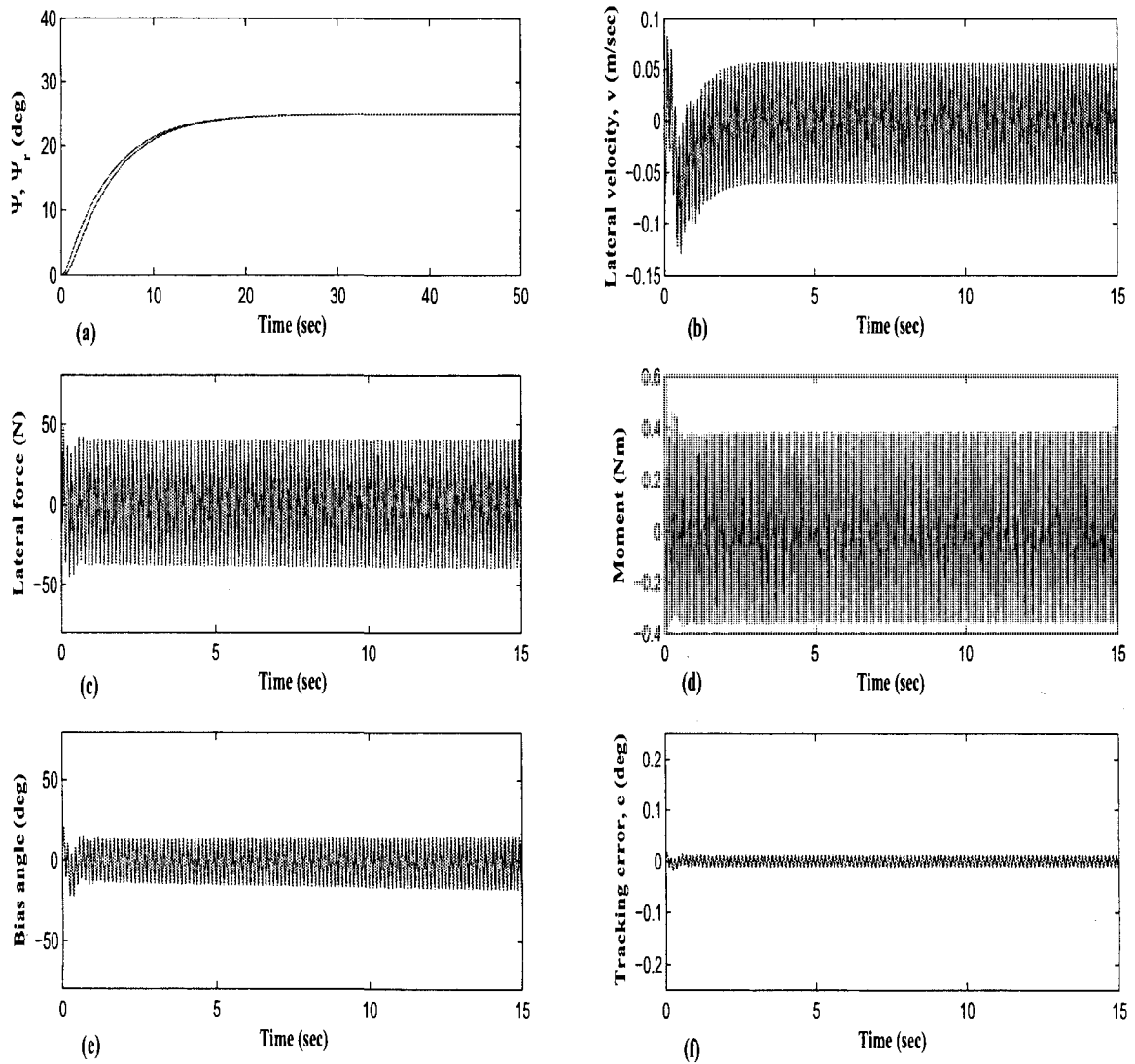


Figure 3.2: Adaptive yaw plane BAUV control: Constant reference trajectory $\psi^* = 25$ deg, $\omega_f = 8$ Hz, nominal parameters

(a) Yaw angle, Ψ , and reference yaw angle, Ψ_r (deg), (b) Lateral velocity, v (m/sec), (c) Lateral force (N), (d) Moment (Nm), (e) Bias angle (deg), (f) Tracking error, e (deg).

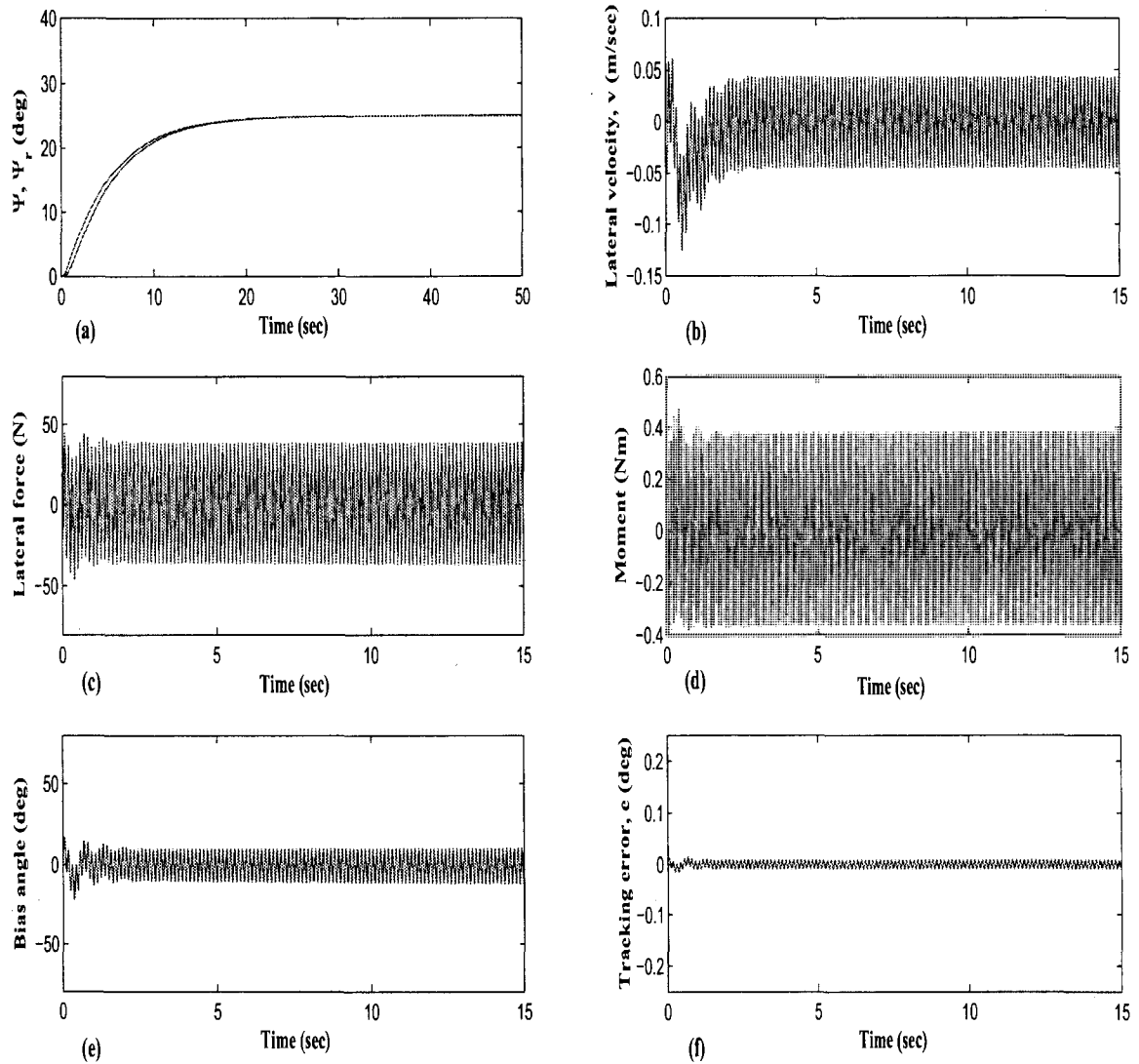


Figure 3.3: Adaptive yaw plane BAUV control: Constant reference trajectory $\psi^* = 25$ deg, $\omega_f = 8$ Hz, -25 % uncertainty

(a) Yaw angle, Ψ , and reference yaw angle, Ψ_r (deg), (b) Lateral velocity, v (m/sec), (c) Lateral force (N), (d) Moment (Nm), (e) Bias angle (deg), (f) Tracking error, e (deg).

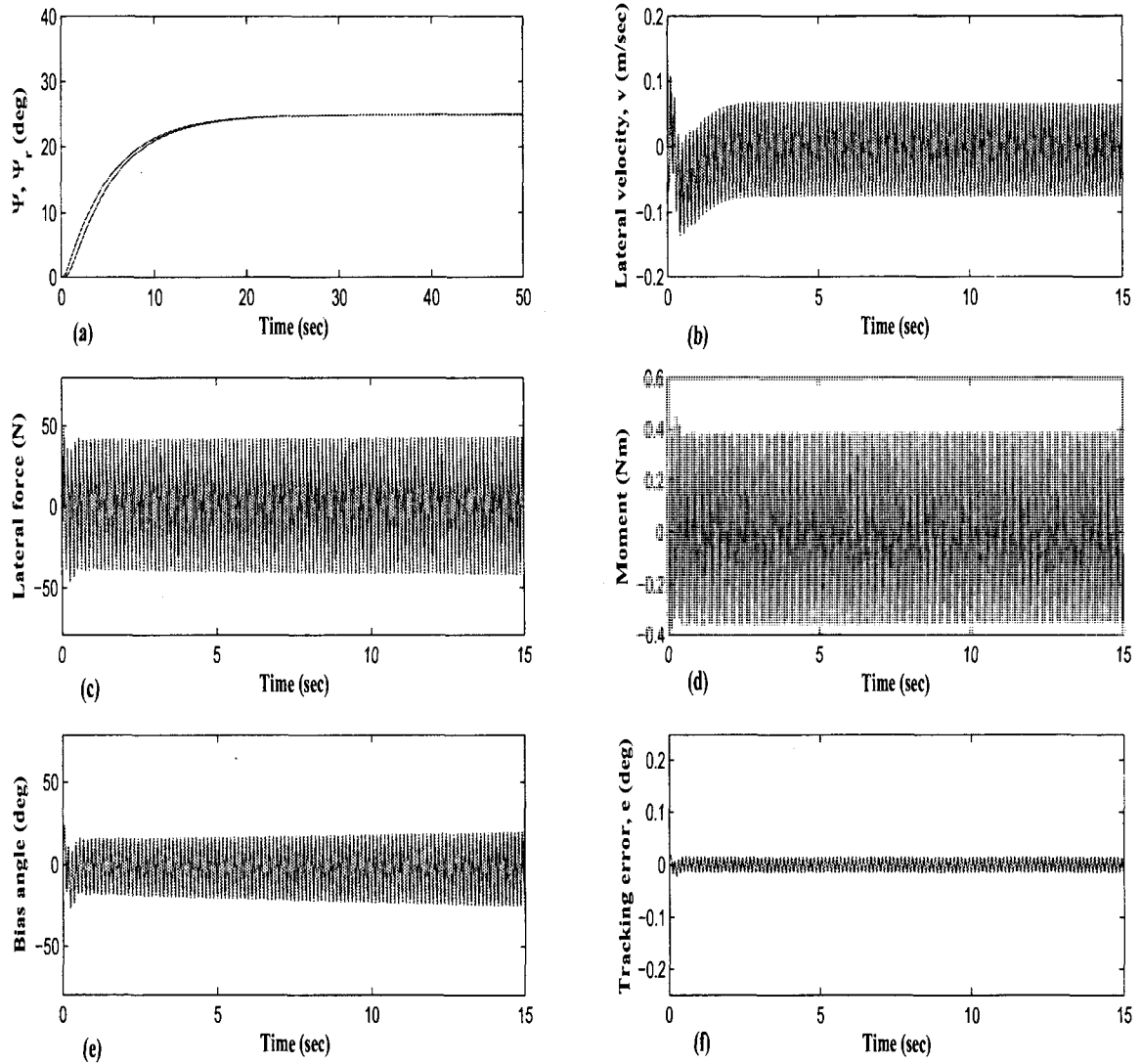


Figure 3.4: Adaptive yaw plane BAUV control: Constant reference trajectory $\psi^* = 25$ deg, $\omega_f = 8$ Hz, +25 % uncertainty
 (a) Yaw angle, Ψ , and reference yaw angle, Ψ_r (deg), (b) Lateral velocity, v (m/sec), (c) Lateral force (N), (d) Moment (Nm), (e) Bias angle (deg), (f) Tracking error, e (deg).

CHAPTER 4

NONLINEAR ROBUST DIVE PLANE CONTROL OF BAUV USING INTERNAL MODEL PRINCIPLE

This chapter presents the design of a robust servoregulator for the control of nonlinear BAUVs based on the nonlinear internal model principle. This design methodology is applicable to complete nonlinear multi-input BAUV models. In this chapter the control of motion in the dive plane is considered. The application of this design methodology for the yaw angle control is shown in chapter 5. The fins are assumed to be oscillating with a combined pitch and heave motion. The mean angle of pitch motion of the fin is used as a control variable. The oscillation of the fins generate unsteady periodic forces. The control law design requires an exosystem of third-order. The nonlinear BAUV model, with the fin forces included, is represented as a nonlinear autonomous system. Then, a nonlinear robust servoregulator is designed for the depth command tracking. The control law has two parts of design. First, an internal model of a k -fold exosystem is derived, where k is a positive integer left to the choice of the designer. Then, a stabilizer is designed for the stabilization of the closed loop system. It is seen that all the harmonic components of order up to k of the tracking error are suppressed. Simulation results are presented in the end of the chapter, which show that in spite of uncertainties in the parameters of the system, the depth is accurately controlled for a given reference command input.

4.1 Problem Definition

It is desired to design a robust servoregulator to achieve set point control of the depth in the dive plane. The physical model of an BAUV in dive plane is shown in Figure. 2.1. The equations of motion of the BAUV in the dive plane Eqn. 2.3 is given in chapter 2. For easy understanding, the mathematical model of an BAUV is again given here [6]

$$\begin{aligned}
 m(\dot{w}_d - uq - z_G \dot{q}^2 - x_G \dot{q}) &= 0.5\rho l^4 z'_q \dot{q} + 0.5\rho l^3 (z'_w \dot{w} + z'_q qu) + 0.5\rho l^2 z'_w w_d u + f_{pd} \\
 I_y \dot{q} + m z_G (\dot{u} + w_d q) - m x_G (\dot{w}_d - uq) &= 0.5\rho l^5 M'_q \dot{q} + 0.5\rho l^4 (M'_w + \\
 M'_q qu) + 0.5\rho l^3 M'_w w_d u - x_{GB} W \cos\theta - z_{GB} W \sin\theta + m_{pd} \\
 \dot{z}_d &= -u \sin(\theta) + w \cos(\theta)
 \end{aligned} \tag{4.1}$$

where θ is the pitch angle; $q = \dot{\theta}$, $x_{GB} = x_G - x_B$, $z_{GB} = z_G - z_B$, $l =$ body length. $\rho =$ density; and z_d is the depth. f_{pd} and m_{pd} are the net force and moment acting on the vehicle due to pectoral fins. The primed variables are the nondimensionalized hydrodynamic coefficients. Here $((x_B, z_B) = 0)$ and (x_G, z_G) denote the coordinates of the center of buoyancy and center of gravity (cg), respectively. The calculation of the fin forces and moment coefficients are given in chapter 2.

Let $z_r = z^*$ be a constant reference signal and $e = z_d - z_r$ be the tracking error. Defining the state vector $x = (x_1, x_2, x_3, x_4)^T = (w_d, q, z_d, \theta)^T \in R^4$, solving Eqn 2.3 and substituting for f_{pd} and m_{pd} from Eqn 2.4, gives the state variable representation of the BAUV of the form

$$\begin{aligned}
 \dot{x} &= Ax + B_v \begin{bmatrix} f_d \\ m_d \end{bmatrix} + n_l(x) \\
 y &= [0, 0, 1, 0]x \\
 e &= y - z_r
 \end{aligned} \tag{4.2}$$

where $n_l(x)$ denotes the vector due to the nonlinear functions of Eqn 2.3. In view of Eqn 2.4 the state equation Eqn 4.2 is a nonlinear time-varying system.

4.2 Third-Order Exosystem

We are interested in representing Eqn 4.2 as a time-invariant system. For this, we select an exosystem

$$\begin{aligned} \begin{pmatrix} \dot{v}_0 \\ \dot{v}_1 \\ \dot{v}_2 \end{pmatrix} &= \begin{pmatrix} 0 & 0 & 0 \\ 0 & 0 & -\omega_f \\ 0 & \omega_f & 0 \end{pmatrix} \begin{pmatrix} v_0 \\ v_1 \\ v_2 \end{pmatrix} \\ &= A_v v \end{aligned} \quad (4.3)$$

where $v = (v_0, v_1, v_2)^T \in R^3$. Define $v_p = (v_1, v_2)^T$. Using Eqn 4.3, one can generate any constant and sinusoidal signals $\sin(n\omega_f t)$ and $\cos(n\omega_f t)$ for any integer n . This can be verified easily. Let $v_0 = 1$, $v_1 = \cos \omega_f t$ and $v_2 = \sin \omega_f t$; then v_1, v_2 satisfy Eqn 4.3, and one can easily show that

$$\begin{aligned} \sin 2\omega_f t &= 2v_1 v_2 \\ \cos 2\omega_f t &= (v_1^2 - v_2^2) \\ \sin 3\omega_f t &= 2v_1^2 v_2 + (v_1^2 - v_2^2)v_2 \\ \cos 3\omega_f t &= (v_1^2 - v_2^2)v_1 - 2v_1 v_2^2 \end{aligned} \quad (4.4)$$

Continuing this process, one can easily show that $\sin(n\omega_f t)$ and $\cos(n\omega_f t)$ can be expressed as homogeneous polynomials, whose each term is monomial in variable v_1 and v_2 of degree n .

As such one can express the fin force and moment as functions of state vector v in the form

$$\begin{pmatrix} f_d(t, \beta) \\ m_d(t, \beta) \end{pmatrix} = \gamma_0(\beta) + \sum_{n=1}^M \gamma_n^s(\beta) \pi_n^s(v_p) + \gamma_n^c(\beta) \pi_n^c(v_p) \quad (4.5)$$

$$= g_f(v, \beta)$$

and $\pi_n^s(v_p) = \sin n\omega_f t$ and $\pi_n^c(v_p) = \cos n\omega_f t$ are homogeneous polynomials in variables v_1 and v_2 degree n , and

$$\begin{aligned}\gamma_0(\beta) &= \begin{pmatrix} f_0^c(\beta) \\ m_0^c(\beta) \end{pmatrix} \\ \gamma_n^s(\beta) &= \begin{pmatrix} f_n^s(\beta) \\ m_n^s(\beta) \end{pmatrix} \\ \gamma_n^c(\beta) &= \begin{pmatrix} f_n^c(\beta) \\ m_n^c(\beta) \end{pmatrix}\end{aligned}$$

Using Eqn 4.5 in Eqn 4.2 gives a time-invariant representation of Eqn 4.2 of the form

$$\dot{x} = A(w)x + g(v_p, \beta, w) + n_l(x, w) \triangleq g_x(x, v, w) \quad (4.6)$$

$$e = x_3 - z^* v_0$$

where $g(v, \beta, w) = B_v g_f(v, \beta)$ and $w = R^p$ denotes the vector consisting of all the unknown parameters of the BAUV model including fin forces. For example, w includes the uncertain parameters of the Fourier coefficients.

Expanding the nonlinear terms of Eqn 4.6 in Taylor series, one can represent Eqn 4.6 in the form

$$\dot{x} = A(w)x + B(w)u_c + E(w)v + n_{l2}(u_c, v, x, w) \quad (4.7)$$

$$e \triangleq H_1 x + H_2 v \triangleq h(x, v_0)$$

where $u_c = \beta$, $H_1 = (0, 0, 1, 0)$, $H_2 = (-z^*, 0, 0)$, n_{l2} denotes nonlinear vector functions of second and higher order terms in β , v_1 , v_2 and x , and

$$B(w) = \frac{\partial g}{\partial \beta}(0, 0, w)$$

$$E(w) = \left[g(0, 0, w), \frac{\partial g}{\partial v_p}(0, 0, w) \right]$$

Note that $E_1 v_0$ ($v_0 = 1$) is a constant vector and E_1 is the first column of E . For the choice of $v_0 = 1$, $v_1 = \cos \omega_f t$, $v_2 = \sin \omega_f t$, the system Eqn 4.2 and Eqn 4.7 are equivalent.

For the purpose of control law derivation, we embed the system Eqn 4.2 in a larger class of system Eqn 4.7 in which we allow $v \in V$, an open set in R^3 . Of course, unknown coefficients of two sinusoids $\sin(\omega_f t)$ and $\cos(\omega_f t)$ can be merged with v_p and remaining unknown parameters are elements of w . We have set the goal for approximate tracking for practical reasons. It will be seen that the design of control law such that e tends to zero is a difficult problem due to time-varying periodic fin forces. The class of control laws of interest is of the form $u_c = k_c(x, x_s)$, where $x_s \in R^{n_c}$ is state vector of a dynamic system

$$\dot{x}_s = g_s(x_s, e) \quad (4.8)$$

for an appropriate choice of vector functions $g_s(x_s, e)$. We observe that the tracking error is an input signal to the dynamical system Eqn 4.8

Define $x_c = (x^T, x_s^T) \in R^{4+n_c}$. Then the closed-loop system can be written as

$$\dot{x}_c = \begin{bmatrix} A(w)x + Bk_c(x, x_s) + E(w)v + n_{l2}(k_c(x, x_s), v, x, w) \\ g_s(x_s, h(x, v_0)) \end{bmatrix} \quad (4.9)$$

$$\triangleq g_c(x_c, v, w)$$

Let the nominal value of the unknown parameter vector w be w^* and $\tilde{w} = w - w^*$ be the perturbation from the nominal value. We assume that $\tilde{w} \in W$, an open set surrounding $\tilde{w} = 0$.

We introduce the following definition to be used later.

Definition: Let V be an open neighborhood of the origin R^3 . A sufficiently smooth function $o^k : V \rightarrow R$ is said to be zero up to the k^{th} order if $o^k(0) = 0$, and its all partial derivatives of order less than or equal to k vanish at $v = 0$.

We are interested in the design of a k^{th} -order nonlinear robust control system (termed k^{th} -order servoregulator) such that the closed-loop system Eqn 4.9 has the following properties.

Property 1: All the eigenvalues of the matrix $\frac{\partial g_c}{\partial x_c}(0, 0, w^*)$ have negative real parts.

Property 2: For all sufficiently small $x_c(0)$, $v(0)$, and \tilde{w} , the trajectory $(x_c(t), v(t))$ of the composite system Eqn 4.9 and Eqn 4.3 satisfies

$$\lim_{t \rightarrow \infty} (e(t) - o^k(v(t))) = \lim_{t \rightarrow \infty} (h(x(t), v(t)) - o^k(v(t))) = 0 \quad (4.10)$$

where k is the chosen positive integer.

The Property 2 implies that steady-state tracking error of the closed-loop system is zero up to k^{th} order. By choosing k large enough, designer can accomplish desired tracking error accuracy in the steady-state.

4.3 Control Law

In this section, the question of existence of a solution of the posed k^{th} -order output regulation is considered. Based on [7,8], the following result is stated.

Theorem 1: Suppose that in the closed-loop system Eqn 4.9, Property 1 holds. Then the closed-loop system also satisfies Property 2 if and only if there exists sufficiently smooth functions $X_c(v, w) = [X^T(v, w), X_s^T(v, w)]^T$ with $X_c(0, w^*) = 0$ which satisfies for $v \in V$ and $\tilde{w} \in \tilde{W}$

$$\begin{aligned} \frac{\partial X_c(v, w)}{\partial v} A_v v &= g_c(X_c(v, w), v, w) \\ \mathbf{e}(v, w) &= \mathbf{h}(X(v, w), v) = o^k(v) \end{aligned} \quad (4.11)$$

It is possible to synthesize a control law to solve the problem of the k^{th} order regulation using the solution of Eqn 4.11. However, it is not easy to solve the partial differential equation Eqn 4.11, and moreover, the solution depends on the unknown parameter w .

4.4 Internal Model

In this section, we now seek a solution for the regulation problem based on the nonlinear internal model principle [8]. This approach avoids the computation of $X_c(v, w)$. To motivate the construction of an internal model, we look into an approximate solution of Eqn 4.11. One can attempt to obtain a solution of Eqn 4.11 by selecting $X_c(v, w) = (X^T(v, w), X_s^T(v, w))^T$ and $U_c(v, w) = k_c(X(v, w), X_s(v, w))$ as polynomial functions of variables v_0, v_1 and v_2 given by

$$\begin{aligned} X(v, w) &= \sum_{l=1}^k X_{lw} v^{[l]} + o^k(v) \\ X_s(v, w) &= \sum_{l=1}^k X_{slw} v^{[l]} + o^k(v) \\ U_c(v, w) &= \sum_{l=1}^k U_{clw} v^{[l]} + o^k(v) \end{aligned} \quad (4.12)$$

where $v^{[1]} = [v_0, v_1, v_2]^T$ and $v^{[l]} = v_p^{[l]} = [v_1^l, v_1^{l-1}v_2, v_1^{l-2}v_2^2, \dots, v_2^l]^T$, for $l = 2, 3, \dots$, and

$$e(v, w) = \mathbf{h}(X(v, w), v) = \sum_{l=1}^k Y_{lw} v^{[l]} + o^k(v) \quad (4.13)$$

Here X_{lw}, X_{slw}, U_{clw} and Y_{lw} are constant matrices of appropriate dimensions depending, perhaps, on w . Each component of the vector polynomial $v_p^{[l]}$ is monomial in variables v_1 and v_2 of degree l . Essentially the elements of $v_p^{[l]}$ form a basis for homogeneous polynomials of degree l in variables v_1 and v_2 . In view of Eqn 4.12, to satisfy Eqn 4.10 it is essential to design a control law which can cancel all the terms of $v^{[l]}$, $l = 1, \dots, k$, occurring in $e(v, w) = \mathbf{h}(X(v, w), v)$ in steady state. This requires construction of a dynamic system (termed internal model of k -fold exosystem) which can produce signals $v^{[l]}$, $l = 1, \dots, k$. The k -fold exosystem can be constructed as follows. First of all $v^{[1]} = (v_0, v_1, v_2)^T$ and $v_p^{[l]}$ satisfy

$$\begin{aligned} \dot{v}^{[1]} &= A_v v^{[1]} \triangleq A^{[1]} v^{[1]} \\ \dot{v}_p^{[l]} &= A_p^{[l]} v_p^{[l]}, l = 2, 3, \dots, k \end{aligned} \quad (4.14)$$

where

$$A_p = \begin{bmatrix} 0 & -\omega_f \\ \omega_f & 0 \end{bmatrix}$$

and $A_p^{[j]}$ are appropriate matrices. (The expressions for $A_p^{[l]}$ and their characteristic polynomials, for $l = 1, \dots, 4$, are collected in the appendix II.A)

Define a state vector

$$v_{kf} = \begin{bmatrix} v^{[1]} \\ \cdot \\ \cdot \\ v_p^{[k]} \end{bmatrix} \quad (4.15)$$

The vector v_{kf} satisfies the differential equation

$$\dot{v}_{kf} = \text{diag}[A^{[1]}, A_p^{[2]}, \dots, A_p^{[k]}]v_{kf} \quad (4.16)$$

$$\triangleq A_{kf}v_{kf}$$

where $A_{kf} = \text{diag}(A^{[1]}, A_p^{[2]}, \dots, A_p^{[k]})$. The system Eqn 4.16 is the k -fold exosystem which generates not only the exogenous signal v , but also the higher order terms of the exogenous signal v_p up to order k . According to the internal model principle, for k^{th} -order robust regulator design [8], one introduces an internal model of k -fold exosystem Eqn 4.16.

The roots of the minimum polynomial of A_{kf} are precisely given by all the distinct members of the following set:

$$\Lambda_k = \{ \lambda \mid \lambda = 0 \text{ and } j\omega_f(l_1 - l_2); l_1 + l_2 = l; l_1, l_2 = 0, 1, \dots, l; l = 1, 2, \dots, k \} \quad (4.17)$$

Now the internal model is constructed using the minimum polynomial of A_{kf} of the form

$$\dot{x}_s = G_1 x_s + G_2 e \quad (4.18)$$

where $x_s \in R^c$ and

$$G_1 = \text{diag} \left(0, \begin{bmatrix} 0 & -\omega_f \\ \omega_f & 0 \end{bmatrix}, \begin{bmatrix} 0 & -2\omega_f \\ 2\omega_f & 0 \end{bmatrix}, \dots, \begin{bmatrix} 0 & -k\omega_f \\ k\omega_f & 0 \end{bmatrix} \right) \quad (4.19)$$

The vector G_2 is chosen such that the pair (G_1, G_2) is controllable. It can be verified that G_2 is given by

$$G_2 = \begin{bmatrix} b_0 \\ 0 \\ b_1 \\ 0 \\ b_2 \\ \cdot \\ \cdot \\ \cdot \\ \cdot \\ 0 \\ b_k \end{bmatrix} \quad (4.20)$$

satisfies the controllability property of pair (G_1, G_2) as long as $b_i \neq 0, i = 0, \dots, k$.

4.5 Stabilizer Design

For completing the design, all one now has to do is to stabilize the closed-loop system. For this purpose, consider the augmented system Eqn 4.7 and Eqn 4.18 given by

$$\frac{d}{dt} \begin{bmatrix} x \\ x_s \end{bmatrix} = \begin{bmatrix} A(w) & 0 \\ G_2 H_1 & G_1 \end{bmatrix} \begin{bmatrix} x \\ x_s \end{bmatrix} + \begin{bmatrix} B(w) \\ 0 \end{bmatrix} u_c + \begin{bmatrix} n_{l2}(u_c, x, v, w) \\ G_2 H_2 v \end{bmatrix} + \begin{bmatrix} E(w) \\ 0 \end{bmatrix} v \quad (4.21)$$

Now one needs to find a control law such that $(x = 0, x_s = 0)$ of the nonlinear system

Eqn 4.21 is exponentially stable for $v = 0$. For exponential stabilization of the origin, it is sufficient to stabilize the linearized model obtained from Eqn 4.21, which for $v = 0$, is given by

$$\begin{aligned} \frac{dx_c}{dt} &= \begin{bmatrix} A(w) & 0 \\ G_2 H_1 & G_1 \end{bmatrix} x_c + \begin{bmatrix} B(w) \\ 0 \end{bmatrix} u_c \\ &\triangleq A_c(w)x_c + B_c(w)u_c \end{aligned} \quad (4.22)$$

where A_c and B_c are defined in Eqn 4.22.

For the system Eqn 4.22, a stabilizing control law exists if [8].

$$\text{rank} \begin{bmatrix} A(w) - \lambda I & B(w) \\ H_1 & 0 \end{bmatrix} = 4 \quad (4.23)$$

for all λ , which are the roots of the minimal polynomial of A_{kf} (that is, for $\lambda = 0$ and $\lambda = \pm j\omega_{fl}, l = 1, 2, 3, \dots, k$). Here I denotes an identity matrix. Of course, the characteristic roots of A_{kf} are the eigenvalues of the internal model matrix G_1 . The matrices A and B of the augmented system Eqn 4.22 depend on the unknown parameter vector w . As such a feedback control law is obtained by the stabilization of Eqn 4.22 at the chosen nominal (known) parameter value w^* . A stabilizing feedback law takes the form

$$u_c = -K_1 x - K_2 x_s \triangleq -K x_c \quad (4.24)$$

where the gain vector K can be computed using either pole assignment technique or the linear optimal control theory such that the closed-loop matrix $A_{cl} = [A_c(w^*) - B_c(w^*)K]$ is Hurwitz.

Here, we design the control law using the optimal control theory. For optimal control, a quadratic performance index

$$J = \int_0^{\infty} (x_c^T Q x_c + r u_c^2) dt \quad (4.25)$$

is chosen, where the weighting matrix Q is a positive definite symmetric matrix and $r > 0$. The optimal gain vector is given by

$$K = r^{-1}B_c^T(w^*)P \quad (4.26)$$

where P_a is the positive definite symmetric matrix, which satisfies the algebraic Riccati equation [9]

$$A_c^T(w^*)P + PA_c(w^*) - PB_c(w^*)r^{-1}B_c^T(w^*)P + Q = 0 \quad (4.27)$$

The weighting matrix Q and r can be chosen to shape the transient responses.

Although the gain vector K is computed for a known nominal value of w , it follows that the closed-loop matrix $A_{cl}(w)$ remains Hurwitz for perturbations $\tilde{w} \in \tilde{W}$, where \tilde{W} is a sufficiently small open set. Thus it follows that the origin $x_c = 0$ of the nonlinear system Eqn 4.21 is exponentially stable for $v = 0$ and for sufficiently small \tilde{w} . In the closed-loop system including the internal model of the k -fold exosystem, one can show that Y_{lw} in the Taylor series expansion of the tracking error Eqn 4.13 are null vectors for small \tilde{w} and $l = 1, \dots, k$. Thus the tracking error $e(t)$ satisfies Eqn 4.10 as $t \rightarrow \infty$, and therefore, the steady-state tracking error is zero up to k^{th} -order.

4.6 Simulation Results

In this section, simulation results for the closed-loop system Eqns 4.1, 4.18 and 4.24 using MATLAB/SIMULINK are presented. The parameters of the model are taken from [17]. The BAUV is assumed to be moving with a constant forward velocity of 0.8 m/sec. The vehicle parameters are $l = 1.282$ m, $m = 4.1548$ kg, $I_y = 0.5732$ kgm², $x_G = 0$, and $Z_G = 0.578802 \times 10^{-8}$ m. The hydrodynamic parameters for the forward velocity of 0.8 m/sec are $z'_q = -0.825 \times 10^{-5}$, $z'_{\dot{w}} = -0.825 \times 10^{-5}$, $z'_q = -0.238 \times 10^{-2}$, $z'_w = -0.738 \times 10^{-2}$, $M'_q = -0.16 \times 10^{-3}$, $M'_{\dot{w}} = -0.825 \times 10^{-5}$, $M'_q = -0.117 \times 10^{-2}$, and $M'_w = 0.314 \times 10^{-2}$. The

pectoral fins are attached at a distance of $d_{cgd} = 0.15$ m. The simulation results are obtained for fin oscillation frequencies of $f = 6$ Hz and $f = 8$ Hz. Of course, the controller design is applicable for any choice of frequency of oscillation of the fins.

Using CFD analysis, the fin forces and the moments coefficients have been obtained for a fixed Strouhal number $S_t = 0.6$, where $S_t = \frac{cf}{U_\infty}$, U_∞ is 0.8 m/sec, f is the frequency of the fin oscillation and c is the chord of the foil. The parameter vectors f_a , f_b , m_a , and m_b used for simulations are

$$\begin{aligned} f_a &= (f_0^c(0), f_1^s(0), f_1^c(0), \dots, f_M^s(0), f_M^c(0))^T \\ f_b &= \left(\frac{\partial f_0^c}{\partial \beta}(0), \frac{\partial f_1^s}{\partial \beta}(0), \frac{\partial f_1^c}{\partial \beta}(0), \dots, \frac{\partial f_s^M}{\partial \beta}(0), \frac{\partial f_c^M}{\partial \beta}(0) \right)^T \\ m_a &= (m_0^c(0), m_1^s(0), m_1^c(0), \dots, m_M^s(0), m_M^c(0))^T \\ m_b &= \left(\frac{\partial m_0^c}{\partial \beta}(0), \frac{\partial m_1^s}{\partial \beta}(0), \frac{\partial m_1^c}{\partial \beta}(0), \dots, \frac{\partial m_s^M}{\partial \beta}(0), \frac{\partial m_c^M}{\partial \beta}(0) \right)^T \end{aligned}$$

where $f_a, f_b, m_a, m_b \in R^{2M+1}$. In the Fourier expansion, four harmonic components, which are dominant, are retained; that is, $M=4$. Then the values of f_a, f_b, m_a, m_b for $M=4$ are

$$f_a = (0, -40.0893, -43.6632, -0.3885, 0.6215, 6.2154, -10.1777, -0.1554, 0.6992)$$

$$f_b = (68.9975, 0.4451, -16.4704, 64.1009, -19.5864, -0.8903, -2.2257, 2.2257, 4.8966)$$

$$m_a = (0, 0.6037, 0.4895, 0, -0.0054, 0, -0.0925, 0, -0.0054)$$

$$m_b = (-0.4986, -0.3739, -0.0935, -0.2493, 0.1246, 0.0312, -0.0312, 0.0935, 0)$$

(Readers may refer to [17] for the details.) It is pointed out that these parameters are obtained using the Fourier decomposition of the fin force and moment, and are computed by multiplying the Fourier coefficients by $\frac{1}{2}\rho.W_a.U_\infty^2$ and $\frac{1}{2}\rho.W_a.c.U_\infty^2$, respectively, where W_a is the surface area of the foil. For simulation, the initial conditions of the vehicle are assumed

to be $x(0) = 0$, and $x_s(0) = 0$.

A smooth reference trajectory $z_r(t)$ converging to z^* , the target depth, using a fourth-order filter

$$G_c(s) = \frac{\lambda_1 \omega_{nc}^2}{(s + \lambda_{c1})(s + \lambda_{c2})(s^2 + 2\zeta_c \omega_{nc} s + \omega_{nc}^2)}$$

is generated, where $\omega_{nc} = 4.95$, $\zeta_c = 0.707$, $\lambda_{c1} = 0.14$ and $\lambda_{c2} = 3.5$ are the real poles.

A simple servocompensator of first-order providing integral error feedback, as well as a compensator representing the internal model of 2-fold exosystem are designed. The latter servocompensator is of fifth-order. For the first-order compensator, $G_1 = 0$, and $G_2 = 0.5$ and for the fifth-order, one has

$$G_1 = \text{diag} \left(0, \begin{bmatrix} 0 & -\omega_f \\ \omega_f & 0 \end{bmatrix}, \begin{bmatrix} 0 & -2\omega_f \\ 2\omega_f & 0 \end{bmatrix} \right)$$

$$G_2 = [0.5, 0, 0.5, 0, 0.5]^T$$

If the input e to the servocompensator is zero, then the first-order system generates constant trajectory, but the fifth-order servocompensator can generate trajectories of the form $c_1 + c_2 \sin(\omega_f t + \theta_1) + c_3 \sin(2\omega_f t + \theta_2)$ by appropriate choice of initial conditions. For the control law design linear optimal control theory is used. For the first-order compensator $Q=1$ and for the fifth-order, Q is an identity matrix of dimension 9×9 , and $r = 0.0001$.

Case I: BAUV control using first-order servocompensator: $\omega_f = 6$ Hz, nominal parameters

The complete closed-loop system including the nominal BAUV model and the first-order servocompensator is simulated for a fin oscillation frequency of 6 Hz. A smooth reference trajectory $z_r(t)$ converging to $z^* = 25$ m is generated. Thus it is desired to steer the BAUV to a depth of 25 m. The optimal controller gains are computed for the nominal BAUV model. Selected

responses are shown in Figure. 4.1. It is observed that the BAUV attains the target depth in little over 30 seconds. We note that, for easy understanding the depth variable z_d is denoted by z in the simulated figures. In steady-state, fin forces, moment, and bias angle exhibit bounded periodic oscillations. Note that the chosen servocompensator has a simple pole at zero and as such it can only suppress any nonzero bias in the tracking error. We observe that indeed, average tracking error is zero, but periodic oscillations including the fundamental component (six Hz) and higher harmonics persist. The magnitude of the tracking error e is observed to be around 0.08 m. The maximum control magnitude is around 8 deg. The peak control force needed is 12 N and the control moment is 0.15 Nm.

Case II: BAUV control using first-order servocompensator: $\omega_f = 6$ Hz, -25% uncertainty

Now simulation is done to examine the effect of uncertainties in the control force and moment coefficients. For this purpose the elements of the vectors f_a , f_b , m_a and m_b are perturbed by a factor of 0.75 for simulation; that is, the perturbed values of these vectors are 25% lesser than the nominal values. However, the controller gains used in Figure. 4.1 computed for the nominal values are retained. Selected plots are provided in Figure. 4.2. It is again noted that with the servocompensator of first-order, the oscillatory components of the tracking error are not suppressed. But, the average value of the tracking error is zero. The magnitude of the tracking error is 0.05 m. The maximum control magnitude and the response time to attain the target depth are of the same order as in Figure. 4.1.

Simulation is also done for fin force coefficients with +25% uncertainty (perturbed values are 1.25 times the nominal values) using the nominal controller. In this case also, a smooth control to the desired depth is accomplished. (In order to save space, the results are not shown

here).

Case III: BAUV control using internal model of 2-fold exosystem: $\omega_f = 6$ Hz, nominal parameters

For attenuating the dominant oscillatory components of the tracking error, it is essential to synthesize servocompensator of higher-order. For the purpose of illustration, a servocompensator of fifth-order is designed using internal model of 2-fold exosystem. Selected responses for the nominal BAUV model are shown in Figure. 4.3. It is seen that desired depth is smoothly attained. The magnitude of the tracking error is significantly smaller compared to that of Figure. 4.1. Interestingly, the designed servocompensator suppresses the constant bias, fundamental and second harmonic components in the tracking error response, and only oscillations of frequency 18 Hz and higher remain. Although, one can design a higher order compensator, we observe that even this fifth-order servocompensator yields maximum error little over 0.01 m, which is negligible for practical purposes. The maximum control magnitude is observed to be around 30 deg. The target depth is attained in a little over 30 secs as in Figure. 4.1.

Case IV: BAUV control using internal model of 2-fold exosystem: $\omega_f = 6$ Hz, +25% uncertainty

Now simulation is done to examine the robustness of the control system. It is assumed that the fin force coefficients are 25% greater than the nominal values, but the nominal control system used for Figure. 4.3 is retained. Selected responses are shown in Figure. 4.4. Similar to Figure. 4.3, we observe that the vehicle attains the desired depth and controller is able to suppress the bias, fundamental and second harmonics in the tracking error response. Compared to Figure. 4.3, the tracking error magnitude in Figure. 4.4 is a little higher at 0.02 m, but the maximum control magnitude and the target depth response time are of the same magnitude.

Case V: BAUV control using first-order servocompensator: $\omega_f = 8$ Hz, nominal parameters

The frequency of the pectoral fin oscillation is set at 8 Hz and the performance of the first-order servocompensator is evaluated. Of course, for 8 Hz the fin force and moment coefficients have changed, and the feedback gains of the controller are redesigned, using the same values of Q and r. The responses are shown in Figure. 4.5. It is observed that the average tracking error is zero, but the oscillatory components in the tracking error are still present. The simulation results shown in Figure. 4.5 are some what similar to the results obtained in Figure. 4.1. Though, the tracking error pattern in Figure. 4.5 and Figure. 4.1 are the same, the magnitude of the tracking error in Figure. 4.5 is 0.025 m, lesser than that in Figure. 4.1. The maximum control magnitude and the target depth response time in both Figure. 4.5 and Figure. 4.1 are almost the same.

Case VI: BAUV control using first-order servocompensator: $\omega_f = 8$ Hz, +25% uncertainty

An uncertainty of +25% is introduced in the fin force coefficients for simulation. The results using the nominal controller of Figure. 4.5 are shown in Figure. 4.6. The magnitude of the tracking error in Figure. 4.6 is 0.04 m, whereas in Figure. 4.5 it was 0.025 m. The target depth response time is close to 35 secs. The maximum control magnitude is around 8 deg.

Case VII: BAUV control using internal model of 2-fold exosystem: $\omega_f = 8$ Hz, nominal parameters

It is assumed that the fins are oscillating at 8 Hz. For obtaining improved responses, a fifth-order servocompensator for the nominal values of the parameters is designed. Simulation results of the nominal BAUV are shown in Figure. 4.7. We observe that target depth is attained and oscillations of fundamental and second harmonic in the tracking error are

suppressed. Compared to the case of first-order servocompensator in Figure. 4.5, we observe significant reduction in the peak magnitude of the steady-state tracking error. The magnitude of the tracking error is 0.004 m in Figure. 4.7 which is substantially lesser than the tracking error magnitude of 0.025 m in Figure. 4.5. The maximum control magnitude is around 30 deg as in the case of Figure. 4.3. The target depth is reached in little over 30 secs.

Case VIII: BAUV control using internal model of 2-fold exosystem: $\omega_f = 8$ Hz, -25% uncertainty

To examine the robustness of the designed controller an uncertainty of -25% is added to the nominal values of the vectors f_a , f_b , m_a and m_b for simulation. The selected responses are shown in Figure. 4.8. The tracking error magnitude for the chosen uncertainty is around 0.002 m. The maximum control magnitude and the target depth response time are similar in both Figures. 4.7 and 4.8.

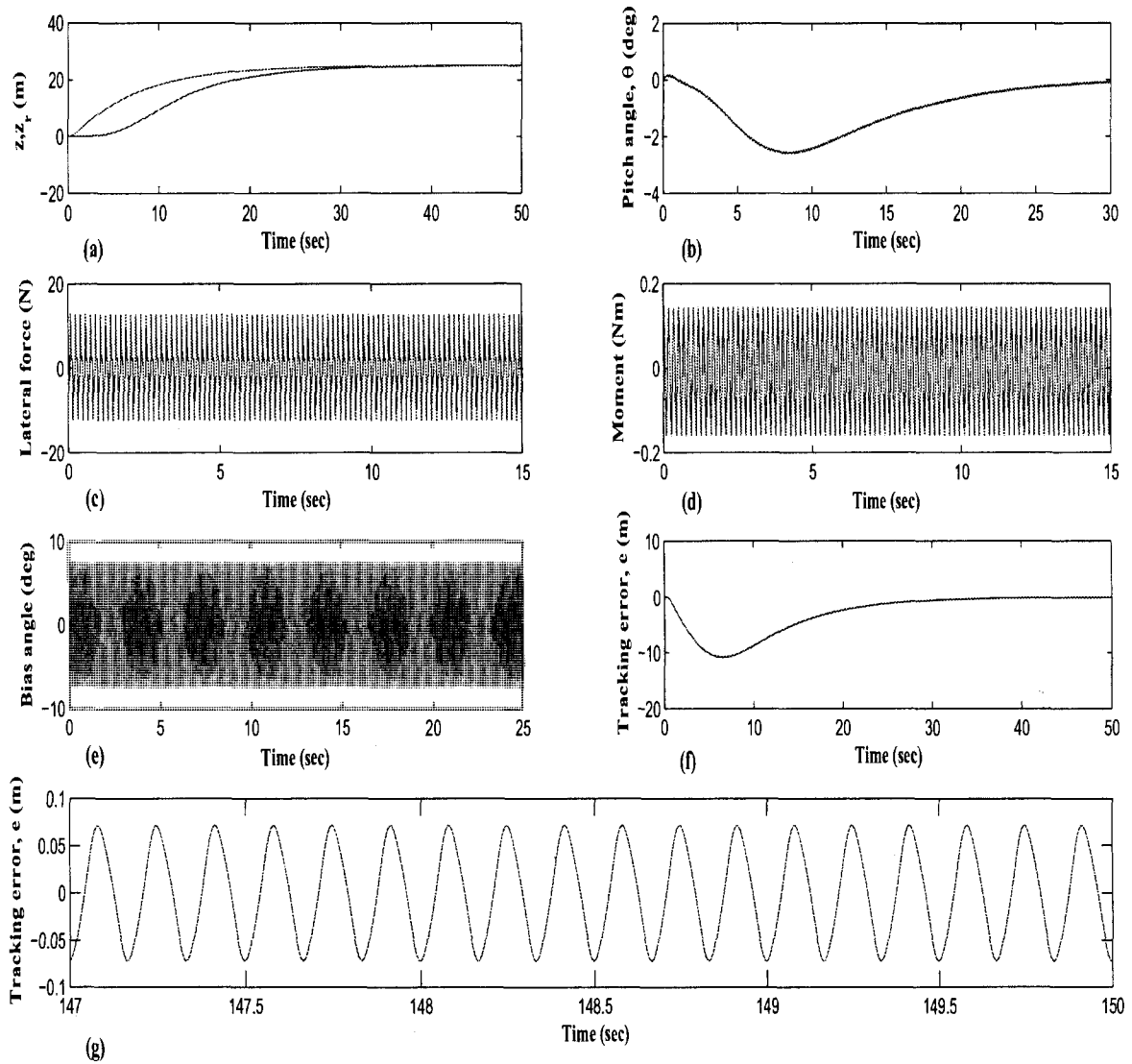


Figure 4.1: BAUV control using first-order servocompensator: $\omega_f = 6$ Hz, nominal parameters (a) Dive plane depth, z , and reference depth, z_r (m), (b) Pitch angle, θ (deg), (c) Lateral force (N), (d) Moment (Nm), (e) Bias angle (deg), (f) Tracking error, e (m), (g) Tracking error plotted for smaller time interval, e (m)

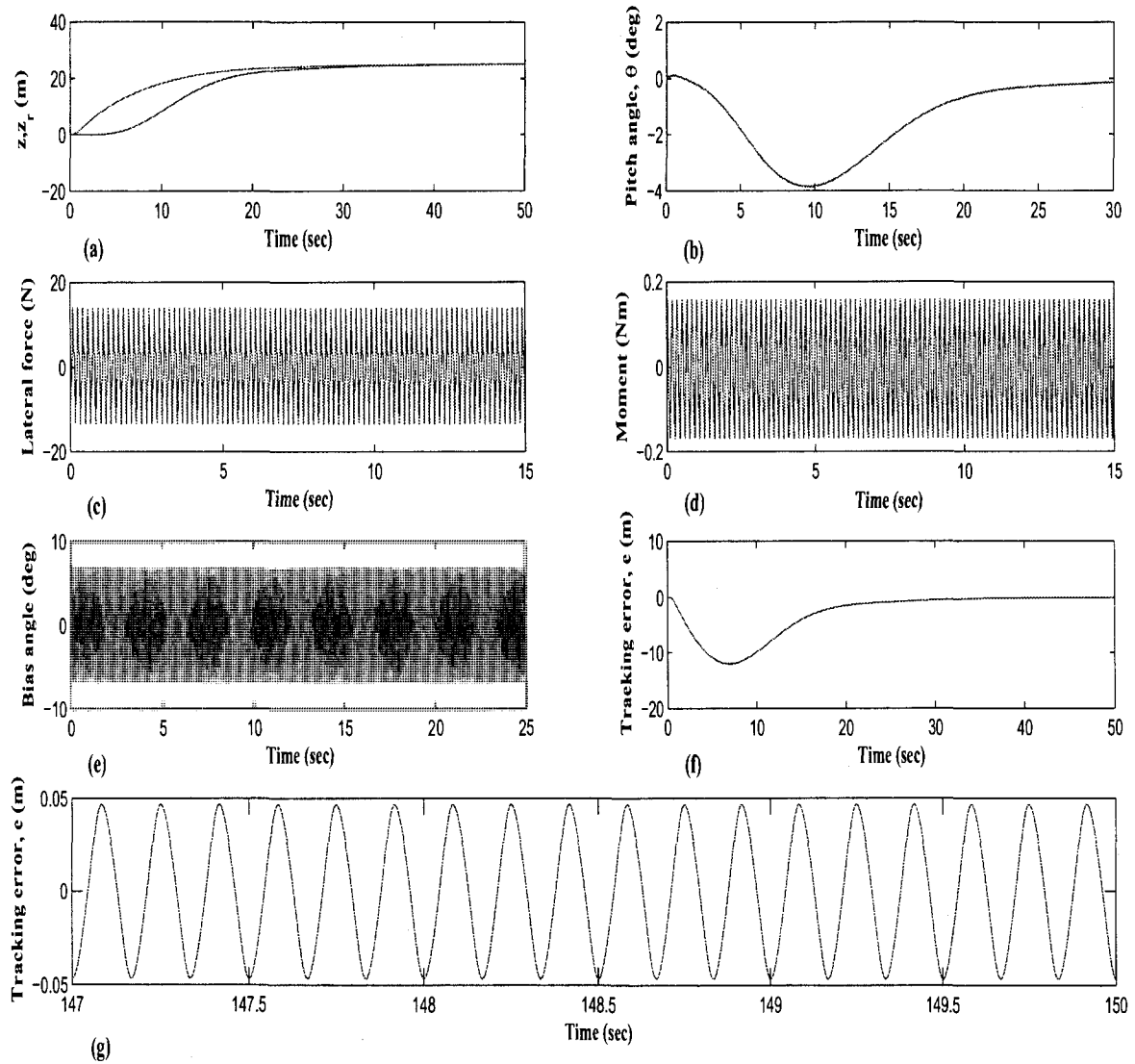


Figure 4.2: BAUV control using first-order servocompensator: $\omega_f = 6$ Hz, -25% uncertainty
(a) Dive plane depth, z , and reference depth, z_r (m), (b) Pitch angle, θ (deg), (c) Lateral force (N), (d) Moment (Nm), (e) Bias angle (deg), (f) Tracking error, e (m), (g) Tracking error plotted for smaller time interval, e (m)

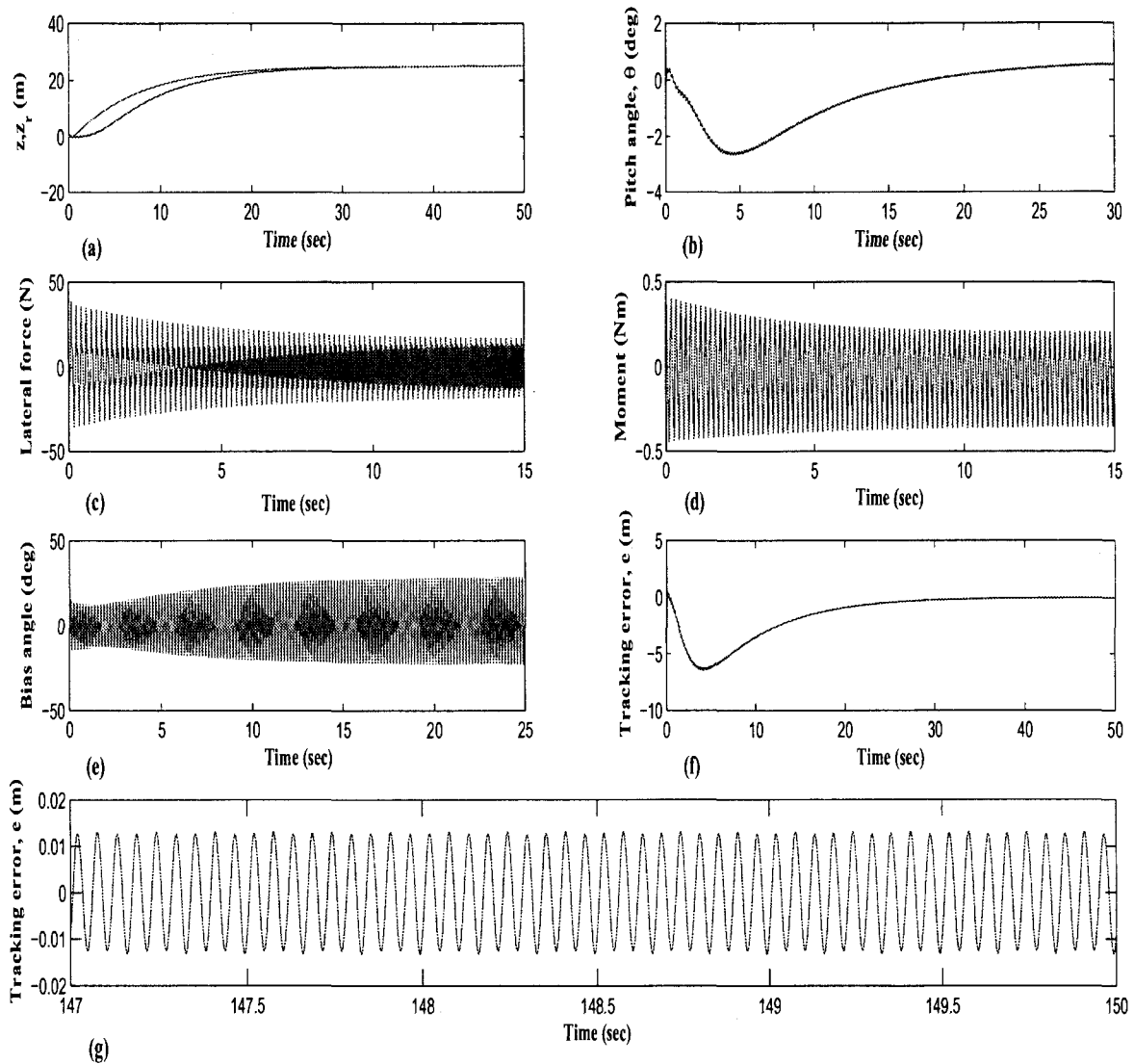


Figure 4.3: BAUV control using internal model of 2-fold exosystem: $\omega_f = 6$ Hz, nominal parameters

(a) Dive plane depth, z , and reference depth, z_r (m), (b) Pitch angle, θ (deg), (c) Lateral force (N), (d) Moment (Nm), (e) Bias angle (deg), (f) Tracking error, e (m), (g) Tracking error plotted for smaller time interval, e (m)

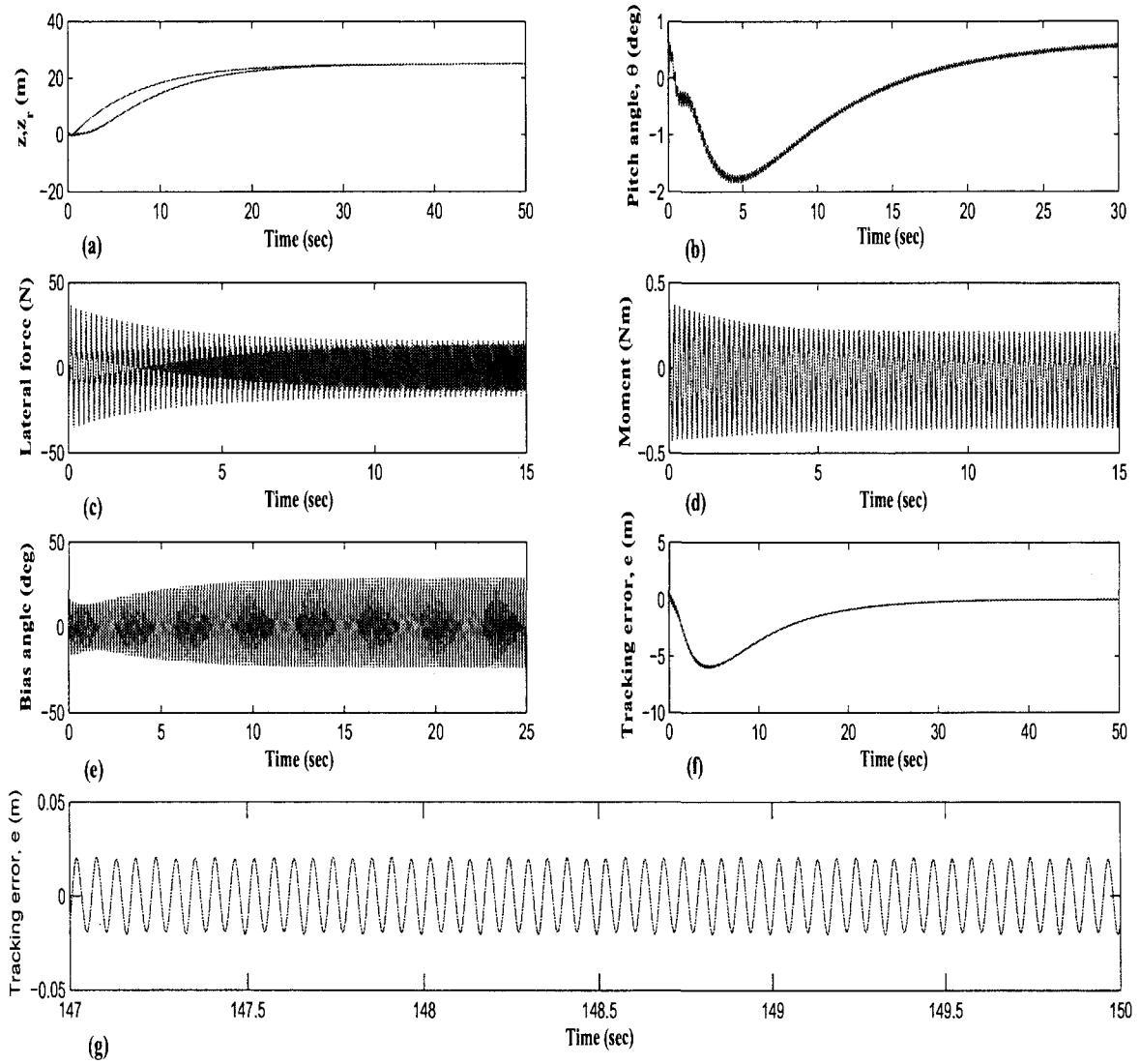


Figure 4.4: BAUV control using internal model of 2-fold exosystem: $\omega_f = 6$ Hz, +25% uncertainty

(a) Dive plane depth, z , and reference depth, z_r (m), (b) Pitch angle, θ (deg), (c) Lateral force (N), (d) Moment (Nm), (e) Bias angle (deg), (f) Tracking error, e (m), (g) Tracking error plotted for smaller time interval, e (m)

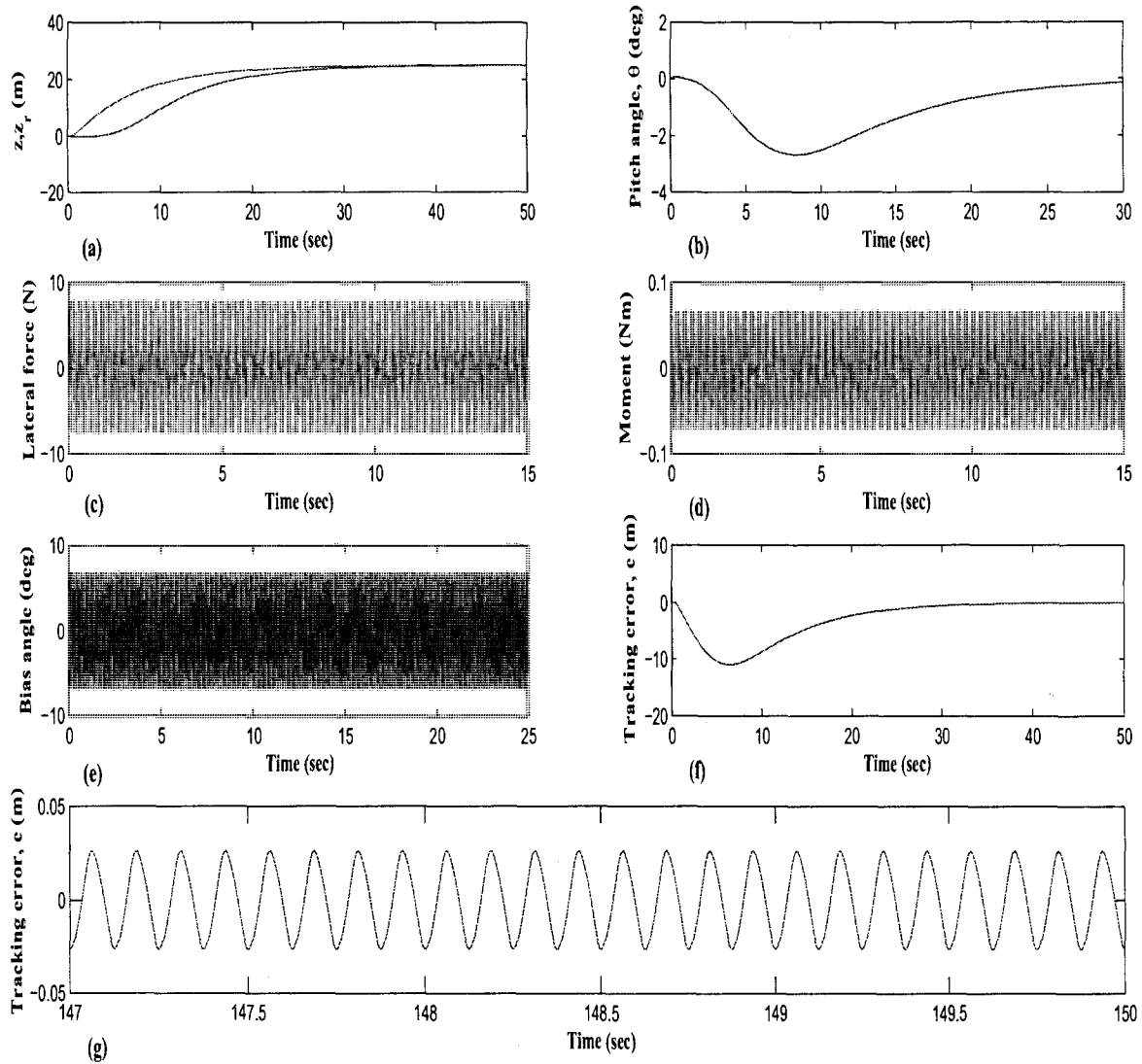


Figure 4.5: BAUV control using first-order servocompensator: $\omega_f = 8$ Hz, nominal parameters (a) Dive plane depth, z , and reference depth, z_r (m), (b) Pitch angle, θ (deg), (c) Lateral force (N), (d) Moment (Nm), (e) Bias angle (deg), (f) Tracking error, e (m), (g) Tracking error plotted for smaller time interval, e (m)

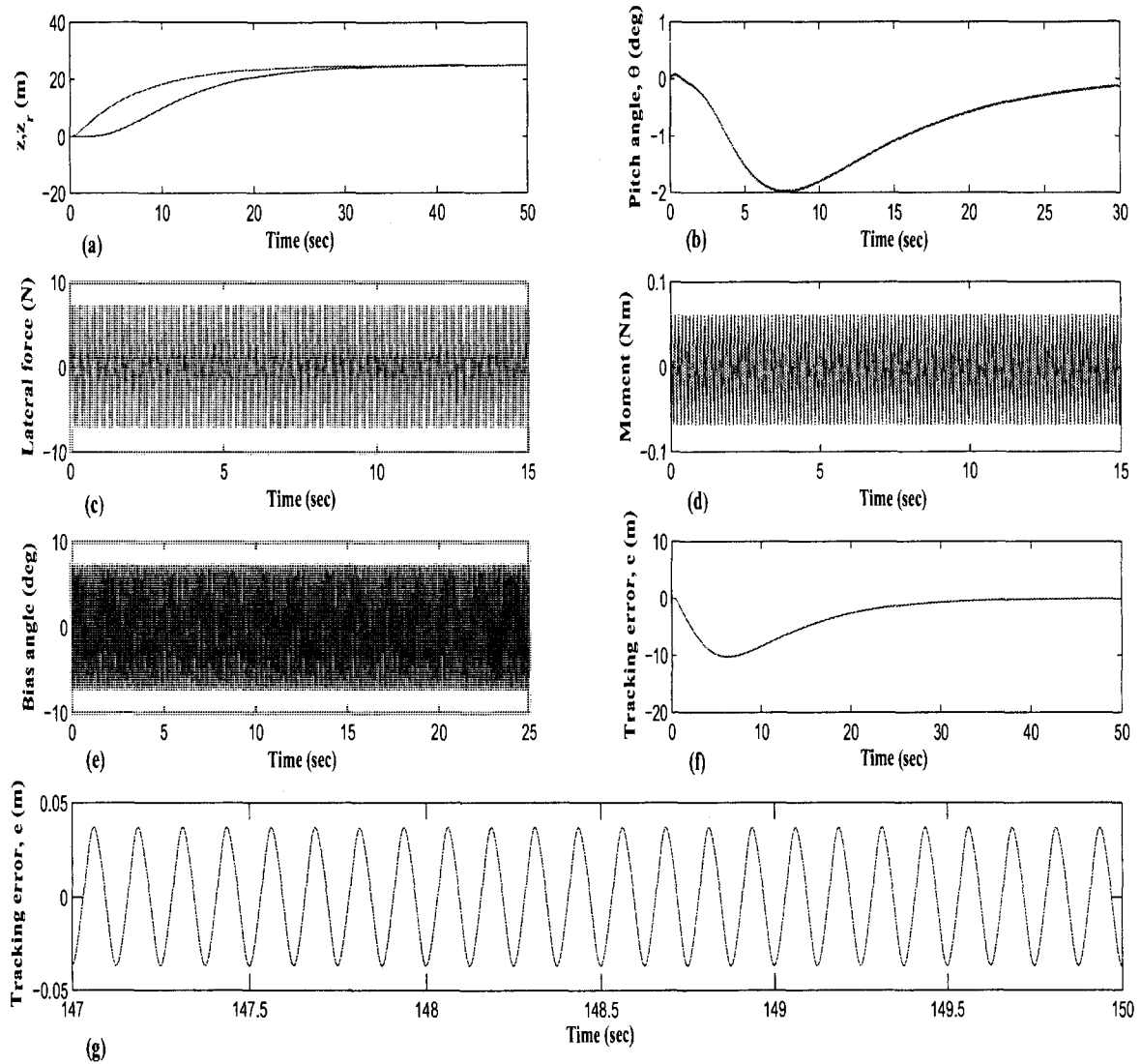


Figure 4.6: BAUV control using first-order servocompensator: $\omega_f = 8$ Hz, +25% uncertainty
 (a) Dive plane depth, z , and reference depth, z_r (m), (b) Pitch angle, θ (deg), (c) Lateral force (N), (d) Moment (Nm), (e) Bias angle (deg), (f) Tracking error, e (m), (g) Tracking error plotted for smaller time interval, e (m)

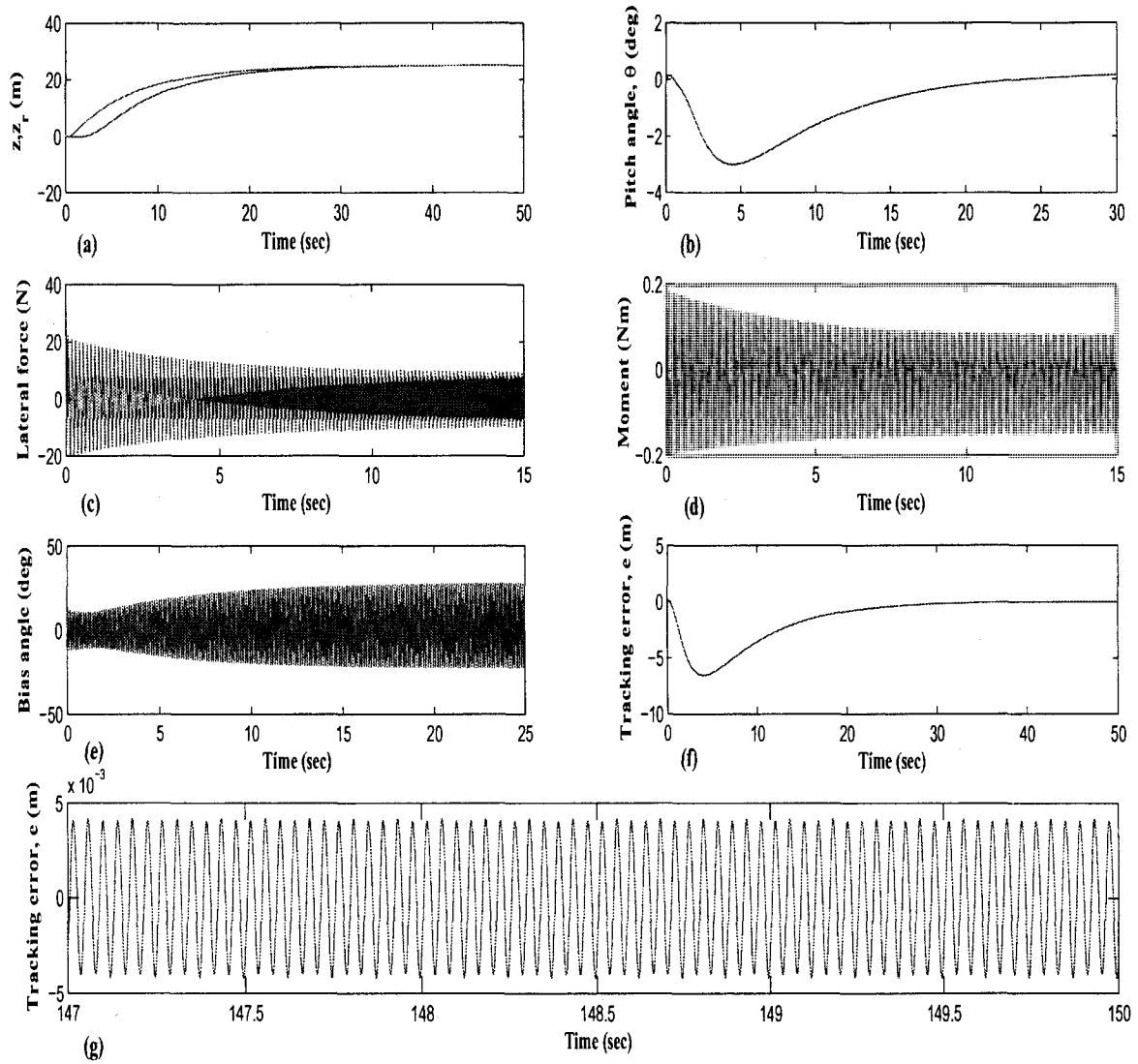


Figure 4.7: BAUV control using internal model of 2-fold exosystem: $\omega_f = 8$ Hz, nominal parameters

(a) Dive plane depth, z , and reference depth, z_r (m), (b) Pitch angle, θ (deg), (c) Lateral force (N), (d) Moment (Nm), (e) Bias angle (deg), (f) Tracking error, e (m), (g) Tracking error plotted for smaller time interval, e (m)

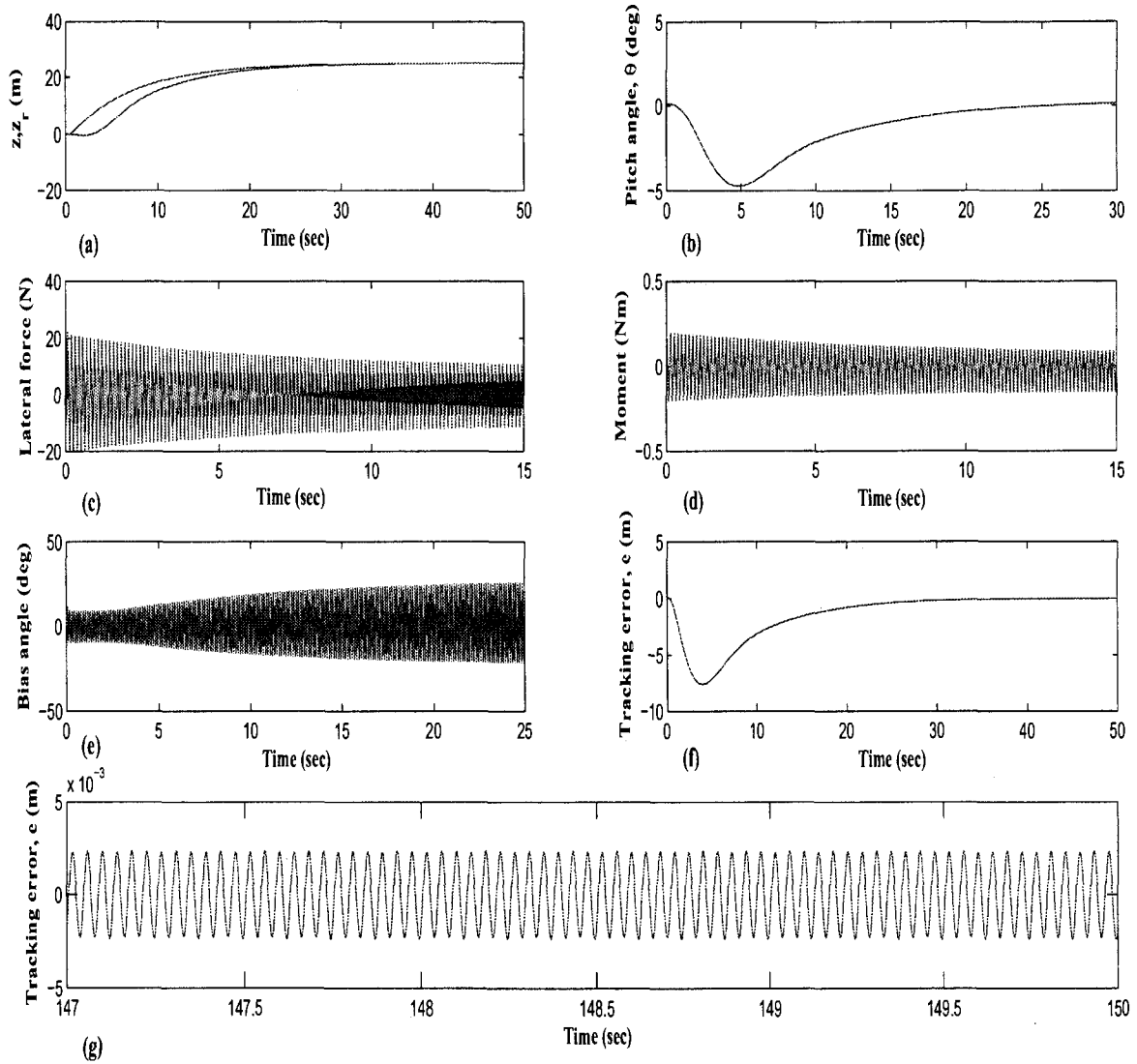


Figure 4.8: BAUV control using internal model of 2-fold exosystem: $\omega_f = 8$ Hz, -25% uncertainty

(a) Dive plane depth, z , and reference depth, z_r (m), (b) Pitch angle, θ (deg), (c) Lateral force (N), (d) Moment (Nm), (e) Bias angle (deg), (f) Tracking error, e (m), (g) Tracking error plotted for smaller time interval, e (m)

CHAPTER 5

NONLINEAR ROBUST YAW PLANE CONTROL OF BAUV USING INTERNAL MODEL PRINCIPLE

This chapter presents the control of BAUVs in the yaw plane based on the nonlinear internal model principle. A similar application of the internal model principle was seen in chapter 4, for the control of an BAUV in dive plane. In this chapter, the BAUV control using pectoral-like fins is considered in the yaw plane. The fins are assumed to be oscillating with a combined sway and yaw motion. The bias angle of the angular motion of the fin is taken as the control input. The yaw angle is taken as the output variable. The oscillating pectoral fins produce large unsteady periodic forces. A continuous-time state variable representation of the nonlinear BAUV is considered for the design of a closed-loop control system for the set point control of the yaw angle. For the purpose of a robust nonlinear servoregulator design, an exosystem of third-order is considered. The third-order exosystem converts the time-variant state variable representation of the BAUV into time-invariant form. An internal model of a k -fold exosystem is designed for the derivation of the control law, where k is a design parameter which decides the accuracy of the yaw angle command tracking. For any choice of k , the simulation results show that all the harmonic components of the tracking error of order up to k can be suppressed. For nonlinear BAUVs the physical systems parameters and hydrodynamic coefficients are poorly known. The control law design, including the internal model and stabilizer design is adapted from chapter 4. Despite the uncertainties in the BAUV

system parameters, the simulation results show that the set point control of the yaw angle is achieved precisely.

5.1 Problem Formulation

Our objective is to design a robust servoregulator for controlling the yaw angle of an BAUV in the yaw plane. The physical model of an BAUV in the yaw plane is given in Figure. 2.2. The mathematical model of an BAUV in the yaw plane is described in chapter 2, but for the convenience of the readers it is again presented here. The equations of motion of a neutrally buoyant vehicle is described by [35]

$$\begin{aligned}
 m(\dot{v} + Ur + X_G \dot{r} - Y_G r^2) &= Y_{\dot{r}} \dot{r} + (Y_{\dot{v}} \dot{v} + Y_r Ur) + Y_v Uv + f_{py} \\
 I_z \dot{r} + m(X_G \dot{v} + X_G Ur + Y_G vr) &= N_r \dot{r} + (N_{\dot{v}} \dot{v} + N_r Ur) + N_v Uv + m_{py} \\
 \dot{\psi} &= r
 \end{aligned} \tag{5.1}$$

where ψ is the heading angle to be controlled, $r = \dot{\psi}$ is the yaw rate, v is the lateral velocity along the Y_B -axis, $(X_G, Y_G) = (X_G, 0)$ is the coordinate of the center of gravity with respect to O_B , m is the mass, and I_z is the moment of inertia of the vehicle. $Y_{\dot{v}}, N_r, Y_v$, etc are the hydrodynamic coefficients, and f_{py} and m_{py} are the net fin force and moment. The global position coordinates X and Y of the vehicle are described by the kinematic equations

$$\begin{aligned}
 \dot{X} &= U \cos(\psi) - v \sin(\psi) \\
 \dot{Y} &= U \sin(\psi) + v \cos(\psi)
 \end{aligned} \tag{5.2}$$

The constant reference signal is given by $\psi_r = \psi^*$ and $e = \psi - \psi_r$ is the tracking error. Defining the state vector $x = (x_1, x_2, x_3)^T = (v, r, \psi)^T \in R^3$, solving Eqn 5.1 and substituting f_{py} and m_{py} using Eqn 2.4, gives the state variable representation of the BAUV given by the

system

$$\begin{aligned}\dot{x} &= Ax + B_v \begin{pmatrix} f_y \\ m_y \end{pmatrix} + n_l(x) \\ y &= [0, 0, 1]x \\ e &= x_3 - \psi_r\end{aligned}\tag{5.3}$$

where $n_l(x)$ denotes the terms due to the nonlinear functions of Eqn 5.1. In view of Eqn 2.4 the state equation Eqn 5.3 is a nonlinear time-varying system. For control law design convenience $n_l(x)$ is neglected and only the linearized components of Eqn 5.2 are considered. But, for simulation purposes the entire BAUV model in Eqn 5.2 is considered.

5.2 Exosystem and Control Law Design

In order to express Eqn 5.3 in a time-invariant form, a third-order exosystem is designed

$$\begin{aligned}\begin{pmatrix} \dot{v}_0 \\ \dot{v}_1 \\ \dot{v}_2 \end{pmatrix} &= \begin{pmatrix} 0 & 0 & 0 \\ 0 & 0 & -\omega_f \\ 0 & \omega_f & 0 \end{pmatrix} \begin{pmatrix} v_0 \\ v_1 \\ v_2 \end{pmatrix} \\ &= A_v v\end{aligned}\tag{5.4}$$

where $v = (v_0, v_1, v_2)^T \in R^3$. Define $v_p = (v_1, v_2)^T$. (Readers can find the detailed exosystem design in section 4.2, in chapter 4.) The control law design comprises the design of an internal model and the stabilizer. The internal model is derived in section 4.4, in chapter 4. The final form of the internal model is given by

$$\dot{x}_s = G_1 x_s + G_2 e$$

where $x_s \in R^c$ is defined in Eqn 4.8 and

$$G_1 = \text{diag} \left(0, \begin{bmatrix} 0 & -\omega_f \\ \omega_f & 0 \end{bmatrix}, \begin{bmatrix} 0 & -2\omega_f \\ 2\omega_f & 0 \end{bmatrix}, \dots, \begin{bmatrix} 0 & -k\omega_f \\ k\omega_f & 0 \end{bmatrix} \right)$$

The vector G_2 is chosen such that the pair (G_1, G_2) is controllable. It can be verified that G_2 is given by

$$G_2 = \begin{bmatrix} b_0 \\ 0 \\ b_1 \\ 0 \\ b_2 \\ \cdot \\ \cdot \\ \cdot \\ \cdot \\ 0 \\ b_k \end{bmatrix}$$

satisfies the controllability property of pair (G_1, G_2) as long as $b_i \neq 0, i = 0, \dots, k$.

The stabilizing feedback law is given by

$$u_c = -K_1 x - K_2 x_s \triangleq -K x_c$$

where the gain vector K can be computed using either pole assignment technique or the linear optimal control theory. The stabilizer design is explained in detail in section 4.5 of chapter 4. To avoid redundancy in details, the complete derivation of the stabilizer design is not shown here.

5.3 Simulation Results

The closed-loop system Eqns 5.1, 4.18 and 4.24 are simulated for yaw angle control using MATLAB/SIMULINK and the results are presented in this section. Constant time-varying reference trajectories are employed for tracking, and the performance of the robust servoregulator in the presence of uncertainties is examined. The parameters of the model are taken from [15]. The BAUV is assumed to be moving with a constant forward velocity of 0.8 m/sec. The vehicle parameters are $l = 1.391$ m, mass=18.826 kg; $I_z = 1.77$ kgm², $X_G = -0.012$, $Y_G = 0$. The hydrodynamic parameters for a forward velocity of 0.8 m/sec are $Y_{\dot{r}} = -0.3781$, $Y_{\dot{v}} = -5.6198$, $Y_r = 1.1694$, $Y_v = -12.0868$, $N_{\dot{r}} = -0.3781$, $N_{\dot{v}} = -0.8967$, $N_r = -1.0186$, and $N_v = -4.9587$. simulations have been carried out for fin oscillation frequencies of $f = 6$ Hz and $f = 8$ Hz. Of course, the control law is applicable for higher choice of fin frequencies too.

As seen in section 4.6 of chapter 4, a fixed Strouhal number $S_t = 0.6$ is considered for the fin force and moment coefficients. The parameter vectors f_a , f_b , m_a , and m_b used for simulations are

$$\begin{aligned} f_a &= (f_0^c(0), f_1^s(0), f_1^c(0), \dots, f_M^s(0), f_M^c(0))^T \\ f_b &= \left(\frac{\partial f_0^c}{\partial \beta}(0), \frac{\partial f_1^s}{\partial \beta}(0), \frac{\partial f_1^c}{\partial \beta}(0), \dots, \frac{\partial f_s^M}{\partial \beta}(0), \frac{\partial f_c^M}{\partial \beta}(0) \right)^T \\ m_a &= (m_0^c(0), m_1^s(0), m_1^c(0), \dots, m_M^s(0), m_M^c(0))^T \\ m_b &= \left(\frac{\partial m_0^c}{\partial \beta}(0), \frac{\partial m_1^s}{\partial \beta}(0), \frac{\partial m_1^c}{\partial \beta}(0), \dots, \frac{\partial m_s^M}{\partial \beta}(0), \frac{\partial m_c^M}{\partial \beta}(0) \right)^T \end{aligned}$$

where $f_a, f_b, m_a, m_b \in R^{2M+1}$. The values of f_a, f_b, m_a, m_b for $M=4$ are

$$f_a = (0, -40.0893, -43.6632, -0.3885, 0.6215, 6.2154, -10.1777, -0.1554, 0.6992)$$

$$f_b = (68.9975, 0.4451, -16.4704, 64.1009, -19.5864, -0.8903, -2.2257, 2.2257, 4.8966)$$

$$m_a = (0, 0.6037, 0.4895, 0, -0.0054, 0, -0.0925, 0, -0.0054)$$

$$m_b = (-0.4986, -0.3739, -0.0935, -0.2493, 0.1246, 0.0312, -0.0312, 0.0935, 0)$$

(Readers may refer to [15] for the details.) For simulation, the initial conditions of the vehicle are assumed to be $x(0) = 0$, and $x_s(0) = 0$.

Simulations were carried out for a constant reference trajectory ψ_r converging to $\psi^*=25$ deg. As seen in section 4.6 of chapter 4, a fourth-order filter of the form

$$G_c(s) = \frac{\lambda_1 \omega_{nc}^2}{(s + \lambda_{c1})(s + \lambda_{c2})(s^2 + 2\zeta_c \omega_{nc} s + \omega_{nc}^2)}$$

is generated, where $\omega_{nc} = 4.95$, $\zeta_c = 0.707$, $\lambda_{c1} = 0.14$ and $\lambda_{c2} = 3.5$ are the real poles.

A first-order servocompensator and a fifth-order servocompensator are designed. The values of the constant matrices (G_1 , G_2) used in servocompensator design in section 4.6 of chapter 4 are retained here. The controller gains are calculated using linear optimal control theory technique. For the first-order compensator $Q=1$ and for the fifth-order, Q is an identity matrix of dimension 8×8 , and $r = 0.001$.

Case I: BAUV control using first-order servocompensator: $\omega_f = 6$ Hz, nominal parameters

The first-order servocompensator along with the nominal BAUV parameters are simulated. The fins are assumed to be oscillating at a frequency of 6 Hz. We are interested in steering the BAUV at an yaw angle of 25 deg. A constant reference trajectory $\psi_r(t)$ converging to $\psi^* = 25$ deg is generated. The closed-loop responses are shown in Figure. 5.1. Optimal control theory technique is used to compute the controller gains. It is seen that the set point control of the yaw angle is reached in little over 25 seconds and other simulation parameters show bounded oscillations. A selected portion of the tracking error is simulated to highlight the non-zero bias suppression. In accordance with the theory, it is observed that the designed first-order servocompensator has the ability to suppress only non-zero bias of the tracking error, whereas

the fundamental component (six Hz) and higher harmonics are still present. The magnitude of the tracking error e is observed to be around 0.025 deg. The lateral control force produced by the fins is 30 N and the control moment is 0.25 Nm. The maximum control input required is 20 deg and this can be easily provided by the fins.

Case II: BAUV control using first-order servocompensator: $\omega_f = 6$ Hz, -25% uncertainty

In the previous case, simulations were carried out for nominal fin force and moment coefficients. To examine the robustness of the designed servocompensator, uncertainties are introduced in the control force and moment coefficients. The constant vectors f_a , f_b , m_a and m_b are perturbed by a factor of 0.75 for simulation; that is, the perturbed values of these vectors are 25% lesser than the nominal values. The controller gains used in case I are retained. The closed-loop responses are shown in Figure. 5.2. Even in the presence of uncertainties in the force and moment coefficients, the behavior of the servocompensator is similar to case I. The average value of the tracking error is zero, whereas the higher harmonics in the tracking error are still present. The magnitude of the tracking error is 0.05 deg, which is almost similar to Figure. 5.1. The maximum control magnitude in this case too is 20 deg and the response time to reach the desired reference yaw angle is around 25 seconds.

Case III: BAUV control using internal model of 2-fold exosystem: $\omega_f = 6$ Hz, nominal parameters

To suppress the higher oscillatory harmonics in the tracking error, a servocompensator of fifth-order is designed using internal model of 2-fold exosystem. Selected responses for the nominal BAUV model are shown in Figure. 5.3. The reference trajectory target is reached in little over 25 seconds. As expected, the constant bias, fundamental and second harmonic components in the tracking error are suppressed, and only oscillations of frequency 18 Hz and

higher remain. It is also observed that the magnitude of the tracking error is 0.001 deg, which is much lower than that in Figure. 5.1. In this case a fifth-order servocompensator is designed, but servocompensators of higher orders can be designed for suppression of higher frequencies present in the tracking error. The maximum control magnitude is observed to be around 25 deg. The response time for reaching the desired heading angle is little over 30 secs.

Case IV: BAUV control using internal model of 2-fold exosystem: $\omega_f = 6$ Hz, +25% uncertainty

The fin force coefficients are assumed to be 25 % greater than the nominal values for examining the robustness of the servocompensator. Simulated results are shown in Figure. 5.4. The behavior of the closed-loop system in the presence of uncertainties is found to be similar to the nominal fin force coefficients . The zero-bias, fundamental and second harmonic components are suppressed, with all other simulation parameters bounded, as found in case III.

Case V: BAUV control using first-order servocompensator: $\omega_f = 8$ Hz, nominal parameters

Simulations similar to cases I - IV are carried out for a pectoral fin oscillation frequency of 8 Hz. In this case, the performance of a first-order servocompensator is evaluated. The fin force, moment coefficients and the feedback gains have been recalculated for a fin frequency of 8 Hz. For the feedback controller gain calculation using the optimal control theory technique, the values of Q and r are retained. The responses are shown in Figure. 5.5. As seen earlier in Figure. 5.1, the average tracking error is zero, but the oscillatory components in the tracking error still exist. The magnitude of the tracking error is 0.001 deg. It is observed that better controller performances are achieved for higher fin oscillation frequencies.

Case VI: BAUV control using first-order servocompensator: $\omega_f = 8$ Hz, +25% uncertainty

The robustness of the first-order servocompensator was tested for a fin oscillation frequency of 6 Hz in case II. Here, the fin oscillation frequency is set at 8 Hz. The fin force and moment coefficients are perturbed by a factor of 1.25. The results are shown Figure. 5.6. The magnitude of the tracking error is 0.01 deg. The response time is close to 30 seconds. The maximum control magnitude is around 20 deg.

Case VII: BAUV control using internal model of 2-fold exosystem: $\omega_f = 8$ Hz, nominal parameters

In case III it was seen that, by using an fifth-order servocompensator the higher harmonics in the tracking error could be suppressed up to 18 Hz. Now, simulations are carried out at a fin oscillation frequency of 8 Hz and the results are shown in Figure. 5.7. A smooth maneuvering of the BAUV to the reference target is observed. As seen in Figure. 5.3, the constant bias, fundamental component and the second harmonics in the tracking error are suppressed. Interestingly, magnitude of the tracking has significantly reduced for $\omega_f = 8$ Hz. In Figure. 5.3, the magnitude of e was 0.001 deg, whereas, in Figure. 5.7 it is 0.0005 deg. This confirms our claim that for higher fin oscillation frequencies, better responses are obtained. As in the case of all other simulations, the control input required is stable at around 20 deg to 30 deg.

Case VIII: BAUV control using internal model of 2-fold exosystem: $\omega_f = 8$ Hz, -25% uncertainty

An uncertainty factor of -25% is introduced and the fin force coefficients are perturbed by a factor of 0.75. The simulated results are shown in Figure. 5.8. Frequencies greater than 24 Hz alone are seen in the tracking error response. This confirms the robust nature of the designed fifth-order servocompensator.

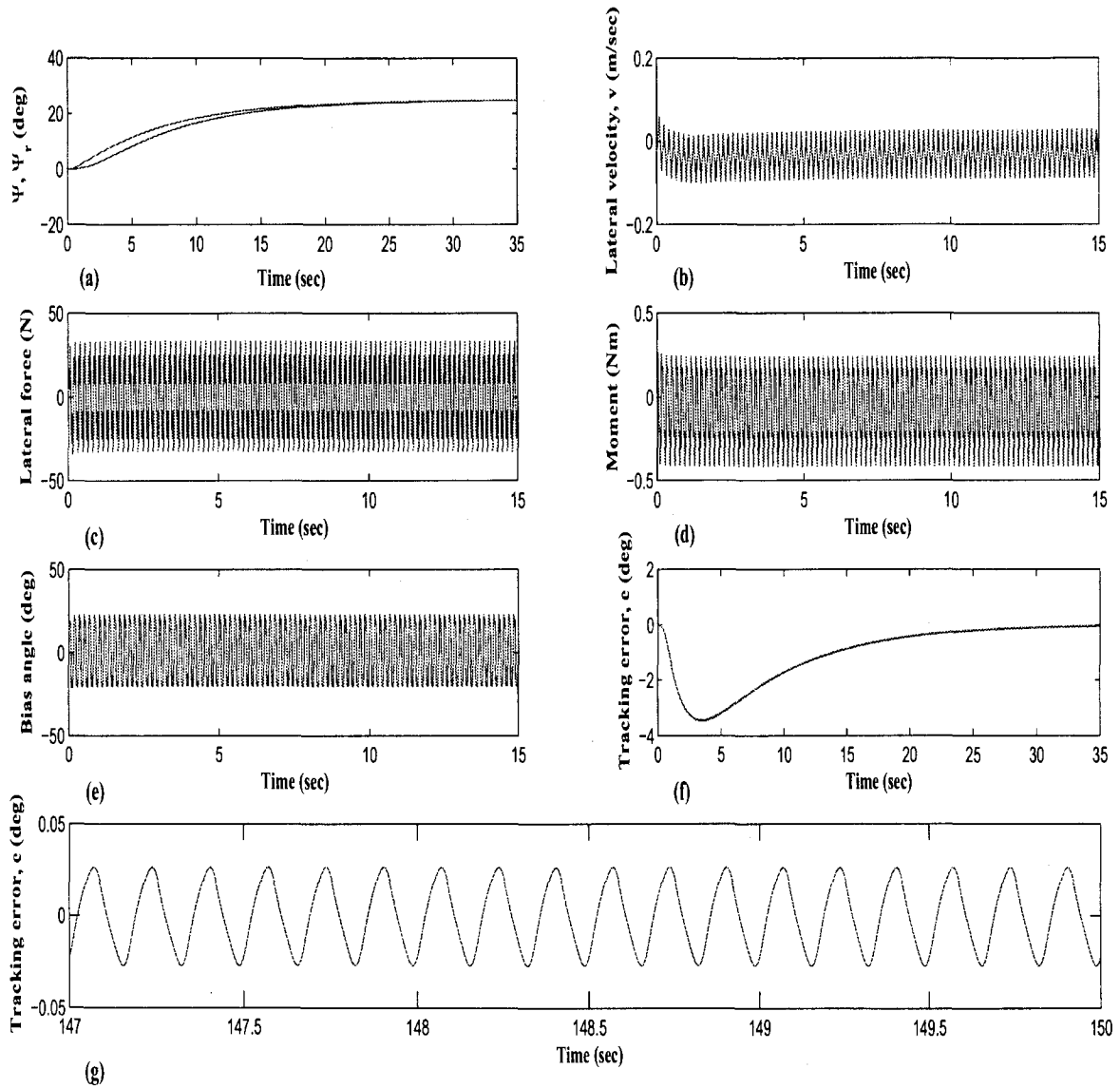


Figure 5.1: BAUV control using first-order servocompensator: $\omega_f = 6$ Hz, nominal parameters (a) Yaw angle, Ψ , and reference yaw angle, Ψ_r (deg), (b) Lateral velocity, v (m/sec), (c) Lateral force (N), (d) Moment (Nm), (e) Bias angle (deg), (f) Tracking error, e (deg), (g) Tracking error plotted for smaller time interval, e (deg).

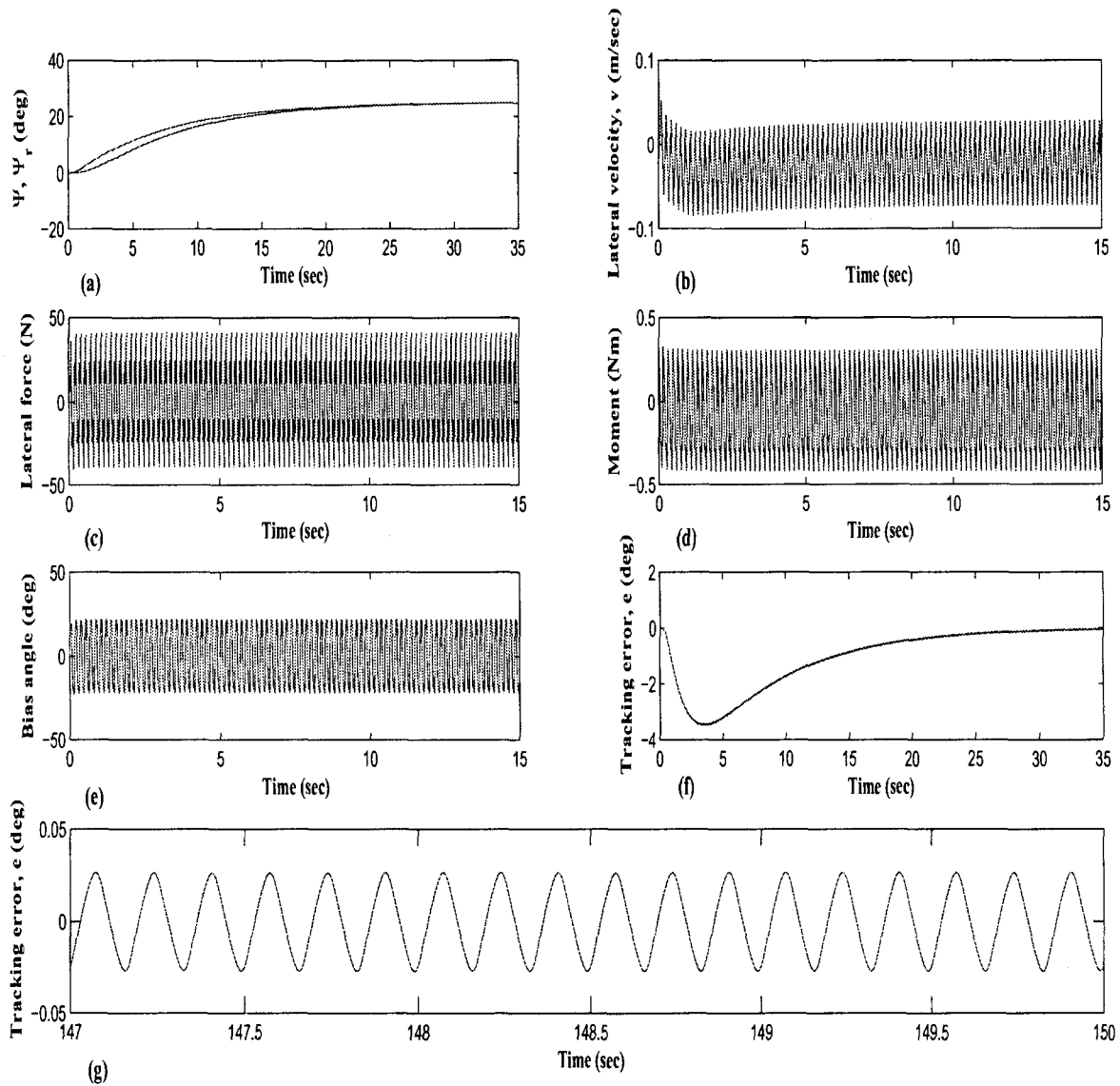


Figure 5.2: BAUV control using first-order servocompensator: $\omega_f = 6$ Hz, -25% uncertainty
(a) Yaw angle, Ψ , and reference yaw angle, Ψ_r (deg), (b) Lateral velocity, v (m/sec), (c) Lateral force (N), (d) Moment (Nm), (e) Bias angle (deg), (f) Tracking error, e (deg), (g) Tracking error plotted for smaller time interval, e (deg).

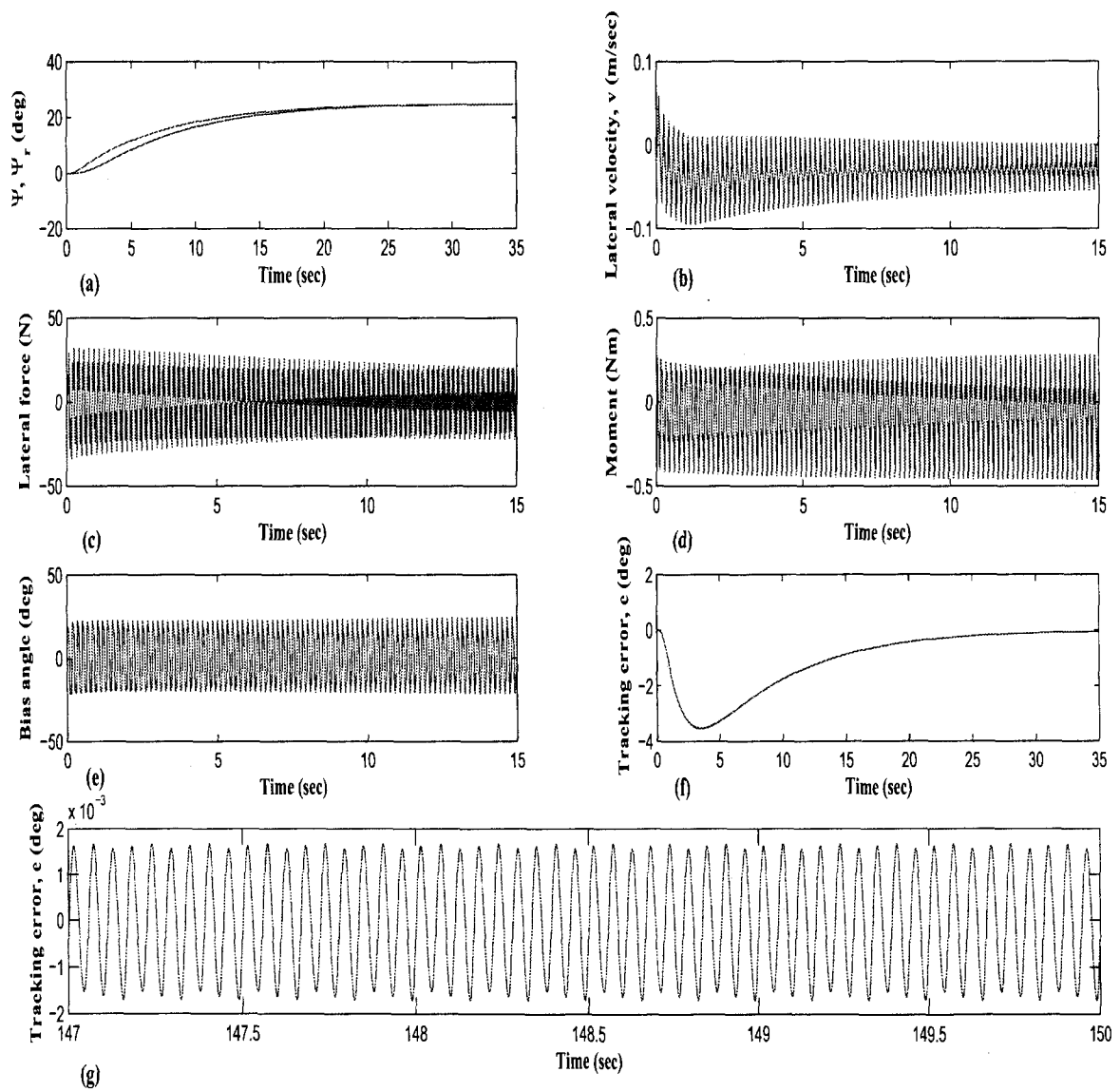


Figure 5.3: BAUV control using internal model of 2-fold exosystem: $\omega_f = 6$ Hz, nominal parameters

(a) Yaw angle, Ψ , and reference yaw angle, Ψ_r (deg), (b) Lateral velocity, v (m/sec), (c) Lateral force (N), (d) Moment (Nm), (e) Bias angle (deg), (f) Tracking error, e (deg), (g) Tracking error plotted for smaller time interval, e (deg).

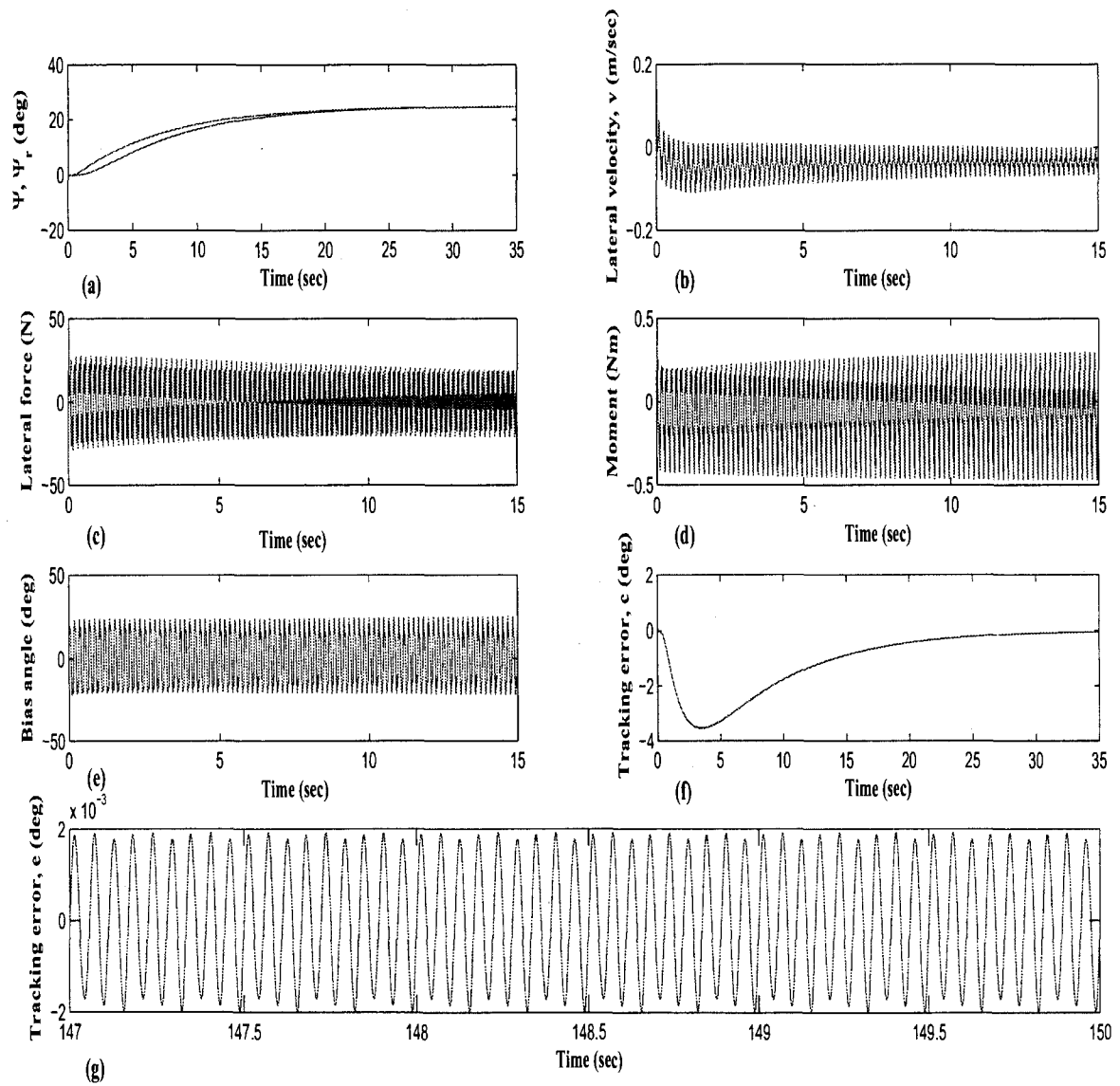


Figure 5.4: BAUV control using internal model of 2-fold exosystem: $\omega_f = 6$ Hz, +25% uncertainty

(a) Yaw angle, Ψ , and reference yaw angle, Ψ_r (deg), (b) Lateral velocity, v (m/sec), (c) Lateral force (N), (d) Moment (Nm), (e) Bias angle (deg), (f) Tracking error, e (deg), (g) Tracking error plotted for smaller time interval, e (deg).

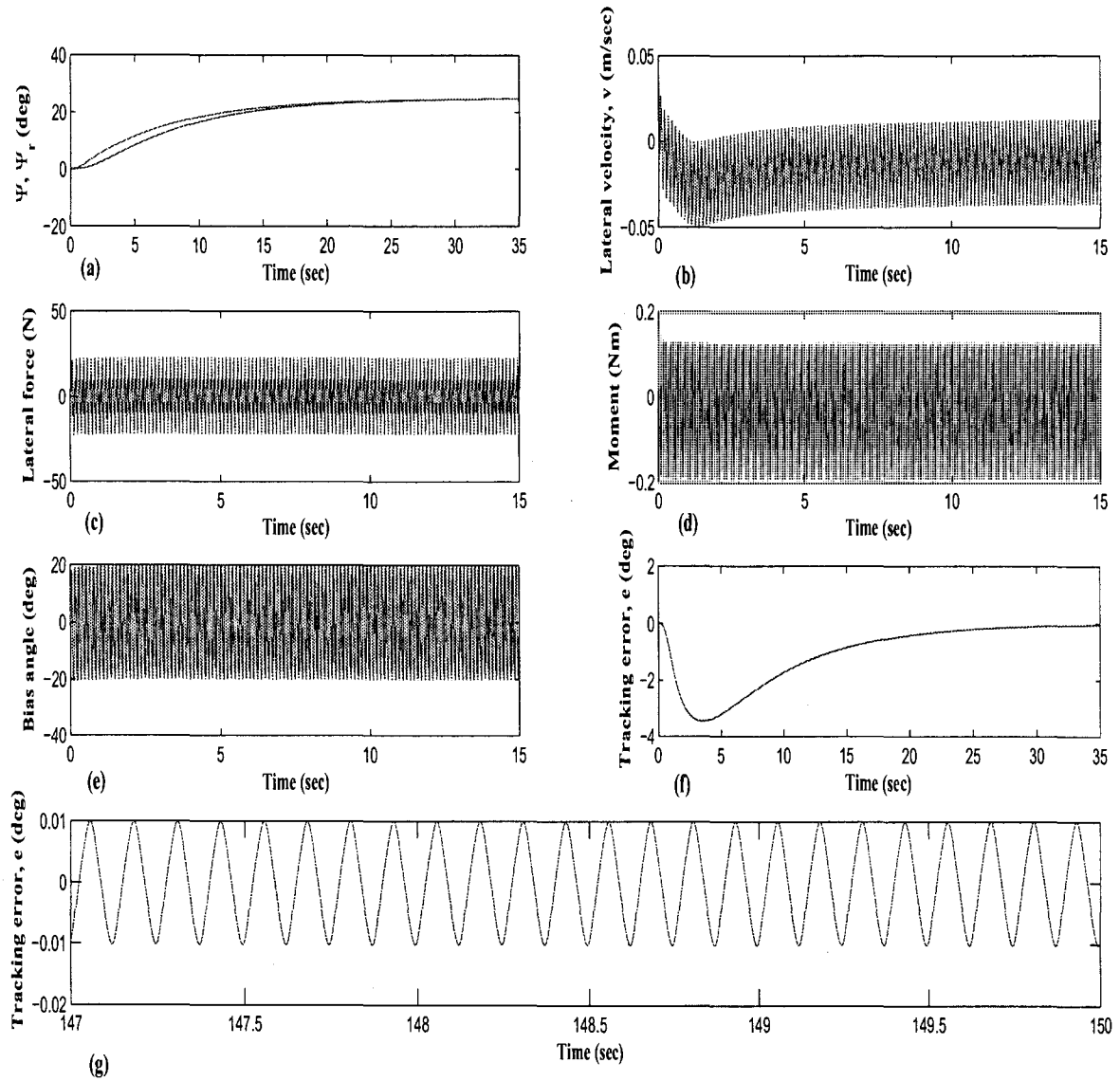


Figure 5.5: BAUV control using first-order servocompensator: $\omega_f = 8$ Hz, nominal parameters (a) Yaw angle, Ψ , and reference yaw angle, Ψ_r (deg), (b) Lateral velocity, v (m/sec), (c) Lateral force (N), (d) Moment (Nm), (e) Bias angle (deg), (f) Tracking error, e (deg), (g) Tracking error plotted for smaller time interval, e (deg).

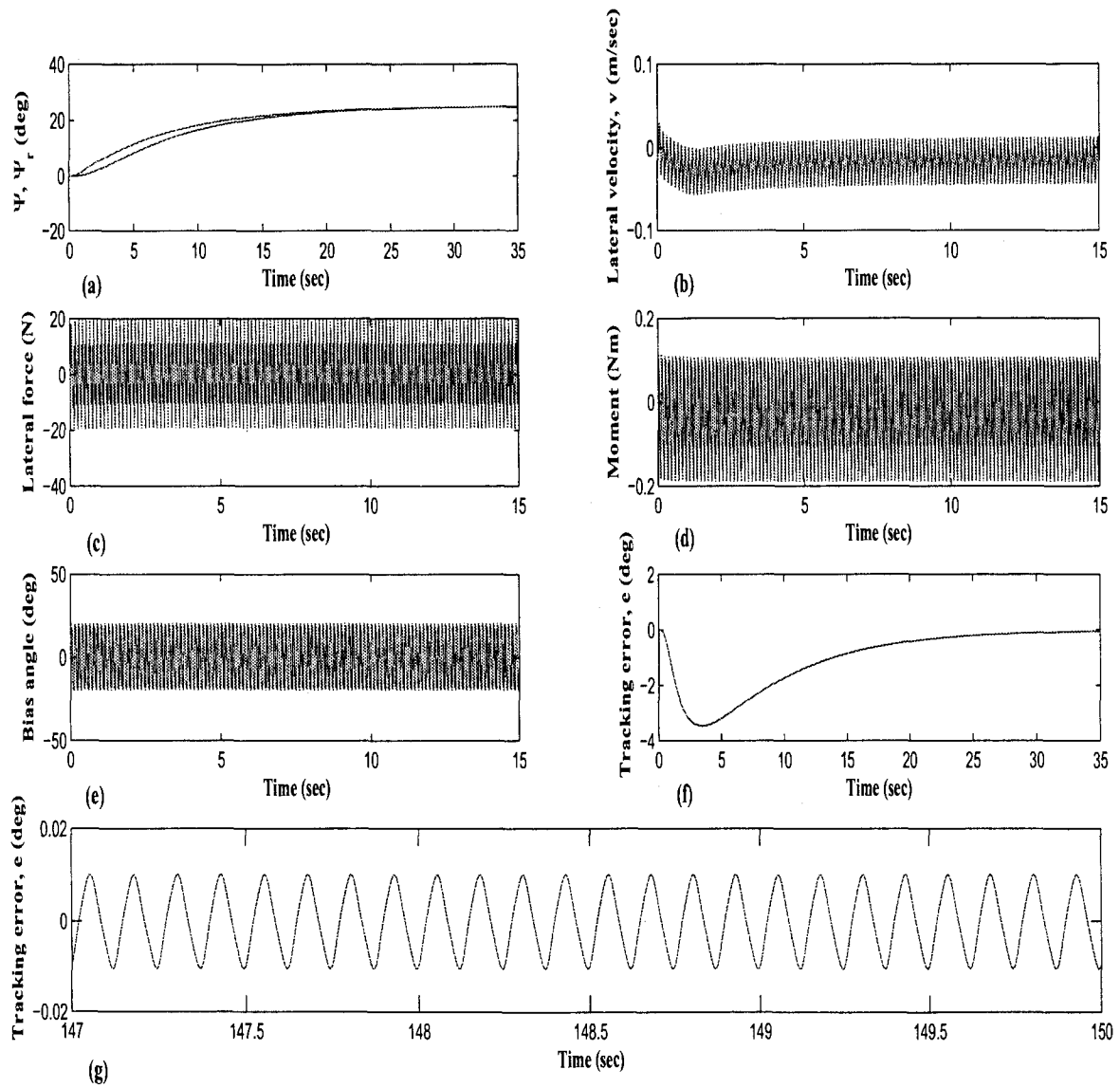


Figure 5.6: BAUV control using first-order servocompensator: $\omega_f = 8$ Hz, +25% uncertainty
 (a) Yaw angle, Ψ , and reference yaw angle, Ψ_r (deg), (b) Lateral velocity, v (m/sec), (c) Lateral force (N), (d) Moment (Nm), (e) Bias angle (deg), (f) Tracking error, e (deg), (g) Tracking error plotted for smaller time interval, e (deg).

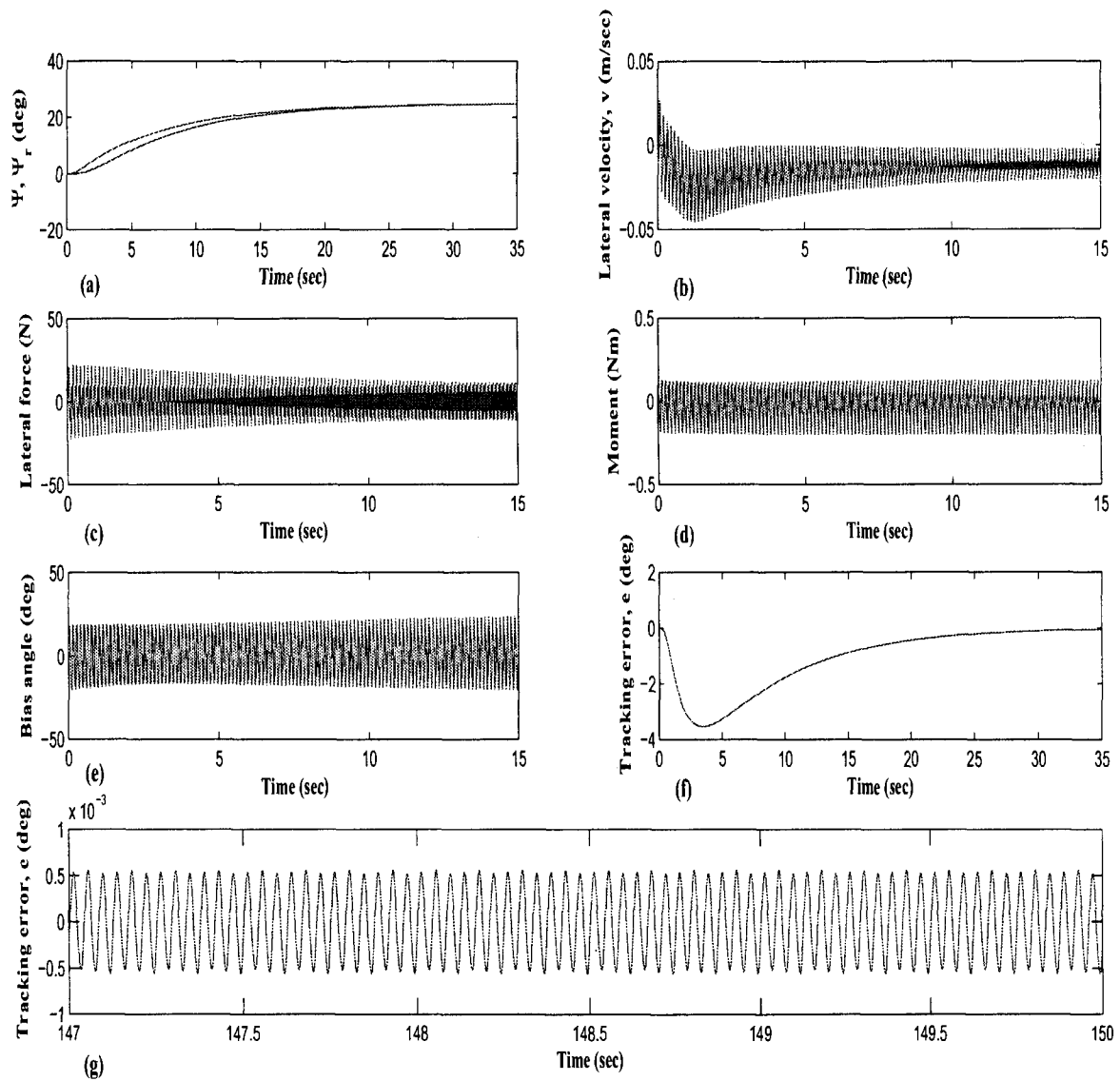


Figure 5.7: BAUV control using internal model of 2-fold exosystem: $\omega_f = 8$ Hz, nominal parameters

(a) Yaw angle, Ψ , and reference yaw angle, Ψ_r (deg), (b) Lateral velocity, v (m/sec), (c) Lateral force (N), (d) Moment (Nm), (e) Bias angle (deg), (f) Tracking error, e (deg), (g) Tracking error plotted for smaller time interval, e (deg).

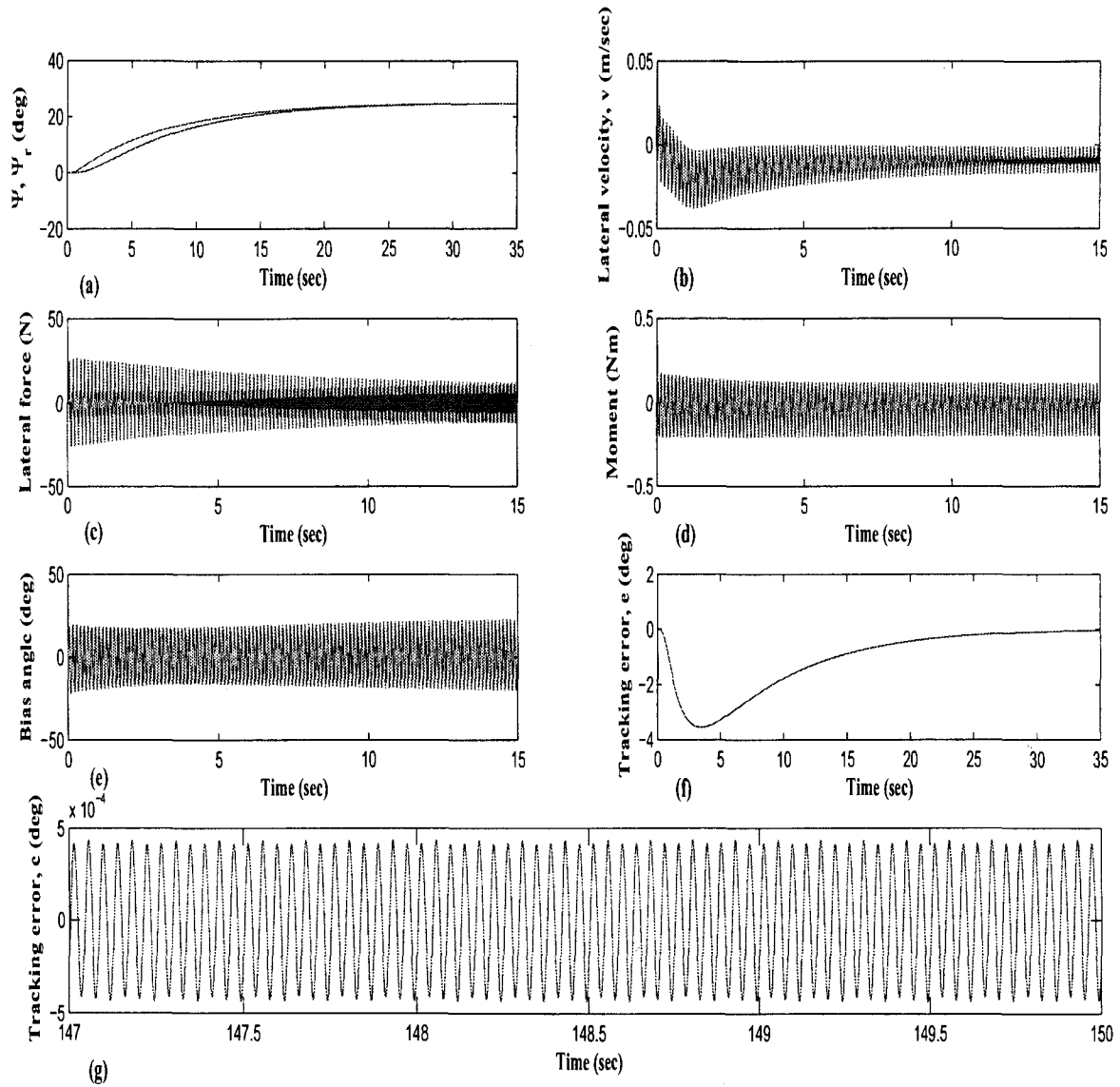


Figure 5.8: BAUV control using internal model of 2-fold exosystem: $\omega_f = 8$ Hz, -25% uncertainty

(a) Yaw angle, Ψ , and reference yaw angle, Ψ_r (deg), (b) Lateral velocity, v (m/sec), (c) Lateral force (N), (d) Moment (Nm), (e) Bias angle (deg), (f) Tracking error, e (deg), (g) Tracking error plotted for smaller time interval, e (deg).

CHAPTER 6

MODULAR DIVE PLANE ADAPTIVE CONTROL OF BAUV USING MECHANICAL PECTORAL FINS

In this chapter, a sampled-data adaptive control system for dive plane control of BAUVs using the pectoral-like fins is presented. The pectoral fins attached to the BAUV are assumed to be oscillating with combined pitch and heave motion. The bias angle of the pitch motion of the fin is considered as a control input variable. Periodic forces generated by flapping pectoral fins are modeled by using the computational fluid dynamics method. The parameters of the nonlinear BAUV model including the fin forces and moments are assumed to be unknown. This entails the design of a parameter identifier to estimate the nonlinear BAUV system parameters. A modular sampled-data adaptive control consisting of the identifier and a stabilizer system is designed for the depth control of the BAUV. For the synthesis of the control law, only the output variable (depth) is measured. The design of a stabilizing control law requires an internal model of the exosignals. Here, the constant reference signal and also the constant disturbance input together are taken as the exosignals. The derived control system accomplishes accurate depth command tracking as well as the disturbance rejection. The control system is applicable to both minimum phase and non-minimum phase BAUV systems. The simulation results are presented which show precise depth trajectory control in spite of parametric uncertainties and constant disturbance input.

6.1 Problem Statement

We are interested in designing an indirect adaptive servoregulator for the control of an BAUV in the dive plane using mechanical pectoral fins. The equations of motion of an BAUV in the dive plane is given in chapter 2. The model of an BAUV in dive plane is given in Fig. 2.1. For easy understanding the equations are given again [6]

$$\begin{aligned}
 m(\dot{w}_d - uq - z_G \dot{q}^2 - x_G \dot{q}) &= 0.5\rho l^4 z'_q \dot{q} + 0.5\rho l^3 (z'_w \dot{w} + z'_q qu) + 0.5\rho l^2 z'_w w_d u + f_{pd} \\
 I_y \dot{q} + mz_G(\dot{u} + w_d q) - mx_G(\dot{w}_d - uq) &= 0.5\rho l^5 M'_q \dot{q} + 0.5\rho l^4 (M'_w + \\
 M'_q qu) + 0.5\rho l^3 M'_w w_d u - x_{GB} W \cos\theta - z_{GB} W \sin\theta + m_{pd} \\
 \dot{z}_d &= -u \sin(\theta) + w \cos(\theta)
 \end{aligned} \tag{6.1}$$

where θ is the pitch angle; $q = \dot{\theta}$, $x_{GB} = x_G - x_B$, m is the mass of the vehicle, $z_{GB} = z_G - z_B$, l = body length. ρ = density; and z_d is the depth. f_{pd} and m_{pd} are the net force and moment acting on the vehicle due to the pectoral fins. The primed variables are the nondimensionalized hydrodynamic coefficients. Here $((x_B, z_B) = 0)$ and (x_G, z_G) denote the coordinates of the center of buoyancy and center of gravity (cg), respectively. Readers can refer to chapter 2 for control force and moment calculation details. Defining a state vector $x = (x_1, x_2, x_3, x_4)^T = (w_d, q, z_d, \theta) \in R^4$, solving Eqn. 6.1 and substituting for f_{pd} and m_{pd} from Eqn 2.4, gives the state variable representation of the BAUV of the form

$$\begin{aligned}
 \dot{x} &= Ax + B \begin{bmatrix} f_d \\ m_d \end{bmatrix} + n_l(x) \\
 y &= [0, 0, 1, 0]x
 \end{aligned} \tag{6.2}$$

where $n_l(x)$ consists of the nonlinear terms of model Eqn 6.1. For the purpose of design, second-order nonlinear function $n_l(x)$ will be ignored.

The output $y = z_d$ is the controlled variable. The values of matrices A and B and the Fourier coefficients of the control force and moments in Eqn 2.4 are unknown. Let $z_r = z_r^*$ be a constant reference signal. we are interested in derivation of an adaptive control system for the depth trajectory control using only output feedback. The control system has a modular structure consisting of an identifier and a stabilizer. Both constant and sinusoidal exponential trajectories are considered for smooth depth trajectory tracking and the depth tracking error $(z_d(t) - z_r(t))$ is desired to asymptotically converge to zero. In the next section a parameter identifier will be designed to determine the unknown BAUV system parameters.

6.2 Estimation of BAUV System Parameters

In this section design of a parameter identifier is considered. Once the BAUV parameters are ascertained, an adaptive control law can be designed for desired depth trajectory tracking. The system in Eqn 6.2 is time-varying. It is desired to obtain a discretized form of Eqn 6.2 for the purpose of convenient design.

The control input $u_c = \beta$ is varied at regular intervals with a sampling time $T = x_0 T_0$, where x_0 is an integer, and $T_0 = (2\pi/w_0) = 1/f_0$ is the fundamental period of fin oscillation. The pitch bias angle in the sampled form is given by

$$u_c(t) = u_c(kT) = u_{ck}, t \in [kT, (k+1)T), k = 0, 1, 2, \dots \quad (6.3)$$

and discretizing the linear vector differential equation, one obtains discrete-time representation from Eqn 6.2 given by

$$\begin{aligned} x[(k+1)T] &= A_d x(kT) + B_d u_{ck} + D_d \\ y(kT) &= C_p x(kT) \end{aligned} \quad (6.4)$$

where A_d and B_d are the discretized constant matrices and D_d is a constant vector. Of course

A_d , B_d and D_d are unknown. Readers may find a complete derivation of the discrete-time model in [17]. We now need to estimate A_d , B_d and D_d .

The system Eqn 6.4 is found to be observable and can be conveniently expressed in observable canonical form. A state transformation of system Eqn 6.4 exists, where $v = Qx$. The new system is of the form [36]

$$v[(k+1)T] = \begin{bmatrix} -a_3 & 1 & 0 & 0 \\ -a_2 & 0 & 1 & 0 \\ -a_1 & 0 & 0 & 1 \\ -a_0 & 0 & 0 & 0 \end{bmatrix} v(kT) + \begin{bmatrix} b_3 \\ b_2 \\ b_1 \\ b_0 \end{bmatrix} u_{ck} + \begin{bmatrix} d_{u3} \\ d_{u2} \\ d_{u1} \\ d_{u0} \end{bmatrix}$$

$$\triangleq A_0 c(kT) + B_0 u_{ck} + D_0$$

$$y(kT) = \begin{bmatrix} 1 & 0 & 0 & 0 \end{bmatrix} x(kT) = C_d v(kT) \quad (6.5)$$

where $A_0 = QA_dQ^{-1}$, $B_0 = QB_d$, $C = C_pQ^{-1}$, $D_0 = QD_d$, and $v(kT)=[v_1(kT), \dots, v_4(kT)]$ is the new state vector. The transfer function of the BAUV relating $y(kT)$ and $u_c(kT)$ is given by

$$G(z) = \frac{b_3z^3 + b_2z^2 + b_1z + b_0}{z^4 + a_3z^3 + a_2z^2 + a_1z + a_0} = \frac{N(z, n_z)}{P(z, n_p)} \quad (6.6)$$

where $n_z = (b_0, b_1, b_2, b_3)$ and $n_p = (a_0, a_1, a_2, a_3)$ are the numerator and denominator polynomials of $G(z)$. z is the z -transform variable. we are interested in obtaining estimates of the unknown parameters b_i and a_i . Using Eqn 6.5, the linearly parametric output equations are given by

$$y[(k+1)T] = -a_3y(kT) + v_2(kT) + b_3u_{ck} + d_{u3}$$

$$y[(k+2)T] = -a_3y[(k+1)T] - a_2y(kT) + v_3(kT) + b_3u_{c(k+1)} + b_2u_{ck} + d_{u3} + d_{u2}$$

$$y[(k+3)T] = -a_3y[(k+2)T] - a_2y[(k+1)T] - a_1y(kT) + v_4(kT) + b_3u_{c(k+2)}$$

$$+b_2u_{c(k+1)} + b_1u_{ck} + d_{u3} + d_{u2} + d_{u1}$$

$$\begin{aligned} y[(k+4)T] = & -a_3y[(k+3)T] - a_2y[(k+2)T] - a_1y[(k+1)T] - a_0y(kT) + b_3u_{c(k+3)} \\ & + b_2u_{c(k+2)} + b_1u_{c(k+1)} + b_0u_{ck} + d_{u3} + d_{u2} + d_{u1} + d_{u0} \end{aligned} \quad (6.7)$$

z is the discrete domain operator, (i.e. $z(kT) = [(k+1)T]$), Using Eqn 6.7

$$z^4y(kT) = (b_3z^3 + b_2z^2 + b_1z + b_0)u_{c(kT)} - (a_3z^3 + a_2z^2 + a_1z + a_0)y(kT) + d^* \quad (6.8)$$

where d^* is a constant. For identifying the unknown parameters b_i , a_i and d^* , we consider a stable parameter estimator polynomial of the form

$$\Lambda(z) = z^4 + \lambda_3z^3 + \lambda_2z^2 + \lambda_1z + \lambda_0 \quad (6.9)$$

Then operating Eqn 6.8 by $\Lambda^{-1}(z)$ gives

$$\frac{z^4}{\Lambda(z)}y(kT) = \frac{b_3z^3 + b_2z^2 + b_1z + b_0}{\Lambda(z)}u_{c(kT)} - \frac{a_3z^3 + a_2z^2 + a_1z + a_0}{\Lambda(z)}y(kT) + \frac{d^*}{\Lambda(z)} \quad (6.10)$$

We note that

$$z^4\Lambda^{-1}(z) = 1 - (\lambda_3z^3 + \lambda_2z^2 + \lambda_1z + \lambda_0)\Lambda^{-1}(z)$$

Eqn 6.10 gives

$$\begin{aligned} y(kT) = & \frac{b_3z^3 + b_2z^2 + b_1z + b_0}{\Lambda(z)}u_{c(kT)} + \\ & \frac{[(\lambda_3 - a_3)z^3 + (\lambda_2 - a_2)z^2 + (\lambda_1 - a_1)z + (\lambda_0 - a_0)]}{\Lambda(z)}y(kT) + \frac{d^*}{\Lambda(z)} \end{aligned} \quad (6.11)$$

The unknown numerator and denominator coefficients of the BAUV system transfer function are expressed in the parametric vector form

$$\theta_p^* = [b_0, b_1, b_2, b_3, (\lambda_0 - a_0), (\lambda_1 - a_1), (\lambda_2 - a_2), (\lambda_3 - a_3), d^*]^T \in R^9$$

$$\begin{aligned} \phi_p(kT) = & \left[\frac{1}{\Lambda(z)}u_{c(kT)}, \frac{z}{\Lambda(z)}u_{c(kT)}, \right. \\ & \left. \frac{z^2}{\Lambda(z)}u_{c(kT)}, \frac{z^3}{\Lambda(z)}u_{c(kT)}, \frac{1}{\Lambda(z)}y(kT), \frac{z}{\Lambda(z)}y(kT), \right. \end{aligned}$$

$$\left[\frac{z^2}{\Lambda(z)} y(kT), \frac{z^3}{\Lambda(z)} y(kT), \Lambda^{-1}(z) 1 \right]^T \in R^9 \quad (6.12)$$

where, $\phi_p(kT)$ is the regressor vector. Eqn 6.11 can be written as

$$y(kT) = \theta_p^{*T} \phi_p(kT) \quad (6.13)$$

The regressor vector $\phi_p(kT)$ is obtained from $\beta(kT)$, $y(kT)$ and the unit step sequence. There exist many parameter identification schemes to obtain an estimate of the parameter vector θ^* . For simplicity, here a normalized gradient algorithm is considered for the identification of these parameters.

Let the $\theta_p(kT)$ be an estimate of θ_p^* . Define the estimation error

$$\epsilon(kT) = \theta_p^T(kT) \phi_p(kT) - y(kT), \quad k \in 0, 1, 2, \dots \quad (6.14)$$

Using Eqn 6.13 in Eqn 6.14 gives

$$\epsilon(kT) = \tilde{\theta}_p^T(kT) \phi_p(kT)$$

where

$$\tilde{\theta}_p(kT) = \theta_p(kT) - \theta_p^* \quad (6.15)$$

is the parameter error vector. For the derivation of the identifier [13, 40], a normalized quadratic cost function

$$J(\theta) = \frac{\epsilon^2}{2m^2} = \frac{\tilde{\theta}_p^T(kT) \phi_p(kT) \phi_p^T(kT) \tilde{\theta}_p(kT)}{m^2} \quad (6.16)$$

is minimized, where m is the normalizing signal. The steepest descent direction of $J(\theta_p)$ is $-\left(\frac{\partial J}{\partial \theta}\right) = -\left(\frac{\epsilon}{m^2} \phi_p(kT)\right)$, which suggests the adaptive update law for $\theta_p(kT)$ given by

$$\begin{aligned} \theta_p[(k+1)T] &= \theta_p(kT) - \frac{\Gamma \phi_p(kT) \epsilon(kT)}{\kappa_0 + \phi_p^T(kT) \phi_p(kT)} \\ \theta_p(0) &= \theta_{p0}, k \in 0, 1, 2, \dots \end{aligned} \quad (6.17)$$

where Γ is a positive definite symmetric matrix (denoted as $\Gamma > 0$) satisfying $0 < \Gamma < 2I$ (I denotes an identity matrix), the normalizing signal $m = [k_0 + \phi_p^T(kT)\phi_p(kT)]^{\frac{1}{2}}$, and $k_0 > 0$ being a design parameter.

The stability analysis of this identifier can be done using a Lyapunov function

$$V(\tilde{\theta}_p) = \tilde{\theta}_p^T \Gamma^{-1} \tilde{\theta}_p \quad (6.18)$$

and then showing that

$$V(\tilde{\theta}_p(k+1)T) - V(\tilde{\theta}_p(kT)) \leq -\alpha_1 \frac{\epsilon^2(kT)}{m^2(kT)} \quad (6.19)$$

for $\alpha_1 = (2 - \lambda_{max}(\Gamma)) > 0$, where $\lambda_{max}(\cdot)$ denotes the maximum eigenvalue of Γ . Using Eqn 6.19, one can show that the algorithm Eqn 6.16 guarantees that $\theta(kT), \frac{\epsilon(kT)}{m(kT)} \in L^\infty$ (the set of bounded sequences) and $\frac{\epsilon(kT)}{m(kT)}, (\theta[(k+1)T] - \theta(kT)) \in L^2$ (the set of square summable sequences). (See [40] for the details.)

The elements of the regressor vector $\theta_p(kT)$ can be obtained using two filters having state variable forms given by

$$\begin{aligned} w_1[(k+1)T] &= A_\lambda w_1(kT) + b_\lambda u(kT), \\ w_2[(k+1)T] &= A_\lambda w_2(kT) + b_\lambda y(kT) \end{aligned} \quad (6.20)$$

where $w_i \in R^4$,

$$A_\lambda = \begin{bmatrix} 0 & 1 & 0 & 0 \\ 0 & 0 & 1 & 0 \\ 0 & 0 & 0 & 1 \\ -\lambda_0 & -\lambda_1 & -\lambda_2 & -\lambda_3 \end{bmatrix}, \quad b_\lambda = \begin{bmatrix} 0 \\ 0 \\ 0 \\ 1 \end{bmatrix}$$

Then it easily follows that $\phi_p(kT) = [w_1^T(kT), w_2^T(kT), \Lambda^{-1}(z)1]^T$. A simplification in the regressor is possible if one ignores the exponentially decaying signal of $\Lambda^{-1}(z)1$. Since $\Lambda^{-1}(z)1$

tends to the constant sequence $\lambda_f = (1 + \lambda_0 + \lambda_1 + \lambda_2 + \lambda_3)^{-1}$, one can replace ϕ_{p9} by λ_f^{-1} , where ϕ_{pi} denotes the i^{th} elements of ϕ_p .

6.3 Adaptive Output Feedback Control Law

The parameter identifier designed in the previous section provides an estimate of the unknown numerator and denominator coefficients of the transfer function in Eqn 6.6, and the constant d^* . In this section an indirect adaptive output feedback method will be used for the control of BAUV for tracking constant trajectories. The adaptive control law is designed to counter the effects of the constant disturbance input D_0 as well.

For a reference output signal $z_r(kT)$, satisfying the

$$Q_m(z)z_r(kT) = 0$$

and for a disturbance input satisfying

$$Q_m(z)D_0 = 0 \tag{6.21}$$

where, $Q_m(z)$ is a monic polynomial, an output feedback control input is to be found for asymptotic tracking of $z_r(kT)$. A constant signal in the z -domain is given by, $y_{ms}(z) = l_1 \frac{z}{z-1}$ ($l_i \in R$), $Q_m(z) = (z - 1)$. According to the internal model principle, $Q_m^{-1}(z)$ should be operated with the transfer function ($G(z)$) of the BAUV for solving the output regulation problem [43].

The adaptive control law is designed using a two step approach. First the parameters of the BAUV Eqn 6.4 are considered to be known, but the disturbance signal D_0 is assumed to be unknown, and a control law is derived. Once this control law is obtained with known system parameters, then an adaptive control law is designed to adaptively update the control law parameters from the adaptive estimates of the parameter of the plant (Eqn 6.4) to be

controlled. The stabilizer includes $Q_m^{-1}(z)$ in the forward path. The structure of the closed-loop system is shown in Figure. 6.1. For the controller design, it is required to find the polynomials $C(z)$ and $D(z)$ such that the closed-loop system is asymptotically stable [43].

The control law is given by

$$u_{c(kT)} = \left[\frac{D(z, n_d)}{C(z, n_c)Q_m(z)} \right] (z_r(kT) - z_d(kT)) \quad (6.22)$$

where the stabilizer polynomials D and C are chosen as

$$\begin{aligned} C(z, n_c) &= z^3 + c_2z^2 + c_1z + c_0 \\ D(z, n_d) &= d_4z^4 + d_3z^3 + d_2z^2 + d_1z + d_0 \end{aligned} \quad (6.23)$$

and stabilizer parameter vectors n_c and n_d are given by

$$\begin{aligned} n_c &= (c_0, c_1, c_2) \in R^{n-1} = R^3 \\ n_d &= (d_0, d_1, \dots, d_4) \in R^{n+n_q} = R^5 \end{aligned} \quad (6.24)$$

The degree of the monic polynomial C is given by

$$\delta(C) = (n - 1)$$

where, the state vector x is of dimension $n = 4$ (degree of a polynomial is denoted as δ), and the degree of the numerator polynomial of the stabilizer is given by $\delta(D) = n + n_q - 1 = 4$, where $n_q = \delta(Q_m)$.

By knowing the parameters $N(z, n_z)$ and $P(z, n_p)$, we can use the pole placement control to determine the parameters $D(z, n_d)$ and $C(z, n_c)$ of the stabilizer. A stable monic polynomial $F^*(z)$ with $\delta(F^*) = 2n + n_q - 1 = 8$ of the form

$$F^*(z) = z^8 + f_7z^7 + f_6z^6 + \dots + f_1z + f_0 \quad (6.25)$$

is considered. An appropriate choice of the zeros of F^* has to be made, such that all its zeros are in $|z| < 1$. The closed-loop system with both the parameter identifier and the stabilizer is shown in Figure. 6.1, whose characteristic polynomial is given by

$$\Psi(z) = C(z, n_c)Q_m(z)P(z, n_p) + D(z, n_d)N(z, n_z) \quad (6.26)$$

For the purpose of pole placement control scheme, we have $\Psi(z) = F^*(z)$, further

$$C(z, n_c)Q_m(z)P(z, n_p) + D(z, n_d)N(z, n_z) = F^*(z) \quad (6.27)$$

From Eqn. 6.27, $C(z, n_c)$ and $D(z, n_d)$ can be determined, only if $N(z, n_z)$ and $P(z, n_p)$ are known. Further, for the validation of Eqn 6.27 $N(z, n_z)$ and $(Q_m(z)P(z, n_p))$ need to be co-prime. It is found that that, for the BAUV model in yaw plane the polynomials $N(z, n_z)$ and $P(z, n_p)$ are co-prime. Also, the zeros of $G(z)$ are not the same as the zeros of $Q_m(z)$. (The calculation of (c_i, d_i) of C and D are shown in the appendix II.B.1).

Our objective is to ensure that the tracking error converges to zero. This is made possible by the internal model consisting the reference input signal and the constant disturbance input signal (exosystem) in the forward path. The closed-loop system is found to be stable and hence the tracking error converges to zero.

The control law in Eqn 6.22 can be expressed in a linearly parameterized form [40]. For manipulation of the control law in Eqn 6.22 we introduce a monic stable stabilizer polynomial $\Psi_\mu(z)$ of the form

$$\Psi_\mu(z) = z^4 + \mu_3 z^3 + \mu_2 z^2 + \mu_1 z + \mu_0 \quad (6.28)$$

where, $(\delta(\Psi_\mu(z)) = n + n_q - 1 = 4)$. Operating Eqn 6.22 by $\Psi_\mu^{-1}(z)$ gives

$$u_c(kT) = (\Psi_\mu(z) - C(z, n_c)Q_m(z)) \frac{1}{\Psi_\mu(z)} u_c(kT) + D(z, n_d) \frac{1}{\Psi_\mu(z)} [z_r(kT) - y(kT)] \quad (6.29)$$

Since Ψ_μ and CQ_m are monic polynomials $\delta(\Psi_\mu - CQ_m) < \delta(\Psi_\mu)$. Define

$$\Psi_\mu(z) - C(z, n_c)Q_m(z) = [l_0, l_1, l_2, l_3] \nu(z) \triangleq l^T \nu(z)$$

$$D(z, n_d)\Psi_\mu^{-1}(z) = d_4 + [d_{a0}, d_{a1}, d_{a2}, d_{a3}]\nu(z) \triangleq d_4 + d_a^T\nu(z) \quad (6.30)$$

where $\nu(z) = [1, z, z^2, z^3]^T \in R^4$. (The vectors l and d_a are given in the appendix II.B.2.) The control law Eqn 6.29 can now be written in the form

$$u_{c(kT)} = l^T w_\beta(kT) + d_a^T w_e(kT) + d_4[z_r(kT) - z_d(kT)] \quad (6.31)$$

where $w_\beta(kT)$ and $w_e(kT)$ satisfy the state equations

$$w_\beta[(k+1)T] = A_\mu w_\beta(kT) + B_\mu u_{c(kT)}$$

$$w_e[(k+1)T] = A_\mu w_e(kT) + B_\mu(z_r(kT) - z_d(kT)) \quad (6.32)$$

where

$$A_\mu = \begin{bmatrix} 0 & 1 & 0 & 0 \\ 0 & 0 & 1 & 0 \\ 0 & 0 & 0 & 1 \\ -\mu_0 & -\mu_1 & -\mu_2 & -\mu_3 \end{bmatrix} \quad B_\mu = \begin{bmatrix} 0 \\ 0 \\ 0 \\ 1 \end{bmatrix} \quad (6.33)$$

For the derivation of the control law Eqn 6.31, the parameters of the model were assumed to be known. Now an adaptive control law design is considered, with unknown BAUV model parameters. By certainty equivalence principle, parameter estimate θ_p of θ_p^* is assumed to be true parameter vector of the BAUV and the compensator is designed. The stabilizer parameter vectors are calculated at each sampling instant, for every value of the parameter estimate. The modified stabilizer equation is given

$$C(z, n_c)Q_m(z)P(z, \hat{n}_p) + D(z, n_d)N(z, \hat{n}_z) = F^*(z) \quad (6.34)$$

where $\hat{n}_z = (\hat{b}_0, \hat{b}_1, \hat{b}_2, \hat{b}_3)$ and $\hat{n}_p = (\hat{a}_0, \hat{a}_1, \hat{a}_2, \hat{a}_3)$ are estimated at every sampling instant from a_i and b_i . The stabilizer vectors n_c and n_d are updated at each sampling instant based on the estimated BAUV system parameters. The vectors l , d_a and d_4 are also computed at

each sampling instant to obtain the control law Eqn 6.31. It is seen that the tracking error $z_d(kT) - z_r(kT)$ converges to zero [13] and all the signals are bounded.

Remark 1: For convenience, the polynomials $\Lambda(z)$, $F^*(z)$ and $\Psi_\mu(z)$ are taken as $\Lambda(z) = z^4$, $F^*(z) = z^8$ and $\Psi_\mu(z) = z^4$.

Remark 2: The designed servoregulator also has the capability to reject arbitrary periodic wave forces on the BAUV at each sampling instant, provided, the frequency of the wave forces are known. Also, the frequency of the wave force disturbance should coincide with the frequency of oscillation the fin. The control law already has the capability to reject any constant disturbance input D_0 .

6.4 Simulation Results For Depth Trajectory Tracking

In this section, simulation results for the depth trajectory tracking of the closed-loop system Eqn 6.1 and Eqn 6.2 using MATLAB/SIMULINK are presented. The nonlinear BAUV system parameters are taken from [17]. The vehicle parameters are $l = 1.282$ m , $m = 4.1548$ kg, $I_y = 0.5732$ kgm², $x_G = 0$, and $Z_G = 0.578802 \times 10^{-8}$ m. The hydrodynamic parameters for the forward velocity of 0.8 m/sec are $z'_q = -0.825 \times 10^{-5}$, $z'_w = -0.825 \times 10^{-5}$, $z'_q = -0.238 \times 10^{-2}$, $z'_w = -0.738 \times 10^{-2}$, $M'_q = -0.16 \times 10^{-3}$, $M'_w = -0.825 \times 10^{-5}$, $M'_q = -0.117 \times 10^{-2}$, and $M'_w = 0.314 \times 10^{-2}$. The pectoral fins are attached at a distance of $d_{cgd} = 0.03$ m. The BAUV is assumed to be moving with a constant forward velocity of 0.8 m/sec. The pectoral fins are considered to be oscillating at a frequency of $\omega_f = 8$ Hz.

A fixed Strouhal number $S_t = 0.6$ is used for the calculation of normal fin forces and control moment, where $S_t = \frac{c_h f}{U_\infty}$, U_∞ is 0.8 m/sec, f is the frequency of the fin oscillation and c_h is the chord of the foil. Then the values of f_a, f_b, m_a, m_b for $M=4$ are

$$f_a = (0, -6.8175, -8.2597, -0.1748, 0.1311, -0.3496, -4.0643, 0, 0)$$

$$f_b = (74.3671, -11.0173, -26.0410, -38.5607, -21.0331, -3.2551, 2.2535, 5.5087, 2.2535)$$

$$m_a = (0, 0.0803, 0.1193, 0.0023, 0, 0, -0.0138, 0.0023, 0)$$

$$m_b = (-0.6178, -0.3681, 0.2235, -0.1840, -0.0263, -0.0526, -0.0131, 0.0131, 0.0263)$$

These parameters are obtained using the Fourier decomposition of the fin force and moment, and are computed by multiplying the Fourier coefficients by $\frac{1}{2}\rho.W_a.U_\infty^2$ and $\frac{1}{2}\rho.W_a.c_h.U_\infty^2$, respectively, where W_a is the surface area of the foil. For simulation, the initial conditions of the vehicle are assumed to be $x(0) = 0$.

Although, the design has been done to track constant reference trajectories, simulation for tracking of constant and sinusoidal time-varying reference trajectories is considered. Furthermore, nonlinear functions of Eqn 6.2 are retained for simulation. The objective is reference command tracking and constant disturbance input rejection. The BAUV is controlled to move at a constant forward velocity of 0.8 m/sec by some control mechanism. The pectoral fins are attached between the cg and the nose of the vehicle. The number of unstable zeros in the transfer function of the BAUV model depends of the distance (d_{cgd}) of the fin from the cg . It is found that for any choice of values of the d_{cgd} , there is at least one unstable zero present in the discretized BAUV model transfer function, hence the system is always non-minimum phase. The modification of the controlled output variable to derive a minimum phase system is discussed in [17]. Since, the adaptive closed-loop feedback control law is applicable to both minimum phase and non-minimum phase systems, we leave the system to be in non-minimum phase form, with one zero outside the unit disk in the complex plane. It is found that there is a single unstable zero if the fins are attached closer to the cg , but two unstable zeros are present if the fin distance from the cg exceeds a critical value. In our case, d_{cgd} is chosen such that the BAUV transfer function has only one unstable zero.

The stabilizer designed for the indirect adaptive control law is in discrete form. Hence the control input u_c is sampled and changed to a new value at $T = T_0$ sec, where $T_0 = 1/f$ is the fundamental period of the fin force (f_d) and moment (m_d). The update law is given by Eqn 6.22. The gains in Eqn 6.22 are chosen as $\Gamma = 0.01I_{9 \times 9}$, $0 < \Gamma < 2I$ and k_o is set to 1. The simulation results are obtained for a reference depth of 2 meters in the dive plane, for both constant and sinusoidal trajectories. The distance of the fin d_{cgd} from the cg is critical and is chosen to be 0.02 m. For this value of d_{cgd} the discrete-time BAUV system is found to be in non-minimum phase with one unstable zero at 24.3685 (outside the unit circle in the complex plane). The other zero and pole values for the BAUV transfer function are 24.3685, -0.2261, 0.5540 and 1.0000, 0.3675, 0.9854, 1.0000, respectively. The parameter coefficients for the parameter identifier ($\lambda_i, i = 0, 1, 2, 3$ and the stabilizer $\mu_i, i = 0, 1, \dots, 3$) are taken as zero, for convenient design.

The zero and pole locations of the stabilizer transfer function is calculated by Eqn 6.34. For this purpose, it is necessary to assign the zero location for the stable monic polynomial $F^*(z)$ in Eqn 6.34. There is no standard procedure to determine the zero locations and a pole matching technique is employed here. It is to be noted that better responses for the closed-loop system can be obtained by appropriately choosing the zeros of $F^*(z)$. In our case, we have chosen $F^*(z)$ to be

$$F^*(z) = z^4(z^2 - 0.1^2)(z - 0.3)(z + 0.2)$$

Case I: Dive plane depth control, constant depth reference trajectory, $z_r = 2$ m, fin oscillation frequency 8 Hz, parameter uncertainty: +20 %

The complete closed-loop systems Eqn 6.2 and Eqn 6.31 are simulated for a fin oscillation frequency of 8 Hz. A constant reference trajectory z_r converging to $z_r^* = 2$ m is taken. Simulation results are shown for a constant reference trajectory with a depth magnitude of 2

m. Of course, the designed adaptive control law will steer the BAUV to any given reference depth, but it will take a longer time to attain the steady state target depth and also the control input required will be higher. The output response characteristics also depend on the nature of the input reference command. Here, the reference trajectory is carefully chosen using appropriate command shaping methods to ensure a smooth maneuver of the BAUV to the target depth at smaller bias angles. The command trajectory $z_r(t)$ is given by

$$z_r = z_r^* * \frac{\pi}{180} * [1 - \exp(0.09 * v * T)]$$

where $z_r^* = 2$ m, v is just a simulation variable which is introduced for input command shaping. It is incremented from 0 to 1 in steps of 0.01. In the update control law Eqn 6.22, the initial estimate parameter uncertainty considered is +20% of the actual vector θ_p^* , $\theta_p(0) = 1.2\theta_p^*$. The simulation results are shown in Figure. 6.2. It is observed that the BAUV reaches the target depth accurately in about 35 secs. The maximum control input required is around 40 deg. After the initial transient phase which lasts for around 2 secs, the bias angle required gradually tends to zero. The maximum control input of 40 deg can be supplied by the pectoral fins. Of course, the control input to be provided can be shared between multiple oscillating fins, which also reduce the time taken to attain the target reference depth. The pitching angle goes up to a maximum of 1 deg and then slowly begins to oscillate around zero once the transient phase is overcome. The normal force (f_d) and the control moment (m_d) produced by the oscillating fins are around 50 N and 0.3 Nm, respectively. Once the control bias angle input falls to zero, the control force and moment begin to oscillate with zero offset making the time average zero. Even though the bias angle is zero in steady state, there is still a forward thrust present which is necessary for the propulsion of the vehicle in the forward direction. In spite of the parameter uncertainties, reference trajectory tracking is achieved in the dive plane and also the the impact of the input disturbance vector is nullified.

Case II: Dive plane depth control, Sinusoidal depth reference trajectory, $z_r = 2$ m, fin oscillation frequency 8 Hz, parameter uncertainty: +20 %

The adaptive control law was designed to track the constant reference trajectories. The internal model of the exosignals was obtained only for constant reference trajectory. Hence, the transfer function $Q_m^{-1}(z)$ was derived as $\frac{1}{z-1}$. Despite the adaptive control law design restricted to constant command tracking alone, it was observed that the accurate tracking of sinusoidal commands can also be accomplished. The initial estimate parameter uncertainty considered is +20% of the actual vector θ_p^* , $\theta_p(0) = 1.2\theta_p^*$. The sinusoidal reference input is of the form

$$z_r = z_r^* * \frac{\pi}{180} * [1 - \exp(0.09 * v * T)] * [\sin(0.5 * v * T)]$$

where $z_r^* = 2$ m, v is just a simulation variable which is introduced for input command shaping. It is incremented from 0 to 1 in steps of 0.01. The simulation results are shown in Figure. 6.3. It is observed that the response of the actual output quickly converges to the reference command trajectory. The maximum input bias angle required is around 60 deg. This higher value of the bias angle is attributed to the time-varying reference trajectory. Though the control input required is 60 deg, it can still be supplied by the pectoral fins. The steady state value of the bias angle is zero. The pitch angle (θ) is observed to around 2 deg. The pitch angle reduces to zero after the initial transient phase. The fin control force (f_d) and moment (m_d) are 80 N and 0.5 Nm, respectively.

The simulations were also performed for under-estimated initial values. It has been found that better closed-loop responses are obtained for the over-estimation of the initial estimate $\theta_p(0)$.

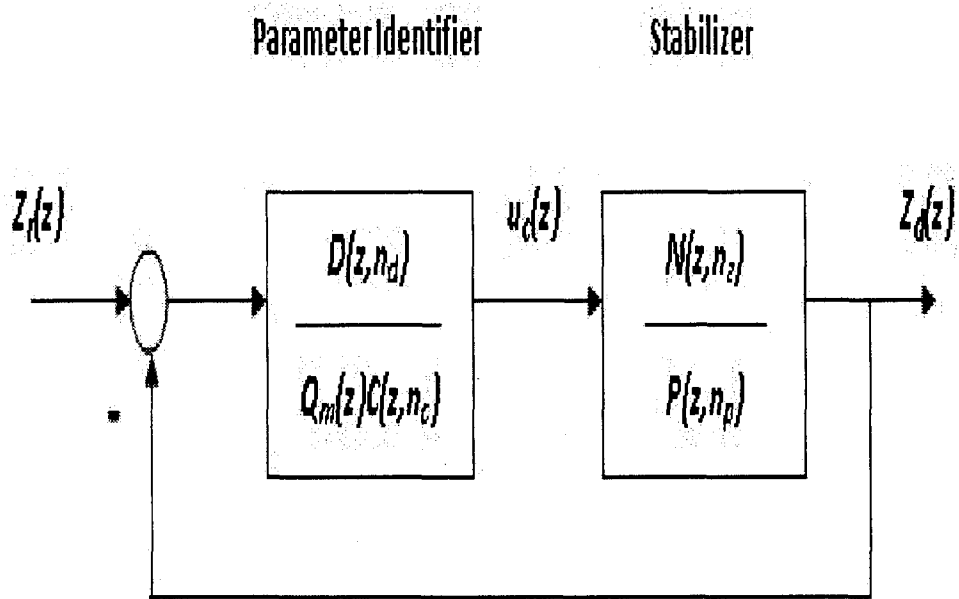


Figure 6.1: Closed-loop BAUV system

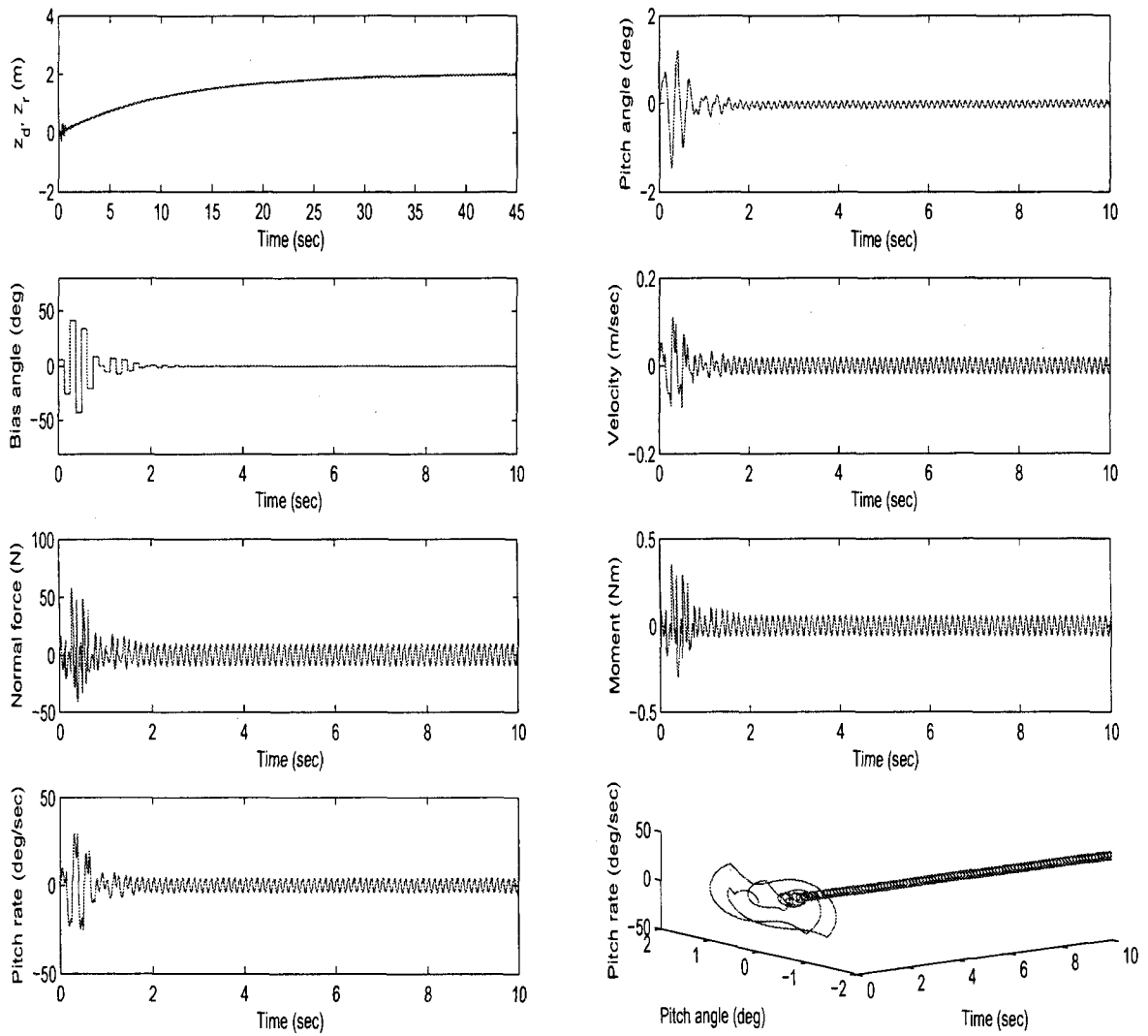


Figure 6.2: BAUV depth control for constant reference command, frequency of fin oscillation $\omega_f = 8$ Hz, parameter uncertainty: + 20 %
 (a) Dive plane depth, z_d , and Reference depth, z_r (m), (b) Pitch angle, θ (deg), (c) Bias angle (deg), (d) Velocity (m/sec), (e) Normal force (N), (f) Moment (Nm), (g) Pitch rate (deg/sec), (h) Pitch rate (deg/sec), and Pitch angle (deg).

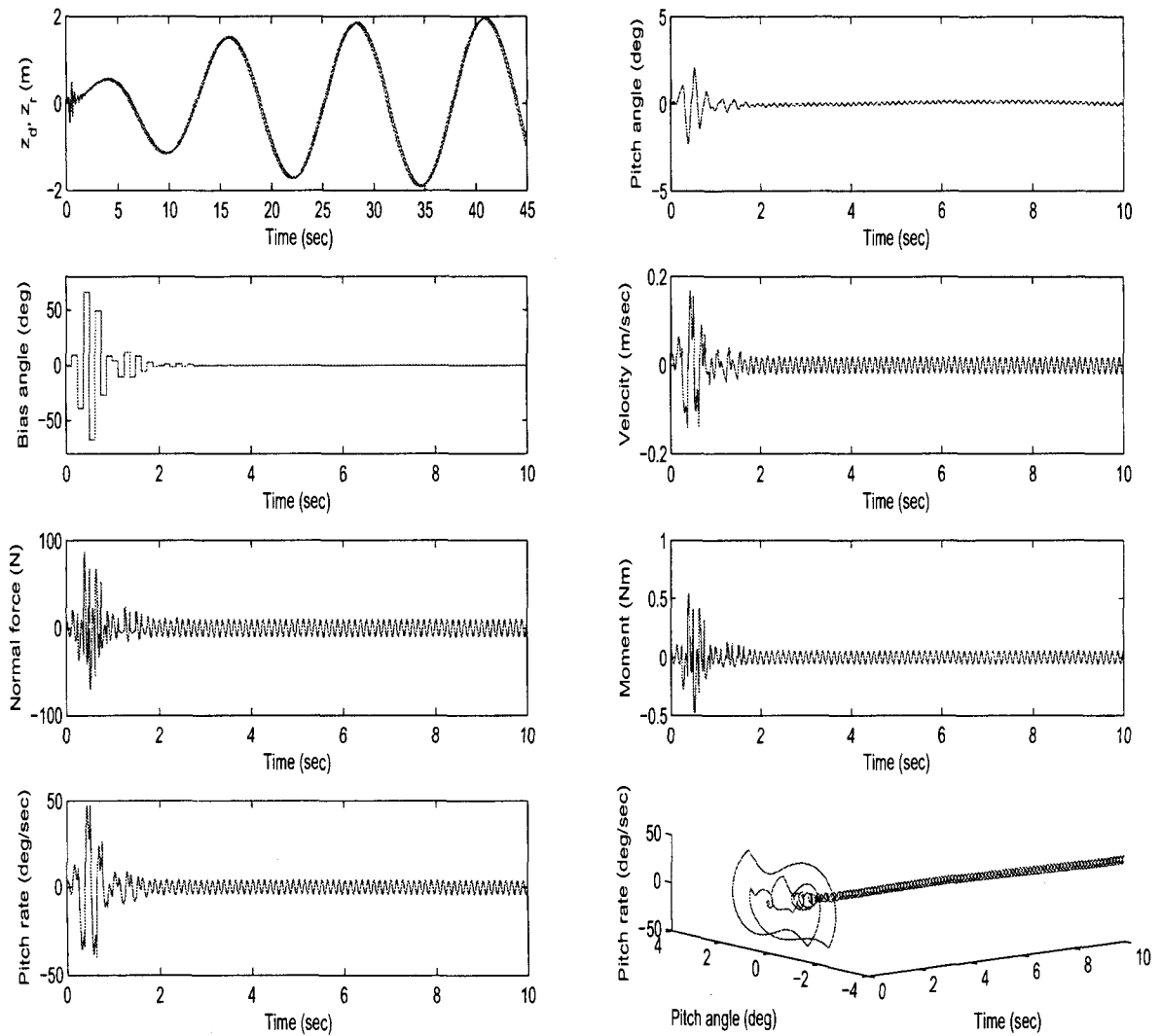


Figure 6.3: BAUV depth control for sinusoidal reference command, frequency of fin oscillation $\omega_f = 8$ Hz, parameter uncertainty: + 20 %
 (a) Dive plane depth, z_d , and Reference depth, z_r (m), (b) Pitch angle, θ (deg), (c) Bias angle (deg), (d) Velocity (m/sec), (e) Normal force (N), (f) Moment (Nm), (g) Pitch rate (deg/sec), (h) Pitch rate (deg/sec), and Pitch rate (deg).

CHAPTER 7

CONCLUSION

In this research work, multiple control design methods were analyzed for the control of an BAUV in yaw and dive planes using pectoral-like fins. Also, both continuous-time and discrete-time controllers were designed and their performances were simulated. The mathematical model of the BAUV had inherent nonlinearities present in them. For control law design, the nonlinearities were neglected, whereas, the original BAUV system model was considered for simulation. For all the different control designs implemented, the bias angle of the fin was taken as the lone control input. Depending on the planar motion of the BAUV, the output variable was either the depth (dive plane) or the yaw angle (yaw plane).

In chapter 3, an adaptive servoregulator was designed for the control of BAUVs in yaw plane. The parameters of the BAUV model including the hydrodynamic coefficients are unknown. The adaptive controller could be efficiently designed without the knowledge of the system parameters. For design purposes, averaging of the fin force and moment was done. The yaw angle and its derivative alone were considered for feedback. The designed controller required the tuning of a single gain alone. Simulation results showed that the set point control of the yaw angle was achieved in spite of the uncertainties in the system parameters. Also, the performance of the controller was examined for perturbations in the fin force and control moment.

In chapter 4, a new design methodology for the control of BAUVs using pectoral-like os-

cillating fins was presented. For the dive plane control, a pair of pectoral-like harmonically heaving and pitching fins were used. The bias angle of pitch motion of the fin was treated as a control input. For the purpose of design, an exosystem of third-order was introduced and the original time-varying nonlinear system was embedded in a larger class of time-invariant nonlinear system. For robust design, an internal model of k -fold exosystem was introduced. The augmented system, including the internal model, was stabilized using optimal control theory. In the closed-loop system including the internal model of the k -fold exosystem, harmonic components of order up to k of the tracking error are suppressed. This special property is not possible using averaging method or discretization approach reported in literature. A simple servocompensator using only integral error feedback and a fifth-order servocompensator were designed. Simulation results were obtained, which showed robust depth control performance. Interestingly, the internal model of 2-fold exosystem was capable of attenuating the depth tracking error to a negligible level in spite of uncertainties in the system parameters. It was seen that flexibility exists in the choice of weighting matrices for shaping responses using optimal control theory. In chapter 5, similar design methodology was adopted for the control BAUVs in yaw plane.

In chapter 6, an indirect adaptive closed-loop control law was designed for the depth control of a BAUV in the dive plane using mechanical pectoral fins. The pectoral fins were considered to be oscillating with pitching and heaving motions. The oscillating fins produce periodic forces. The control force and moment coefficients of the fins are computed using Fourier decomposition methods. The control force produced by the pectoral fins is a function of the bias angle. The bias angle is taken as the control input. The depth variable z_d is taken as the output variable. Since the hydrodynamic coefficients and the system parameters of the BAUV model are unknown, a parameter identifier was designed to determine the system

parameters. For the convenient design of a parameter estimator, a sampled-data control system was derived. The transfer function of the BAUV model was found to be non-minimum phase, with one unstable zero. An adaptive feedback control law was designed for the reference command tracking and the rejection of constant input disturbance. The depth tracking error was also desired to converge to zero. For the purpose of control law design, an internal model of exosignals was obtained for constant reference signals. The pole-zero coefficients of the stabilizer were determined using pole matching methods. Simulation results showed that an precise depth trajectory tracking can be achieved in spite of the uncertainties in the system parameters. Though the control law was designed for constant reference trajectory tracking, it was observed that accurate sinusoidal trajectory tracking can also be achieved.

The advantage of the adaptive control law lies in its application to both minimum-phase and non-minimum phase BAUV models.

APPENDIX I

SYSTEM PARAMETERS

1. Hyrdrodynamic coefficents for BAUV model in dive plane[6]

$$l = 1.282 \text{ m}$$

$$m = 4.1548 \text{ kg}$$

$$I_y = 0.5732 \text{ kgm}^2$$

$$x_G = 0$$

$$Z_G = 0.578802 \times 10^{-8} \text{ m}$$

$$U = 0.8 \text{ m/sec}$$

$$z'_q = -0.825 \times 10^{-5}$$

$$z'_w = -0.825 \times 10^{-5}$$

$$z'_q = -0.238 \times 10^{-2}$$

$$z'_w = -0.738 \times 10^{-2}$$

$$M'_q = -0.16 \times 10^{-3}$$

$$M'_{\dot{w}} = -0.825 \times 10^{-5}$$

$$M'_q = -0.117 \times 10^{-2}$$

$$M'_w = 0.314 \times 10^{-2}.$$

2. Hyrdrodynamic coefficents for BAUV model in yaw plane[35]

$$l = 1.391 \text{ m}$$

$$\text{mass}(m) = 18.826 \text{ kg}$$

$$I_z = 1.77 \text{ kgm}^2$$

$$X_G = -0.012$$

$$Y_G = 0$$

$$U = 0.8 \text{ m/sec}$$

$$Y_{\dot{r}} = -0.3781$$

$$Y_{\dot{v}} = -5.6198$$

$$Y_r = 1.1694$$

$$Y_v = -12.0868$$

$$N_{\dot{r}} = -0.3781$$

$$N_{\dot{v}} = -0.8967$$

$$N_r = -1.0186$$

$$N_v = -4.9587.$$

APPENDIX II

MATHEMATICAL CALCULATIONS

A. Matrices $A_p^{[k]}$ and minimum polynomials

$$A_p^{[2]} = \begin{bmatrix} 0 & 2\omega_f & 0 \\ -\omega_f & 0 & \omega_f \\ 0 & -2\omega_f & 0 \end{bmatrix}$$

$$A_p^{[3]} = \begin{bmatrix} 0 & 3\omega_f & 0 & 0 \\ -\omega_f & 0 & 2\omega_f & 0 \\ 0 & -2\omega_f & 0 & \omega_f \\ 0 & 0 & -3\omega_f & 0 \end{bmatrix}$$

$$A_p^{[4]} = \begin{bmatrix} 0 & 4\omega_f & 0 & 0 & 0 \\ -\omega_f & 0 & 3\omega_f & 0 & 0 \\ 0 & -2\omega_f & 0 & 2\omega_f & 0 \\ 0 & 0 & -3\omega_f & 0 & \omega_f \\ 0 & 0 & 0 & -\omega_f & 0 \end{bmatrix}$$

Computing the minimum polynomials $p^{[1]}(\lambda)$ of $A^{[1]}$ and $p^{[k]}(\lambda)$ of $A_p^{[k]}$ ($k = 2,3,4$), one finds that

$$p^{[1]} = \lambda(\lambda^2 + \omega_f^2)$$

$$p^{[2]} = \lambda(\lambda^2 + (2\omega_f)^2)$$

$$p^{[3]} = (\lambda^2 + \omega_f^2)(\lambda^2 + (3\omega_f)^2)$$

$$p^{[4]} = \lambda(\lambda^2 + (2\omega_f)^2)(\lambda^2 + (4\omega_f)^2)$$

B.1 Stabilizer parameters (c_i, d_i)

The compensator equation Eqn 6.27 can be further expanded as

$$\begin{aligned} & (z^3 + c_2 z^2 + c_1 z + c_0)(z-1)(z^4 + a_3 z^3 + a_2 z^2 + a_1 z + a_0) + (d_4 z^4 + d_3 z^3 + d_2 z^2 + d_1 z + d_0)(b_3 z^3 + b_2 z^2 + b_1 z + b_0) \\ & = z^8 + f_7 z^7 + f_6 z^6 + f_5 z^5 + f_4 z^4 + f_3 z^3 + f_2 z^2 + f_1 z + f_0 \end{aligned} \quad (7.1)$$

and then converted into matrix form as follows

$$\begin{bmatrix} c_0 & d_0 & c_1 & d_1 & c_2 & d_2 & d_3 & d_4 \end{bmatrix} \times S = \begin{bmatrix} f_0 \\ f_1 \\ f_2 \\ (f_3 + a_0) \\ (f_4 - a_0 + a_1) \\ (f_5 - a_1 + a_2) \\ (f_6 - a_2 + a_3) \\ (f_7 + 1 - a_3) \end{bmatrix}^T \quad (7.2)$$

where

$$S = \begin{bmatrix} -a_0 & (a_0 - a_1) & (a_1 - a_2) & (a_2 - a_3) & (a_3 - 1) & 1 & 0 & 0 \\ b_0 & b_1 & b_2 & b_3 & 0 & 0 & 0 & 0 \\ 0 & -a_0 & (a_0 - a_1) & (a_1 - a_2) & (a_2 - a_3) & (a_3 - 1) & 1 & 0 \\ 0 & b_0 & b_1 & b_2 & b_3 & 0 & 0 & 0 \\ 0 & 0 & -a_0 & (a_0 - a_1) & (a_1 - a_2) & (a_2 - a_3) & (a_3 - 1) & 1 \\ 0 & 0 & b_0 & b_1 & b_2 & b_3 & 0 & 0 \\ 0 & 0 & 0 & b_0 & b_1 & b_2 & b_3 & 0 \\ 0 & 0 & 0 & 0 & b_0 & b_1 & b_2 & b_3 \end{bmatrix}$$

Post multiplying Eqn 7.2 by S^{-1} gives the controller parameters (c_i, d_i) .

B.2 The vectors l and d_a of control law

$$d_a = \begin{bmatrix} (d_0 - d_4\mu_0) & (d_1 - d_4\mu_1) & (d_2 - d_4\mu_2) & (d_3 - d_4\mu_3) \end{bmatrix}^T$$
$$l = \begin{bmatrix} (\mu_0 + c_0) & (\mu_1 - c_0 + c_1) & (\mu_2 - c_1 + c_2) & (\mu_3 - c_2 + 1) \end{bmatrix}^T$$

REFERENCES

1. A. Azuma, *The Bio-Kinetics of Flying and Swimming*. Springer-Verlag, New York, 1992
2. P. R Bandyopadhyay, "Trends in Biorobotic Autonomous Undersea Vehicles," *IEEE Journal of Oceanic Engineering*, 30, pp. 109-139, 2005.
3. P. R Bandyopadhyay , D. N Beal and A. Menozzi, "Biorobotic Insights into how Animals Swim," *J. Exp.Biol*, 211, pp. 206-214, 2008
4. P. R Bandyopadhyay , S. N Singh, D. P Thivierge, A. M Annaswamy, H. A Leinhos, A. R Fredette and D. N Beal, "Synchronization of Animal-Inspired Multiple High-Lift Fins in an Underwater Vehicle Using Olivo-Cerebellar Dynamics," *IEEE Journal of Oceanic Engineering*, 33(4), pp. 563-578, 2008.
5. F. E Fish, "Structure and Mechanics of Nonpiscine Control Surfaces," *IEEE Journal of Oceanic Engineering*, 29, pp. 605-621, 2004.
6. T. I Fossen, *Guidance and Control of Oceanic Vehicles*. Wiley Publications, New York, 1994.
7. J. Huang, "Asymptotic Tracking and Disturbance Rejection in Uncertain Nonlinear Systems," *IEEE Transactions on Automatic Control*, 40, pp. 1118-1122, 1995.
8. J. Huang, *Nonlinear Output Regulation: Theory and Applications*. SIAM, Philadelphia, 2004.
9. T. Kailath, *Linear Systems*. Prentice-Hall, Englewood Cliffs, New Jersey, 1980.

10. N. Kato, "Performance in the Horizontal Plane of a Fish Robot with Mechanical Pectoral Fins," *IEEE Journal of Oceanic Engineering*, 25(1), pp. 121-129, 2000.
11. N. Kato, *Pectoral Fin Controllers. Neurotechnology for Biometric Robots*. MIT Press, Cambridge, Massachusetts, pp. 325-350, 2002.
12. G. V Lauder and E. G Drucker, "Morphology and Experimental Hydrodynamics of Fish Fin Control Surfaces," *IEEE Journal of Oceanic Engineering*, 29, pp. 556-571, 2004.
13. M. S Naik and S. N Singh, "Oscillatory Adaptive Yaw-Plane Control of Biorobotic Autonomous Underwater Vehicles Using Pectoral-Like Fins," *Applied Bionics and Biomechanics*, 4(4), pp. 137-147, 2007.
14. M. S Naik, S. N Singh and R Mittal, "Indirect Adaptive Output Feedback Control of a Biorobotic AUV Using Pectoral-Like Mechanical Fins," *Bioinspiration & Biomimetics*, 4(2), 11 pages, 2009.
15. M Narasimhan, H Dong, R Mittal and S. N Singh, "Optimal Yaw Regulation And Trajectory Control of Biorobotic AUV Using Mechanical Fins Based on CFD Parameterization," *Journal of Fluids Engineering*, 128, pp. 687-698, 2006.
16. M Sfakiotakis, D. M Lane and J. B. C Davies, "Review of Fish Swimming Modes for Aquatic Locomotion" *IEEE Journal of Oceanic Engineering*, 24(2), pp. 237-253, 1999.
17. S. N Singh, A Simha and R Mittal, "Biorobotic AUV Maneuvering by Pectoral Fins: Inverse Control Design Based on CFD Parameterization," *IEEE Journal of Oceanic Engineering*, 29, pp. 777-785, 2004.
18. M. S Triantafyllou, A Techet and F Hover, "Review of Experimental Work in Biomimetic Foils," *IEEE Journal of Oceanic Engineering*, 29, pp. 585-594, 2004.

19. M. S Triantafyllou, A Techet and F Hover, "Review of Experimental Work in Biomimetic Foils," 13th International Symposium on Unmanned Untethered Submersible Technology (UUST), New England center, Durham, New Hampshire, USA, 2003.
20. G. S Triantafyllou and M. S Triantafyllou, "An Efficient Swimming Machine," *Sci. Amer*, 272, pp. 64-70, 1995.
21. I Yamamoto , Y Terada , T Nagamatu and Y Imaizumi, "Propulsion System With Flexible/Rigid Oscillating Fin," *IEEE Journal of Oceanic Engineering*, 20(1), pp. 23-30, 1995.
22. T. Ichikizaki, I. Yamamoto, "Development of Robotic Fish with Various Swimming Functions," Symposium on Underwater technology, Japan, April 2007.
23. M. S. Naik, S. N. Singh, R. Mittal, "Biologically-inspired adaptive pectoral-like fin control system for CFD parameterized AUV," International Symposium on Underwater Technology, Tokyo, Japan. 17th – 20th, April 2007.
24. R. Ramamurti, R. Lohner, and W. Sandberg, "Computation of the unsteady-flow past a tuna with caudal fin oscillation," *Adv. Fluid Mech. Series*, vol 9, pp. 169-178, 1996.
25. P. W. Webb, "Maneuverability - general issues," *IEEE Journal of Oceanic Engineering*, 29, pp. 547-555, July 2004.
26. J. A. Walker, "Kinematics and Performance of Maneuvering Control Surfaces in Teleost Fishes," *IEEE Journal of Oceanic Engineering*, 29, pp. 572-584, 2004.
27. M. W. Westneat, D. H. Thorsen, J. A. Walker, M. E. Hale, "Structure, Function, and Neural Control of Pectoral Fins in Fishes," *IEEE Journal of Oceanic Engineering*, 29, pp. 674-683, July 2004.

28. N. Kato, T. Inaba, "Guidance and control of fish robot with apparatus of pectoral fin motion," IEEE International Conference on Robotics and Automation, Belgium., pp. 446-451, 1998.
29. P. R. Bandyopadhyay, "Maneuvering Hydrodynamics of Fish and Small Underwater Vehicles," Integrative and Comparative Biology, 42(1), pp. 102-117, February 2002.
30. H. S. Udaykumar, R. Mittal, P. Rampungoon, and A. Khanna, " A Sharp Interface Cartesian Grid Method for Simulating Flows with Complex Moving Boundaries," J. Comput. Phys., 174, 345-380, 2001.
31. Nakashimal, "Dynamics of two-joint dolphin-like propulsion mechanism," Nippon Kikai Gakkai Ronbunshu, B Hen/Transactions of the Japan Society of Mechanical Engineers, 62(602), pp. 3607-3613.
32. J. D. W. Madden, N. A. Vandesteeg, P. A. Anquetil, P. G. A. Madden, A. Takshi, R. Z. Pytel, S. R. Lafontaine, P. A. Wieringa, and I. W. Hunter, "Artificial Muscle Technology: Physical Principles and Naval prospects," IEEE Journal of Oceanic Engineering, 29, pp. 706-728, July 2004.
33. R. R. Llinas, E. Leznik, and V. I. Makarenko, "The Olivo - Cerebellar Circuit as a Universal Motor Control System," IEEE Journal of Oceanic Engineering, 29, pp. 631-639, July 2004.
34. P. Ridley, J. Fontan, P. Corke, "Submarine Dynamic Modeling," Australian Conference on Robotics and Automation, Brisbane, Australia, 2003.
35. T. I. Fossen, Guidance and Control of Ocean Vehicles. John Wiley and Sons, New York, 1999.

36. C. T. Chen, *Linear System Theory and Design*. Oxford University Press, 1999.
37. R. Mittal, "Computational Modeling in Biohydrodynamics: Trends, Challenges, and Recent Advances," *IEEE Journal of Oceanic Engineering*, 29, pp. 595-604, 2004.
38. H. Suzuki, N. Kato, T. Katayama, Y. Fukui, "Motion Simulation of an Underwater Vehicle with Mechanical Pectoral Fins Using a CFD-based Motion Simulator," *Symposium on Underwater technology, Japan*, pp. 384 - 390, April 2007.
39. L. Schenato, "Analysis and Control of Flapping Flight: from Biologically to Robotic Insects," Ph. D. Dissertation, University of California, Berkeley, 2003.
40. G. Tao, *Adaptive Control Design and Analysis*. John Wiley and Sons, New Jersey, 2003.
41. P. R. Bandyopadhyay, J. M. Castano, J. Q. Rice, R. B. Philips, W. H. Nedderman, and W. K. Macy, "Low-Speed Maneuvering Hydrodynamics of Fish and Small Underwater Vehicles," *ASME J. Fluids Engg.*, 119, pp. 136-144, 1997.
42. S. Guo, K. Sugimoto, S. Hata, J. Su, K. Oguro, "A new type of underwater fish-like microrobot," *IEEE ICIRS2000.*, pp. 867-872, 2000.
43. P. A. Ioannou, J. Sun, *Robust Adaptive Control*. Prentice-Hall Inc, New Jersey.
44. C.C Lindsey, *Form, Function and Locomotory Habits in Fish*, in *Fish Physiology*, W. S Hoar and D. J Randall, Eds. Academic, New York, ch 1, pp. 1-100, 1978
45. M. Narasimhan, and S. N. Singh, "Adaptive Optimal Control of an Autonomous Underwater Vehicle in the Dive Plane Using Dorsal Fins". *Ocean Engineering*, 33(3-4), pp. 404-416, 2006.

46. M. Narasimhan, and S. N. Singh, "Adaptive Input-Output Feedback Linearizing Yaw Plane Control of BAUV Using Dorsal Fins". *Ocean Engineering*, 33, pp. 1413-1430, 2006.
47. S Mani, S.N Singh, S. K Parimi, and W Yim, "Adaptive Servoregulation of a Projectile Fin Using Piezoelectric Actuator," *Journal of Dynamic Systems Measurement, and Control*, 129, pp. 100-104, 2007.
48. H Kaufmann, I Barkana, and K Sobel, *Direct Adaptive Control Algorithms*. Springer-Verlag, New York, 1998.
49. A Fradkov, I. V Miroshnik, and V. O Nikiforov, *Nonlinear and Adaptive Control of Complex Systems*. Kluwer Academic, Boston, 1999.
50. S Mani, S.N Singh, S. K Parimi, W Yim, and M Trabia, "Adaptive Rotation of a Smart Projectile Fin by Piezoelectric Flexible Beam Actuator," *J. Vib. Control*, 11(8), pp. 1085-1102, 2005.

VITA
Graduate College
University of Nevada, Las Vegas

Subramanian Ramasamy

Local Address:

1555 E Rochelle Avenue, Apt 134
Las Vegas, Nevada 89119

Home Address:

1/7 K.G Layout, Ist Cross Street
Saibaba Colony
Coimbatore, Tamil Nadu
India 641038

Degrees:

Bachelors of Engineering, Electrical and Electronics Engineering, 2006
Mepco Schlenk Engineering College, (Sivakasi)
Anna University, Tamil Nadu, India

Publications:

K. W lee, S Ramasamy, and S. N Singh, Adaptive Sliding Mode 3-D Trajectory Control of F/A-18 Model Via SDU Decomposition. AIAA Guidance, Navigation and Control Conference and Exhibit, Honolulu, Hawaii, August 18th - 21st, 2008.

S Ramasamy, Yaw Plane Robust Control of Nonlinear Biorobotic AUV Using Pectoral Fins 16th International Symposium on Unmanned Untethered Submersible Technology(UUST09), New England Center, University of New Hampshire - Durham, New Hampshire, August 23rd - 26th, 2009.

K. W lee, S Ramasamy, and S. N Singh, Bifurcation of Periodic Orbits in Inferior Olive Neurons. Twentieth International Conference on Systems Engineering), Coventry University, UK, September 8th - 10th, 2009.

Thesis Title:

Biology-Inspired Adaptive and Nonlinear Robust Control of BAUV Using Pectoral-Like Fins

Thesis Examination Committee:

Chairperson, Dr. Sahjendra Singh, Ph.D.
Committee Member, Dr. Venkatesan Muthukumar, Ph.D.
Committee Member Dr. Pushkin Kachroo, Ph.D.
Graduate Faculty Representative, Dr. Woosoon Yim, Ph.D.